NOTICE: When government or other drawings, specifications or other data are used for any purpose other than in connection with a definitely related government procurement operation, the U. S. Government thereby incurs no responsibility, nor any obligation whatsoever; and the fact that the Government may have formulated, furnished, or in any way supplied the said drawings, specifications, or other data is not to be regarded by implication or otherwise as in any manner licensing the holder or any other person or corporation, or conveying any rights or permission to manufacture, use or sell any patented invention that may in any way be related thereto.

ASD-TDR-62-75

DESIGN ANALYSIS OF FINAL RECOVERY PARACHUTES B-70 ENCAPSULATED SEAT AND THE USD-5 DRONE

ASD TECHNICAL DOCUMENTARY REPORT No. ASD-TDR-62-75

APRIL 1962

FLIGHT ACCESSORIES LABORATORY
AERONAUTICAL SYSTEMS DIVISION
AIR FORCE SYSTEMS COMMAND
WRIGHT-PATTERSON AIR FORCE BASE, OHIO

Project No. 6065, Task No. 606503

Prepared under Contract No. AF 33(616)-8371
by Space Recovery Systems, Inc., El Segundo, California
Authors: T. W. Knacke and L. I. Dimmick

NOTICES

When Government drawings, specifications, or other data are used for any purpose other than in connection with a definitely related Government procurement operation, the United States Government thereby incurs no responsibility nor any obligation whatsoever; and the fact that the Government may have formulated, furnished, or in any way supplied the said drawings, specifications, or other data, is not to be regarded by implication or otherwise as in any manner licensing the holder or any other person or corporation, or conveying any rights or permission to manufacture, use, or sell any patented invention that may in any way be related thereto.

ASTIA release to OTS not authorized.

Qualified requesters may obtain copies of this report from the Armed Services Technical Information Agency, (ASTIA), Arlington Hall Station, Arlington 12, Virginia.

Copies of this report should not be returned to the Aeronautical Systems Division unless return is required by security considerations, contractual obligations, or notice on a specific document.

200 - June 1962 - 36-1566 & 1567

ABSTRACT

A performance analysis was conducted on two parachute recovery systems developed by Space Recovery Systems, Inc., for the North American Aviation B-70 encapsulated seat and the Fairchild Stratos Corporation USD-5 surveillance drone. Optimization of aerodynamic and textile design, controlled deployment and opening, and use of a cluster of two independently deployed parachutes for the USD-5 drone resulted in a highly predictable performance, in the highest known drag area per weight ratio for the USD-5 system, and a high velocity capability for the B-70 system.

Equations were developed through data analysis for the opening process and the drag area increase versus time during parachute opening for extended skirt parachutes. These equations permitted a computer analysis of the total parachute deceleration process with computer results showing less than 10% deviation from actual test data. The developed computer method may well be suitable for performance analysis of recovery processes using ribbon, ring slot, and other solid material type parachutes.

PUBLICATION REVIEW

This report has been reviewed and is approved.

FOR THE COMMANDER:

GEORGE A. SOLT, JR.
Chief, Retardation and Recovery
Branch
Flight Accessories Laboratory

TABLE OF CONTENTS

TABLE OF CONTENTS (Continued)

TABLE OF CONTENTS (Continued)

LIST OF FIGURES

LIST OF FIGURES (Continued)

LIST OF FIGURES (Continued)

1.0 INTRODUCTION

1.1 Background

Space Recovery Systems, Inc. (SRS), El Segundo, California, in 1960 successfully completed the recovery system for the encapsulated seat of the B-70 Bomber developed by North American Aviation for the U.S. Air Force, and the aerial recovery and landing system for the USD-5 Drone developed by Fairchild Stratos Corporation for the U.S. Army Signal Corps. In each case, SRS developed the complete system, including system installation, sequencing and ejection subsystems, first-stage deceleration parachute and final recovery parachute assemblies, and the airbag shock absorption system, for the USD-5 Drone.

The requirements of both recovery systems extended beyond the state-of-the-art in such areas as velocity profile, allowable weight and volume, and installation concept. The technical analysis of these two final recovery parachute subsystems is the subject of this report.

Both systems include first-stage deceleration or stabilization parachutes. The B-70 Capsule uses small ribbon parachutes, deployed from the end of telescoping booms, for capsule deceleration and stability augmentation. These parachutes have been successfully tested at Mach 2.3 at 70,000 feet. First-stage deceleration on the USD-5 is accomplished by a single ribbon parachute designed for operation at high subsonic velocities.

1.2 Requirements

The B-70 system required the recovery of a 710-pound encapsulated seat with a sea level rate of descent of 28 fps, an oscillation of less than 15 degrees, an on-the-deck recovery capability at a 90-knot forward velocity, with parachute opening completed 90 feet above ground, and safe deployment velocity of 410 knots TAS at an altitude of 15,000 feet above sea level.

The USD-5 Drone system was designed for the recovery of a 4,800-pound drone at a sea level rate of descent of 23.5 fps with minimum oscillation consistent with proper airbag operation. Maximum parachute deployment force was not to exceed 15,000 pounds at an operational velocity of 250 knots IAS.

Manuscript released by authors October 1961 for publication as an ASD Technical Documentary Report.

1.3 Development Histories

1.3.1 The B-70 Capsule Recovery Parachute: The B-70 Capsule recovery parachute assembly, consisting of recovery parachute, pilot chute, and deployment bag-pilot chute-bridle line, is shown in flight in Figure 1. A 10% extended skirt parachute was selected for the recovery parachute based on the proven reliability, good stability and low opening shock obtained with the 10% extended skirt T-10 troop parachute. Considerable improvements were made in aerodynamic design and in the construction details of the canopy which resulted in an improved speed capability and reduced the volume requirements. Initial calculations based on published data resulted in a 38-foot diameter parachute defined as Type I in this report. The high drag coefficient obtained in Phase I tests led to a reduction in diameter to 35.5 feet (Type II), and subsequently to 34.5 feet (Type III), based on reduced capsule weight. Initial tests were made with guide-surface type pilot chutes. A permanently attached 5-foot diameter conical vane-type pilot chute resulted in controlled parachute deployment and opening and, in connection with reefing, in a reduction in parachute opening force.

The final recovery 34.5-foot nominal diameter 10% extended skirt parachute, weighing 18.5 pounds in one version and 21.3 pounds in another, is described in detail in paragraph 3.2. A rate of descent of 28.5 fps at sea level was obtained with a total capsule weight of 710 pounds. The 21.3-pound parachute has been successfully deployed at 463 knots TAS at an altitude of 15,000 feet and has provided an on-the-deck recovery at 90 knots with a 100-foot safe altitude, thus meeting all requirements. In a test conducted by North American, an inadvertent on-the-deck ejection was made at 570 knots, with the parachute opening at approximately 560 knots, resulting in full on-the-deck recovery. For details, see North American report No. NA61-24-2.

Fifty-two engineering development tests were conducted with the parachute system. Detailed data on the design, performance and qualification of this parachute recovery system are contained in Reference 1, SRS Report 147-588, "Analysis of Parachute Qualification Tests for B-70 Air Crew Encapsulated Seat".

1.3.2 The USD-5 Drone Recovery Parachute: A cluster of two independently, but simultaneously deployed 71-foot diameter conical, fully extended skirt parachutes was originally used for recovery of the USD-5 Drone. Figure 2 shows an in-flight deployment of the parachute cluster assembly.

During the testing, it became obvious that the airbag impact attenuator subsystem was not as effective as had been anticipated, making it desirable to lower the rate of descent in order to decrease the energy absorbed by the airbag system. Experience gained with the 71-foot diameter parachutes and revised packing techniques made it possible to use a 78-foot nominal diameter parachute assembly which still could be packed into the USD-5 Drone parachute compartment.

The individual 78-foot diameter parachute weighs 64.5 pounds. The cluster of two parachutes, deployed at 225 knots IAS, was practically free of oscillation and produced a rate of descent of 22.7 fps (measured by phototheodolite) resulting in an average C_{D_o} of 0.825. These parachutes produce 61 ft^2 of parachute drag area per pound of parachute weight called "specific drag area", $C_D S_o / W_p$. This efficiency value is more than 10% better than any other known recovery parachute, and probably even 15% better when compared on an individual parachute basis. Figure 3 compares the B-70 and USD-5 recovery parachutes with other recovery parachutes now in use.

The USD-5 parachute cluster of two parachutes is deployed independently, left and right of the vertical stabilizer, from a single compartment. This method has proven extremely successful and has solved the difficult problem of how to deploy a single large parachute or a parachute cluster from a compartment located directly in front of the vertical stabilizer.

2.0 DESIGN PHILOSOPHY AND APPROACH

2.1 General Approach

The requirement for high performance, minimum weight and volume, low oscillation and, in the case of the B-70 Capsule, high speed capability required extensive investigation of parachute types and optimization of parachute performance, parachute design, and parachute installation. The following approach was used for both parachute assemblies:

(a) Both parachute assemblies were optimized in aerodynamic design of the parachute canopy and suspension line arrangement with regard to high drag, high stability, and low opening forces.

(b) Textile canopy design and fabrication were optimized for minimum weight by eliminating all excess material, minimizing connection losses, and discarding tradition-bound design concepts in seams, fullness and line connections. (See paragraph 2.3)

(c) The parachute assemblies were designed so as to maintain a completely controlled deployment and opening procedure. This was obtained by a permanently attached pilot chute positioned so that the pilot chute remained inflated during reefed opening and disreefing, and by careful stowing of all parachute parts so as to assure a steady force between pilot chute and parachute attachment point during all phases of deployment and opening. A proper force balance was obtained between snatch force, reefed opening, and final opening.

(d) A new approach was used for the deployment of the cluster of two USD-5 parachutes stowed in front of the vertical stabilizer consisting of individual parachute deployment left and right of the vertical stabilizer.

2.2 Aerodynamic Optimization

The design of a final recovery parachute system for any aerospace vehicle must fulfill some or all of the following requirements:

(a) reliability of opening and operation

(b) low weight and volume

(c) low opening forces within allowable G limits

(d) suitable stability for land and/or water recovery

(e) suitability for cluster use (if required)

(f) low maintenance and service

(g) simplicity of fabrication

Reliability of parachute opening is an inherent characteristic of a particular parachute type documented by statistical analysis of conducted tests. Simultaneously, it requires proper installation and parachute component design so as not to preclude otherwise proper parachute opening. Low weight and volume are products of high individual parachute drag, obtained by applying optimized parachute construction and design features associated with low parachute opening forces. Parachute opening forces depend upon factors inherent in the particular parachute type, but can be controlled by deployment and reefing. Stability is an inherent parachute characteristic for single parachutes of a particular type. The use of relatively unstable parachutes in a cluster provides a stable parachute system if some basic ground rules are observed. Reference 4, the U.S. Air Force Parachute Handbook, WADD Technical Report 55-265, page 2-1-20, and Reference 5, the recently published "Handbook of Astronautical Engineering", chapter 22-5, give summaries of parachute performance. The ribbon parachute and guide-surface parachute are typical high speed deceleration and stabilization parachutes giving good stability, low opening shock but also low drag and a resultant high weight which makes them less suitable for use as final recovery parachutes. Flat circular and flat conical parachutes have proven their reliability in numerous applications and produce a high drag; however, their lack of stability and high individual opening shock makes them less desirable for use as final recovery parachutes. Ring slot and ring sail parachutes have good stability and low opening shock, but low drag coefficients in stable configurations. In the higher drag coefficient range, stability decays rapidly, and weight and volume are considerably higher than that of extended skirt parachutes. Extended skirt parachutes, properly designed, have exhibited a very high drag, a stability of about 5 to 10 degrees and a reasonably low opening shock. In addition, extended skirt parachutes can be optimized in aerodynamic design as well as in construction, and have proven their exceptionally high reliability in applications as the Army T-10 standard troop parachute, and for several missile recovery projects such as the Q-2 and Beech KD-4 Drone. Considerable performance data are available on these parachutes as a result of numerous tests. A 10% extended skirt parachute is used for the B-70 Capsule. Considering the fact that the capsule parachute is a human escape parachute, it was felt practical to benefit from the extensive reliability experience of the Army T-10 parachute. Figure 4 shows drag

coefficient versus the ratio of suspension line length to nominal diameter for several basic parachute types. For the extended type, it can be seen that C_D will increase rapidly with increase in L_s/D_o up to a value of 1.0 and thereafter shows only a very slight improvement with further increase in L_s/D_o. An analysis, comparing the parachute weight required for a given rate of descent and vehicle weight, shows that for a lightweight parachute, an L_s/D_o ratio of 0.95 will give approximately the minimum parachute weight and logically the minimum stowed volume. This ratio was, therefore, used for both the B-70 and the USD-5 extended skirt parachute. A conical, fully extended skirt parachute was selected for the USD-5 Drone based on good experience with fully extended skirt parachutes for drone recovery. Aerodynamic optimization resulted in the high drag coefficient $C_{D_o} = 0.825$ for a cluster of two extended skirt parachutes. In addition, the canopy design was carefully controlled for the purpose of obtaining a canopy shape that complied with the original aerodynamic design after completion.

2.3 Parachute Design Optimization

Great emphasis was placed on eliminating excess weight and volume and updating fabrication and design methods. It is not known why, for example, radial seams in solid material parachutes are traditionally 1 inch wide and section seams are 5/8 inch wide, and why, for example, 7% of fullness (G11-A) is used in the canopy. SRS conducted strength tests of all parachute seams, suspension lines, and riser connections. Based on these tests, the width of all seams was decreased to a point where full effectiveness of the seams was maintained without sacrificing strength or going to difficult fabrication methods. For example, the conventional 1 inch wide seam was reduced to 3/4 inch. A proper ratio was selected between suspension lines and radial seam strength assuming that the material contained in the radial seam could carry a proportionate amount of the load of the suspension lines. Radial seams reinforced with tape were used, whereby the total strength of tape plus material was designed for 90% of the suspension line strength. Special care was taken to maintain proper distribution of the radial tapes. Webbing and tape overlap of required length, but not more, were used. Braided suspension lines, rather than woven suspension lines, were used based on their better strength-weight ratio.

2.4 Deployment Optimization

Particular attention was paid to optimization of the deployment and opening sequence.

2.4.1 The B-70 Parachute Assembly: The deployment sequence of the B-70 parachute assembly is shown in Figure 5. The encapsulated seat is rocketed from the aircraft and stabilized in free fall by the

stabilization parachutes and the dynamic action of the booms. When the capsule has descended to an altitude of 15,000 feet, recovery is initiated by aneroid switches using the following sequence of deployment:

(a) The parachute compartment cover is ejected and deploys the pilot chute, stowed in a bag permanently attached to the cover; cover and deployment bag then detach and descend separately.

(b) The pilot chute, in turn, extracts the main recovery parachute.

(c) The main recovery parachute inflates to the reefed state. After a 2-second time delay, pyrotechnically operated reefing line cutters, mechanically armed at line stretch, sever the reefing line. The recovery parachute then inflates fully and decelerates the capsule to a descent rate at sea level of approximately 28 fps. When seat ejection occurs below 15,000 feet, the recovery sequence takes place immediately.

A positive control of deployment and parachute opening is obtained by a large pilot chute permanently attached by an 18.5-foot bridle line to the vent of the recovery parachute. This long bridle assures that the pilot chute remains inflated during reefed opening and most of the full opening period. The pilot chute drag area is 1.75% of the drag area of the main recovery parachute. This pilot chute performs three functions.

(a) It provides tension between pilot chute and recovery parachute attachment so as not to allow any parts of the parachute to deploy in an uncontrolled (or premature) manner.

(b) It delays the canopy opening into the reefed stage at high speeds, thereby decreasing the opening shock.

(c) It assures a uniform and symmetrical parachute deployment and opening and centers the parachute vent into a cone rather than part of a hemisphere. This results in a stress relief due to the smaller radius of individual parachute parts in the vent area and prevents false vents and unsymmetrical vent loading detrimental to the overall performance.

The suspension lines are stowed in the deployment bag in two parallel groups, thereby allowing a straightforward deployment of the bag without the zigzag motions that occur if the lines are stowed in a single group. The canopy is tied in the deployment bag at regular intervals with special break ties. As the pilot chute starts deployment of the main canopy, it first has to deploy the two suspension line groups out of individual rows of stow pockets and then has to deploy the canopy, which is securely held in place, until the deployment of the lines is complete.

2.4.2 The USD-5 Parachute Subsystem: The deployment of the USD-5 recovery parachute is based on the same design philosophy, that a positive tension must be maintained on the system at all times. The deployment is as follows; see Figure 6.

(a) At the initiation of recovery, the parachute compartment doors are unlocked and opened. Two drogue guns, mounted forward of the main recovery parachute container, fire small projectiles 45 degrees from the vertical. Connected to each projectile by a short bridle is a pilot chute deployment bag. The drogue projectile pulls the pilot chute deployment bag by this bridle to the limit of the pilot chute riser and then strips the deployment bag from the pilot chute.

(b) The inflated pilot chute deploys an extractor parachute.

(c) Each extractor parachute serves to deploy a main recovery parachute on either side of the vertical tail. The extractor parachute remains attached to the apex of the recovery parachute, thereby producing a well controlled opening sequence of the recovery parachute similar to that employed on the B-70 parachute assembly. The extraction parachute drag area is 0.9% of the drag area of the main or final recovery parachute.

(d) The main recovery parachutes are initially deployed in a reefed condition. After a 6-second delay period, the parachutes are disreefed.

2.5 USD-5 Cluster Deployment

Prior to the development of the USD-5 parachute recovery system, clusters were deployed by using a single extraction parachute and multiple or individual deployment bags jointly extracted by this single extraction parachute. The USD-5 Drone parachute installation with the parachute compartment in front of the high vertical stabilizer was very unfavorable for the deployment of a single parachute or a cluster of parachutes through the use of a single extraction parachute. This was amply demonstrated on several drone projects, especially the Radioplane Q-4 Drone which had numerous changes in the location of the parachute compartment with regard to the vertical stabilizer in order to assure proper deployment of the single main recovery parachute. SRS proposed to use a cluster of two parachutes with each parachute individually deployed right and left of the vertical stabilizer. In addition, the deployment system was laid out so that optimum clearance between individual drogue slugs, pilot chutes, extraction parachutes, and main recovery parachutes could be obtained with regard to the vertical stabilizer. Special care was taken so that the entire deployment procedure of both parachute assemblies was ex-

tremely uniform. The success of this deployment system and the smoothness and uniformity of the deployment method can be seen in Figure 2. Throughout the entire test series on the USD-5 parachute system, no problems occurred that had their source in the method of deployment of the two individual parachutes. Figure 6 illustrates deployment to the left and right of the vertical tail. In addition to a large permanently attached extraction parachute providing tension on all parachute parts during deployment, canted deployment bags are used that position the bags during extraction for adequate clearance past the vertical stabilizer.

3.0 PARACHUTE ASSEMBLY DESCRIPTIONS

3.1 General Discussion

Similarities exist between the B-70 and USD-5 parachute assemblies in that reliability and performance were the prime requisites of their design specifications. In the B-70 system, the obvious reason was a human payload; in the USD-5, a system was needed to return vehicle and reconnaissance data undamaged and suitable for reuse. To achieve these ends, an optimization of components in regard to strength, weight, volume and function was carried out using the latest approaches in the state-of-the-art as outlined in Section 2.0 of this report.

3.2 B-70 Parachute Assembly

The final parachute system consists of the following items: (Figure 7)

(a) A 34.5-foot nominal diameter, 10% extended skirt recovery parachute attached with individual two-legged risers, one on either side of the container, which are mounted atop the escape capsule.

(b) The recovery parachute deployment bag.

(c) A 5-foot nominal diameter conical vane-type pilot chute connected permanently to the recovery parachute deployment bag and the apex of the recovery parachute by an 18.5-foot bridle.

(d) The pilot chute deployment bag connected to the pilot chute by means of an apex break tie and to the parachute compartment cover by a three-legged steel cable.

The 34.5-foot diameter recovery parachute has 36 gores (see gore pattern, Figure 7) and 36 suspension lines, each of 750-pound braided cord, MIL-C-7515 Type III. The canopy is fabricated primarily of 1.1 oz/sq yd nylon cloth, MIL-C-7020 Type I, with the upper 10% of the canopy area fabricated of 2.25 oz/sq yd nylon cloth, MIL-C-7350 Type I. The radial seam employed for the design of the recovery parachute consisted of 4 rows of stitches over a seam width of 3/4 inches as shown in Figure 7.

The suspension lines are connected in two groups via 2-ply bridles of 1-3/4 inch 10,000-pound webbing, MIL-W-4088 Type XIX, to the capsule attachment points. The parachute incorporates a reefing line of 750-pound braided cord, MIL-C-7515 Type III, passing through three 2-second delay reefing line cutters, Ordnance Associates Type OA-D2.

The recovery parachute deployment bag is a shaped design forming to the contour of the container with separate canopy and suspension line compartments. Each compartment is closed by the suspension line locking loop method. Suspension lines are stowed in two parallel groups in stow loops designed to provide a detention force of 15 to 25 pounds; this permits good deployment at high as well as low speeds.

Connection between the pilot chute, deployment bag and recovery parachute apex is made by a continuous bridle, 18.5 feet long, which is integral with the deployment bag and pilot chute. In this way, forces can initially be transmitted into the deployment bag reinforcement webbing and, subsequently, into the apex of the recovery parachute.

3.3 USD-5 Parachute Assembly

The USD-5 parachute assembly is a twin system; therefore, only one side will be discussed for the sake of clarity and to avoid repetition. Each half assembly consists of the following items (Figure 8):

(a) A 78-foot nominal diameter, 25 degrees conical, fully extended skirt parachute with a 32.4-foot riser connected with its sister assembly to the ground disconnect. From this common point (ground disconnect), a three-member vehicle riser connects the entire assembly to the vehicle.

(b) The recovery parachute deployment bag.

(c) The extractor parachute. This is a 7-foot nominal diameter ring slot parachute permanently attached to the main recovery parachute. The use of an extractor parachute was the most economical way, from weight considerations, to extract the large main recovery parachute. Use of a single pilot chute capable of extracting the main recovery parachute would have required a drogue gun and slug of inordinate size.

(d) The extractor parachute deployment bag.

(e) The box type pilot chute with a nominal diameter of 2.25 feet which is permanently attached to the extractor parachute deployment bag.

(f) The pilot chute deployment bag. This bag is permanently attached to the drogue gun slug by a short bridle and to the apex of the pilot chute by a break cord.

The 78-foot diameter recovery parachute has 64 gores (see gore pattern, Figure 8) and 64 suspension lines. The canopy is fabricated from 1.1 oz/sq yd nylon cloth, MIL-C-7020 Type I. The suspension lines are 400-pound braided cord, MIL-C-7515 Type III. The radial seam was 3/4 inches wide and consisted of 4 rows of stitching as shown in Figure 8.

The canopy is reefed with a 750-pound braided nylon cord reefing line using three 6-second delay reefing line cutters, Ordnance Associates Type OA D2-6.

The recovery parachute deployment bag is of shaped design conforming to the contour of the parachute container. Separate compartments for canopy and suspension lines are used with each compartment closed by the suspension line locking loop method. The extractor parachute riser is unsymmetrically attached, thereby obtaining a canted position after extraction.

The pilot chute is a 2.25-foot nominal diameter parachute of box-type construction with four gores and four suspension lines.

Figure 8 is a data chart giving the essentials of the USD-5 main parachute assembly.

4.0 TEST PROGRAM AND RESULTS

4.1 Test Programs

4.1.1 B-70 Test Program: The B-70 parachute tests were conducted in four phases. Phase I consisted of rate of descent and stability tests. Phases II and III consisted of structural integrity tests using a representative deployment system and a cylindrical drop test vehicle as test carrier. The Phase II tests were conducted at low altitude, and the Phase III tests at 15,000 feet. The Phase IV tests were systems tests at velocities and altitudes selected to cover the specified flight recovery envelope.

The original test program, as proposed by Space Recovery Systems, consisted of twenty aerial drop tests.

Due to changes in the design of the parachute, which were introduced because of performance characteristics and changes in capsule weight, a total of 24 Rate of Descent Tests were conducted. Instrumentation difficulties made it necessary to conduct a total of 24 Structural Integrity Tests in order to obtain sufficient data for qualifying the parachute system.

The 48 tests mentioned above, together with four recovery system tests, resulted in a total drop test program of 52 tests.

4.1.2 USD-5 Test Program: The drop test program consisted of four phases.

4.1.2.1 Phase I, Recovery Parachute: Phase IA comprised Rate of Descent and Stability Tests consisting of six tests at 130 knots drop velocity and 2,000 feet altitude, using a drop weight of 2,400 pounds for single and 4,800 pounds for double parachute systems.

Phase IB tests covered structural integrity of the parachute assembly; seven tests, ranging from drop velocities of 150 knots to velocities at which the damage suffered by the parachute would not permit the successful recovery of the USD-5 Drone.

Phase IC included the trajectory analysis drop tests. The exact number of drops were to be determined by analysis of test results.

4.1.2.2 Phase II, Deceleration Parachute: Five successful tests were to be conducted with a high speed deceleration parachute using cylindrical test vehicle dropped from a B-66 aircraft. This parachute assembly is not a subject of this report.

4.1.2.3 Phase III, Recovery System (Dummy Drone): The Phase III series was to consist of eight successful drops to prove the compatibility of the complete drone recovery system. The test vehicle was a dummy drone of steel construction ballasted to simulate the USD-5 Drone. These drops were to be made with a B-47 aircraft from low altitude at velocities from 150 knots to 250 knots indicated air speed, and drop weights of 4,800 pounds and 7,200 pounds.

4.1.2.4 Phase IV, Recovery System (Stripped Drone): The Phase IV recovery system tests were to be conducted with a "stripped" version of the USD-5 Drone to be dropped from a B-52 aircraft.

4.2 B-70 Parachute Test Results

4.2.1 Test Summary: The B-70 parachute test results are shown in the aerial drop test summaries, Figures 9, 10, 11, 12 and 13. The several recovery parachutes employed during the test program are shown in Table I.

TABLE I

B-70 Recovery Parachute Types

Type	Description
I	38-foot diameter (L_s/D_o = 1.0)
II	35.5-foot diameter (L_s/D_o = 0.87)
III	34.5-foot diameter (L_s/D_o = 0.87)
IIIA	34.5-foot diameter (L_s/D_o = 0.95)

The various pilot chutes tested are listed in Table II.

TABLE II

B-70 Pilot Chute Types

Type	Description	Part No.	Suspension Line Length (feet)
I	48-inch guide surface, ribless	GFE	4.0
II	60-inch guide surface, ribless	GFE	5.0
III	68-inch octagonal - flat	GFE	5.7
IV	5-foot solid conical, vane	SRS 588-054 Type II	7.5
V	5-foot solid conical, vane	SRS 588-320	5.0

4.2.2 Rate of Descent: Rate of Descent was obtained by (1) dropline, and (2) photo-theodolite (Askania) measurements. Figures 14, 15 and 16 are representative plots of altitude versus time obtained from photo-theodolite data. Slopes taken from these plots give rate of descent. Figure 17 is a summary of rate of descent and drag coefficient data obtained on the various B-70 parachute types.

4.2.3 Stability: A total of 18 drops were analyzed to determine the oscillation characteristics of the parachute assembly at ground impact. This included five tests with parachute Type I, 12 drops with Type III, and one drop with Type IIIA. Sixteen drops were analyzed from 70mm Hulcher photographs; two were plotted using the angle of oscillation from photo-theodolite data. The analysis of the Hulcher photographs was accomplished by trigonometric evaluation of physical measurements. The mathematical derivation of the analysis is found in Appendix I. The method used was to plot the magnitude of oscillation versus time and the distance traveled by the suspended load during the oscillation of the parachute. Three of the analysis sheets, Figures 18, 19 and 20, are typical examples. The average impact oscillation for the Type III recovery parachute is 8.5 degrees. It is interesting to note that while the oscillation occurring during the descent did occasionally exceed 15 degrees, this generally occurred just before ground impact (see Figures 18 and 19) when turbulent air conditions were most likely to exist.

4.2.4 Force and Velocity: A total of 19 tests were instrumented for obtaining force by telemetry and strain gage links, velocity versus time by kine-theodolite, and photo coverage by Hulcher cameras. On 15 tests, two of these values were obtained and on only four tests were all three values obtained. The difficulty in obtaining proper coverage is partially explained by the fact that the main emphasis in this program was placed on meeting schedules and operational requirements rather than on gathering data.

Parachute force and velocity versus time for test numbers 29, 33, 48, 51 and 54 are presented in Figures 21, 22, 23, 24 and 25, together with event photographs of the parachute opening.

Two drops (13 and 14) made at 240 knots without reefing resulted in recovery, but produced damage to canopies at opening force of 14,000 pounds. These two tests served to substantiate the need for single-stage reefing. As deployment velocities increased through drops 15, 17 and 19, a relatively high disreefing force occurred, making it necessary to increase the length of the reefing line from 75 inches to 106 inches. Subsequent tests reflect the improved balance between reefed forces and fully open forces, see Figure 24.

4.2.5 Structural Integrity: Specifications required an operational speed of 325 knots (550 fps) at sea level, and 410 knots (693 fps) True Air Speed (TAS) at 15,000 feet with an ultimate safety factor of 1.5.

Figure 26 shows that the maximum parachute force at a velocity of 550 fps at sea level is approximately 6,100 pounds. An extrapolation of the curve indicated that the ultimate load of 9,150 pounds, equal to 1.5 times operational load, would result from a drop velocity of approximately 640 fps (378 knots), or a 16% higher velocity. The one test conducted at this over-speed condition (drop 57) resulted in full recovery with light damage to the parachute; however, no force records were obtained. Drops 13 and 14, conducted early in the program with no reefing, showed maximum parachute forces of 13,500 and 12,800 pounds, respectively, with only medium canopy damage. This documents that the parachute is able to withstand forces in excess of the ultimate load specified above. Tests subsequently conducted at the Hurricane Mesa Test Track accomplished "on-the-deck" recovery at 575 knots TAS with only medium parachute damage.

4.2.6 Opening Process: Data plotted in Figure 27 shows parachute deployment time (defined as time from cover ejection to line stretch) and canopy filling time (defined as time from line stretch to fully open canopy). It should be noticed that there is a tendency for filling time to increase at higher speeds. A similar tendency has been observed on drop tests with 28-foot solid flat parachutes featuring a large permanently attached pilot chute.

It appears that the large permanently attached pilot chute has but little influence on filling time at low speed, but has a definite tendency to increase filling time at high speeds.

4.3 USD-5 Parachute Test Results

4.3.1 Test Summary: The USD-5 parachute test results are summarized in the drop test summaries, Figures 28, 29 and 30. The four phases were:

Phase IA, Rate of Descent and Stability
Phase IB, Structural Integrity
Phase II, Deceleration Parachute Tests
Phase III, Recovery System Tests (Dummy Drone)
Phase IV, Recovery System Tests (Stripped Drone)

Two types of recovery parachutes were used having nominal diameters of 71 and 78 feet. The 78-foot parachutes were dropped only in the cluster configuration. The two types of pilot chutes used are described in Table III. With clusters, additional extraction parachutes were used. After drop test Number 11, the extraction parachutes remained permanently attached.

TABLE III

USD-5 Pilot Chute Types

Type	Description	Part No.	Suspension Line Length (feet)
I	68-inch nominal diameter octagonal - flat	GFE	5.7
II	2.25-foot nominal diameter box type	510-2231-1	2.25

4.3.2 Rate of Descent: Figure 31 is a typical plot of rate of descent versus time as taken from Askania photo-theodolite measurements on the 78-foot diameter parachutes. Average rate of descent obtained from photo-theodolite with clusters of two 78-foot diameter parachutes at a drone weight of 4,800 pounds was 22.6 fps, yielding an average drag coefficient (C_{D_o}) of 0.825.

Data on the 71-foot parachutes were gathered from dropline measurements and event time film analysis. Average rate of descent, obtained with clusters of these parachutes, at a weight of 4,800 pounds was 25.9 fps, yielding a drag coefficient (C_{D_o}) of 0.765 per parachute.

4.3.3 Stability: The Hulcher photographs were not available on this program as they were on the B-70 capsule program; therefore, data on the stability of the USD-5 parachute assemblies are qualitative rather than quantitative. However, motion pictures and drop site observation by skilled observers showed oscillation to be from 5 to 10 degrees for single parachutes. The oscillation was practically zero for the cluster of two parachutes.

4.3.4 Force and Velocity: Parachute force and velocity versus time, based on drop test Number 19, are shown in Figures 32 and 33. All drop tests, except Number 1, were made with reefed parachutes. The aerial drop test summaries, Figures 28, 29 and 30, indicate the installed reefing line length on each test.

4.3.5 Structural Integrity: The initial specification required safe deployment at 250 knots Indicated Air Speed (IAS). This was expected to be met with a 71-foot diameter parachute having a reinforced crown. However, when it was found necessary to increase to a 78-foot diameter parachute, the parachute compartment volume would not accommodate the reinforced crown. The requirement was then lowered to 200 knots IAS; the parachute was successfully deployed at this velocity in test. It is felt that reinforcing the crown would allow this parachute to be deployed at considerably higher speed.

4.3.6 Opening Process: In tests with the USD-5, it was noted that deployment and reefed filling time did decrease very little with increase in velocity. This can be attributed to the permanently attached pilot chute.

4.3.7 Cluster Deployment: A total of 23 parachute cluster tests were made with the individually deployed parachutes. At no time during these tests did parachute entanglement or vertical tail avoidance (when a dummy or stripped drone was used) become a problem. Since completion of the test program, the independent cluster deployment system has worked perfectly on all flights where main recovery parachutes were deployed, resulting in 13 successful recoveries to date.

5.0 DATA ANALYSIS

5.1 Approach

The data analysis on both the B-70 and the USD-5 parachute assemblies was made with the clear objective in mind of obtaining data that would allow improved prediction of the performance of present and future parachute systems. Parachute recovery systems are generally designed for decelerating an object from a certain velocity-altitude condition to a low velocity at ground impact, frequently in a desired minimum time or at a minimum altitude. In a parachute performance analysis, therefore, the following factors have to be investigated:

(a) Parachute opening times.

(b) Parachute forces.

(c) Parachute drag area increase versus time for the various stages of parachute opening. This is mandatory for computer analysis.

(d) Proper parachute staging (reefing) for a given parachute drag area profile.

Numerous attempts have been made to solve the problem of parachute opening, and its resultant force-time history, by a strictly analytical approach. So far, only limited success has been achieved, and no system has been developed that is suitable for recovery systems with multiple stage parachutes. A semi-analytical approach is used in this report which was found to be suitable for engineering application and especially for computer analysis. The proposed method agrees, in general terms, with the approach used in Reference 4.

Parachute opening time in the Parachute Handbook (Reference 4) is defined as

$$t_f = \frac{n D_o}{V_s^{.9}} \qquad 5.1$$

where

t_f = Parachute filling time from line stretch to fully opened parachute, seconds

D_o = Parachute nominal diameter, feet

V_s = Velocity at line stretch, respectively begin of filling or disreefing, fps

n = A factor for a particular type of parachute

This formula, developed eighteen years ago for ribbon parachutes at subsonic speeds, gives reasonable results, but does not take into account the many subtle variations in parachute design. The formula is based on the logical assumption that, in accordance with the "law of continuity", a parachute of a particular type and diameter opens in the same traveled distance. This means that a certain column of air has to be swallowed by the canopy in order to open fully.

The Handbook expression for parachute filling time, 5.1, cannot be applied directly to systems where reefing is employed. A correction factor must be applied to the nominal parachute diameter, D_o. Since this factor is related to the ratio of reefed to full open drag areas, the revised expression for filling time for a parachute opening into the reefed condition becomes, in general form:

$$t_{f_1} = \frac{n\, D_o}{V_s^{.9}} \cdot \left(\frac{(C_D S)_R}{(C_D S)_o} \right)^{\frac{1}{2}}$$

with t_{f_1} = reefed fill time, seconds

$(C_D S)_R$ = reefed drag area, square feet

$(C_D S)_o$ = full open drag area, square feet

It is obvious that the expression

$$D_o \cdot \left(\frac{(C_D S)_R}{(C_D S)_o} \right)^{\frac{1}{2}}$$

is the equivalent diameter of the reefed parachute. A similar expression can be formulated for disreef time. Paragraph 5.6 gives exact equations on data for the various fill times and n-factors.

Determination of parachute opening force follows the method developed by Pflanz in Germany (Reference 6). The Pflanz system is based on an exact mathematical approach assuming that a body increases its drag area, $C_D S$, in a known time period, from a small value (start of parachute opening) to a large value (fully opened parachute) in a given mathematical fashion (linear, power, or exponential rate). This method gives forces, travel distance, velocity and time at maximum force.

The opening force calculation in the U.S. Air Force Parachute Handbook is based on this report and can be written in the form:

$$\text{Opening force: } F_o = C_{D_o} \cdot S_o \cdot q \cdot X_o \cdot X_1$$

where:

X_o = The opening shock factor obtained for the infinite load condition from wind tunnel tests

X_1 = The opening shock decreasing factor obtained from Figure 34 (see Reference 4)

In order to determine X_1, it is necessary first to calculate a value for "A" from the expression

$$A = \frac{2W}{\rho \cdot C_D S_o \cdot t_f \cdot g \cdot V_s}$$

The factor, X_1, is based upon a linear drag area increase with canopy filling time, as given in Figure 34 as a function of "A". This system, which assumes that filling time for the various steps will comply with Expression 5.1, and that the drag area will increase linearly with time, is limited for computer analysis. Finding improved methods suitable for computer techniques was one of the prime goals of this analysis.

5.2 Approach to Computer Analysis

In order to utilize computers for the determination of parachute trajectories, it is necessary first to examine the basic problem of parachute opening. For simplicity, it could be assumed that parachute canopy drag area increased linearly with time. However, past experience has shown that such an assumption will, in some cases, lead to a considerable error. Therefore, in order to obtain valid results from the computer, it will be necessary to determine the manner in which canopy drag area changes with respect to time.

For computer programming, it is convenient to use mathematical expressions for this growth rate. From Figure 35, typical possibilities of drag area growth versus time can be seen. When reefing is used, the shape of the growth curves may tend to change since opening into the reefed state is a considerably different process than going to full open. It could be anticipated that only area growth from reefed open to full open would follow the same form as opening without reefing. The expressions which evolve from the analysis of drag area growth generally involve a time ratio raised to some power. This power, called m, would be 1.0 for a linear relationship.

Once a suitable expression has been generated and fed into the computer, the parachute drag area can be permitted to grow with time up to some predetermined limit. This limit might be either maximum drag area, maximum force, or total filling time. For values of m equal to or greater

than 1.0, the computer can work to these maximum values with no difficulty. However, if m is less than 1.0, then a basic problem arises. It is no longer possible to limit the computer to a maximum drag area since this value must be preselected due to the nature of the expression. As a result of this problem, a trial and error method must be employed.

Figure 36 shows a typical drag area-velocity-time diagram of a multiple stage recovery system. Generally known are such initial conditions as velocity, altitude and weight, and the same parameters for final conditions. Limiting factors are usually maximum parachute force (F_o) and, frequently, altitude and time.

Starting at time zero with a filling time from line stretch to the reefed condition, t_{f_1}, and an initial C_DS, the computer will determine the maximum allowable reefed stage drag area so that the permissible force limit will not be exceeded. On the opposite end, the drag area of the final parachute is known from the given conditions of weight and final rate of descent. The terminal velocity of the recovery parachute usually determines its maximum opening velocity based on parachute weight considerations. Minimum compartment volume will generally call for a minimum weight final recovery parachute (USD-5), whereas operational requirements such as recovery of the B-70 capsule may call for high operational speed of the main recovery parachute. This opening speed of the main recovery parachute then determines the size of the deceleration or first-stage parachute, which must be capable of decelerating the vehicle within reasonable time limits to the allowable opening velocity of the main recovery parachute. This can be easily accomplished in a computer analysis if the opening process, that is the drag area increase versus time, is known.

Attention has to be given in the computer analysis to such factors as:

(a) How to handle the force overshoot, the so-called X_o factor

(b) How to handle exponential and power factor type increases in drag area versus time

(c) How are apparent mass effects accounted for?

However, it should be realized that in each computer program, time, drag area, force and altitude vary and that at least two of these, generally time and drag area, have to be varied simultaneously. Therefore, one of these variables must be preselected in order to limit computer runs to reasonable numbers.

5.3 Drag Coefficient

Data on extended skirt parachutes are contained in Reference 4 and in a number of reports published by the USAF 6511th Test Group as AFFTC Technical Notes (References 7 and 8). Reference 4 quotes a drag coefficient spectrum (C_{D_o}) of 0.7 to 0.85 for the extended skirt parachute, with the high value representing small parachutes at low velocities and the low value representing large parachutes at high velocities. Figure 37 shows drag coefficient versus rate of descent, as tabulated in Figure 17, for the extended skirt parachutes used for the USD-5 and B-70 programs in comparison to published data. Considerably higher than published values of drag coefficients were obtained on both the B-70 and the USD-5 parachutes. Points 1 and 2 show the coefficients for the B-70 parachutes and Points 3 and 4 coefficients based on a cluster of two 78-foot diameter and 71-foot diameter USD-5 parachutes. No drag coefficient data were obtained on individual USD-5 parachutes; therefore, no comparison is possible between single parachutes and a cluster of two parachutes. However, there is reason to believe that the difference is probably smaller than the generally accepted 10% values. Drag coefficient data on several other extended skirt parachutes are plotted for comparison.

These rather good results are credited to proper aerodynamic design of the canopy and proper optimization of single parachutes in regard to suspension line and riser length when used in clusters. The high aerodynamic efficiency of the USD-5 parachutes results in a "specific drag area" of 61 square feet of drag area per pound of parachute weight; this is the best value obtained with a parachute now in operational use.

5.4 Stability

The stability of the single B-70 capsule system, as described in Paragraph 4.2.3, is within the limits discussed in the Parachute Handbook. The $\pm$ 5 degree or better stability of the cluster of two USD-5 parachutes is equal to or better than the stability achieved on clusters used for aerial delivery, and sufficient for use with airbag shock absorption systems.

5.5 Independent Deployment of a Cluster of Two Parachutes

The independent deployment of a cluster of two parachutes, as used on the USD-5 Drone, has proven reliable on all tests with the dummy drone, stripped drone, and the actual drone in operational flights; deployment has been reliable and extremely uniform in its individual operation. Film analysis, conducted on many drops with the final assembly, showed no more than a 0.1 second time difference in any phase of the two individual parachute deployments. However, it should be emphasized that this was obtained by a completely controlled and carefully designed deployment and parachute opening system that leaves no part of the parachute deployment procedure to chance, but controls each individual function by maintaining constant tension between the pilot chute and the parachute attachment point on the drone.

5.6 Parachute Opening Time

5.6.1 Method of Evaluation: Parachute opening times have been evaluated from time-coordinated motion picture films and from time-controlled Hulcher 70mm cameras. Practically all B-70 and USD-5 drops were evaluated using ground-to-air as well as air-to-air coverage for comparison. On USD-5 cluster drops, where the times could be determined with sufficient accuracy, filling times for both parachutes are given. Evaluating the time from line stretch to reefed inflation (t_{f_1}) on the 34.5-foot B-70 parachute was difficult due to the large possible variations caused by small time errors which are inherent in motion picture evaluation. Definitions used in the evaluations are shown in Figure 38.

All canopy filling times, reefed and unreefed, were then compared with the formula for filling time (5.1) and the n-factors determined. The evaluated filling times are plotted in Figure 39 for the B-70 tests and in Figure 40 for the USD-5 tests.

5.6.2 Discussion: The following comments on filling time can be made.

(a) The filling time (t_{f_1}) for the unreefed 38-foot diameter B-70 parachute, used in tests 1 through 12, varies uniformly between 1.18 and 1.53 seconds.

(b) The reefed filling time (t_{f_1}) of the 34.5- and 35.5-foot parachutes varies from 0.29 second to about 0.53 second. It was found that no significant difference in filling times was observed in tests conducted at low altitudes (2,000 feet) and high altitudes (15,000 feet).

(c) Disreefing times (t_{f_2}) vary from about 0.8 second to about 1.17 seconds.

It appears that the large pilot chute has a definite influence on filling time.

(d) Disreefing times for the USD-5 vary from about 5.19 seconds to 6.8 seconds.

5.6.3 Determination of n-Factor: Figures 41 and 42 show the n-factors determined from formula 5.1. The n-factor for unreefed parachutes was obtained only with the 34.5-foot diameter parachute; no drops were made with unreefed 78-foot diameter parachutes. A considerable amount of data on n-factors for reefed opening was accumulated due to the fact that diameters were known and velocity at start of filling could be determined with negligible

error from the drop speed and the known drag area of the test vehicle. Only a limited number of n-factors for disreefing could be determined because the velocity at the start of disreefing has to be known for this evaluation. These velocities could be obtained only on drops where full photo-theodolite coverage was obtained.

The data are therefore limited to drops numbered 12, 13, 19 and 45 for the large USD-5 parachutes, and drops 17, 29, 33, 51 and 54 on the smaller 34.5-foot diameter B-70 parachutes. On the nine drops made with unreefed 38-foot diameter parachutes, as shown in Figure 41, an average n-factor of approximately 4.8 was obtained.

Considerable effort was spent in obtaining parachute filling times with good accuracy. This was necessary for determining the n-factor for parachute opening from line stretch to reefed opening due to the short times obtained for the small B-70 as well as the large USD-5 parachutes. Figure 41 shows that the n-factor for inflation into the reefed condition for the 34.5-foot diameter B-70 parachute is reasonably constant, between 15 and 20, in the velocity range of approximately 400 to 650 fps. The n-factor at disreefing is approximately 7 for the large USD-5 parachutes and approximately 4 for the smaller B-70 parachutes.

The following tentative analysis is made of data contained in Figures 41 and 42. The n-factor for a parachute opening from the reefed condition can probably be considered reasonably similar to the n-factor for a parachute opening without reefing. This is based on the fact that the drag area of the reefed parachute is small for both B-70 and USD-5 parachutes, being between 2.5 and 3.5% of the fully opened parachute. This is shown quite well in Figure 41 where the n-factor for unreefed and disreefing parachutes has roughly the same value. The n-factor for the large 78-foot and 71-foot diameter parachutes is approximately 7. However, data from only six tests are available. This larger factor of 7 as compared to 4.8 on the 34.5-foot parachute could be caused by the slight difference in canopy shape, or by the fact that larger parachutes have a proportionately longer filling time. Exact data, however, cannot be derived from such a limited number of tests. The n-value for parachute opening into the reefed condition increases with velocity.

The possibility exists that extended skirt parachute filling time increases at higher speeds. However, it is more likely that this increase is caused by the large pilot chute, which definitely controls opening into the reefed stage, thereby causing the high n-values, of approximately 15 to 20, obtained on the B-70 parachute at 400 fps. No tests were made with reefed parachutes at low speeds; therefore, no data are available on n-factors at low speeds.

Three drops, two with 34.5-foot parachutes and one with a 78-foot parachute, were conducted at 15,000 feet altitudes. In no case was a change in opening time noticeable.

5.6.4 Filling Time Summary: The following equations can now be written for filling times of extended skirt parachutes, using definitions outlined in Figure 38.

(a) Full fill time, t_f (unreefed parachute)

The general formula, 5.1, remains unchanged.

$$t_f = \frac{n \cdot D_o}{V_s \cdot 9}$$

with n-values ranging from 4.0 to 7.0 to be selected from Figures 41 and 42.

(b) Reefed fill time, t_{f_1}

$$t_{f_1} = \frac{n \cdot D_o}{V_{s_1} \cdot 9} \cdot \left(\frac{(C_D \cdot S)_R}{(C_D \cdot S)_o} \right)^{\frac{1}{2}} \qquad 5.2$$

n-values have to be selected from Figures 41 and 42 in a range from 7.0 to approximately 20, dependent on velocity at line stretch, V_{s_1}, and parachute diameter, D_o.

(c) Disreef fill time, t_{f_2}

$$t_{f_2} = \frac{n \cdot D_o}{V_{s_2} \cdot 9} \cdot \left(\frac{(C_D \cdot S)_o - (C_D \cdot S)_R}{(C_D \cdot S)_o} \right)^{\frac{1}{2}} \qquad 5.3$$

n-values are again selected from Figures 41 and 42, dependent on velocity at start of disreef, V_{s_2}, and parachute diameter, D_o. These n-values are similar to values obtained for unreefed parachutes.

No attempt was made within the scope of this project to find a different formulation for filling time than given in Reference 4. However, it appears that this might be well worthwhile to investigate in any future projects of a similar nature.

5.7 Drag Area versus Time

The available data on drag area increase versus time can be divided logically into the following four categories: (1) open unreefed, (2) line stretch to reefed open, (3) reefed open, and (4) disreef to full open. These four areas will be discussed separately.

5.7.1 Unreefed Opening: A sufficient number of tests were conducted with unreefed B-70 parachutes; however, only partial instrumentation in the form of ground-to-air and air-to-air motion picture coverage, but no force data or photo-theodolite trajectory data were obtained. This was sufficient to obtain filling times, but no drag area versus time data could be evaluated. No unreefed parachute drops were performed in the USD-5 program.

5.7.2 Drag Area Increase to Reefed Inflation: Good data for evaluation of drag area increase versus time, consisting of force, velocity and event photography, were obtained on a number of USD-5 drops. Data obtained with the B-70 parachutes were unsuitable for drag area versus time evaluation due to the great fluctuation of parachute force during the short opening times encountered. Filling times were obtained for both programs. Typical plots of drag area versus time for the USD-5 parachutes are shown in Figure 43. Start of inflation was taken at the time when the drag area was 20 ft^2, and all times are determined from this point which is assumed to be full line stretch.

From Figure 43 it can be seen that the trend is for the rate of drag area growth to decrease with time. For the general case, an expression can be developed for drag area growth with respect to time. A graphical analysis of the data revealed the type of function which best described the opening process. If two related variables, plotted on logarithmic coordinates, appear as a straight line, the relation is a power function of the form

$$y = ax^m$$

If an exponential function of the form

$$y = a^{mx}$$

is plotted on semi-logarithmic coordinates, it too will plot as a straight line. The drag area increase was found to be a power function of time. The power m, is the slope of the logarithmic plot. Referring to Figure 44, the expression for drag area increase versus time becomes:

$$(C_D S)_{x_1} = (C_D S)_R \, (t_{x_1}/t_{f_1})^{m_1} \qquad 5.4$$

where

$(C_D S)_{x_1}$ = drag area at time, t_{x_1}, ft^2

$(C_D S)_R$ = drag area at fully open reefed condition, ft^2

t_{x_1} = time from line stretch, seconds

t_{f_1} = time to reefed full open, seconds

m_1 = exponent for reefed opening determined by shape of curve.

The shape of the curve, however, indicates that m_1 will be less than one and a preliminary analysis has established an m value of 0.5 to .52.

It should be noted that no force overshoot ($x_o = 1.0$) was experienced on any tests for parachute opening into the reefed condition. (See Figures 43 and 46.)

5.7.3 Reefed Drag Area: Plots of drag area versus time through the reefed period for the B-70 and the USD-5 tests are presented in Figures 45 and 46. An examination of these figures reveals that reasonably consistent results were obtained. This is particularly true in the case of the USD-5 Drone (see Figure 46) where drag areas in the reefed condition remained essentially constant at a value of approximately 100 ft^2.

5.7.4 Drag Area Increase from Disreef to Full Open: Plots of drag area increase versus time, after parachute disreef, are shown in Figures 47 and 48. Times are from the start of disreefing. All curves have the same general shape showing a steadily increasing rate of growth. A similar system of defining power function or exponential function for drag area increase versus time was used, as described in paragraph 5.7.2. The m-factor again was found to be a power function, but in this case was greater than one. This is exactly the opposite of the drag area growth characteristics of reefed opening. From Figure 44 the drag area growth with respect to time can be expressed as

$$(C_DS)_{x_2} = (C_DS)_R + \left[(C_DS)_o - (C_DS)_R\right] \cdot (t_{x_2}/t_{f_2})^{m_2} \qquad 5.5$$

where

$(C_DS)_{x_2}$ = drag area at time, t_{x_2}, ft^2

$(C_DS)_o$ = drag area at full open condition, ft^2

t_{x_2} = time from disreef, seconds

m_2 = exponent for disreefing determined by shape of curve.

The shape of the drag area curves (Figures 47 and 48) indicates that the value of the exponent, m_2, must be greater than one and from a preliminary analysis, a value on the order of 3 to 4 has been established. A considerable overshoot in drag area, compared to the steady-state drag, occurred on the B-70 parachutes after disreefing. A lower overshoot after disreefing was experienced on the USD-5 parachute. A more detailed discussion is contained in the computer analysis section.

5.7.5 Discussion: From the preceding analysis of parachute drag area variation versus time, the following general conclusions can be made:

(a) The growth of drag area to the reefed condition is not linear, but is a power function with an exponent less than one.

(b) There appears to be no overshoot in drag area when opening into the reefed condition.

(c) Perfect canopy stability was obtained in the reefed condition.

(d) The growth in drag area after disreef is similar to an unreefed parachute and, again, a power function can be applied. The power value determined from test data is greater than one.

(e) Drag area overshoot after disreefing has been neglected since the maximum force point occurs considerably before maximum canopy area has been reached. If necessary, normal overshoot could be programmed into the computer. In this study, drag area increase was halted at the point of full inflation due to the fact that it did not change the maximum force encountered.

(f) It has to be realized that the drag area obtained in this analysis is not drag area in the true classical sense. It actually constitutes the product of instantaneous force divided by instantaneous dynamic pressure and, therefore, includes such effects as influence of apparent mass and other factors influencing the opening process of the parachute. However, as long as these factors are consistent, any computer analysis will be correct in calling this product "instantaneous drag area".

(g) The increase of drag area versus time for an unreefed solid material parachute can be assumed to be similar to the drag area increase after disreefing. The form of drag area increase from line stretch to reefed opening is probably caused by the restriction in opening introduced by reefing which slows the opening rate at fully reefed open to zero in a rather smooth fashion.

5.8 Drag Area Ratios

The coordinated force-velocity-time data obtained on several B-70 and USD-5 parachute tests allowed an evaluation of drag area ratio versus reefing line lengths. Reference 4, Figure 4-5-9, shows drag area ratio versus reefing line diameter ratio. These data are obsolete and have been replaced by results obtained in numerous tests conducted by the 6511th Test Group, and published in summary form by T. W. Knacke in his Purdue Parachute Technology lecture in 1956.

The 6511th Test Group conducted, as part of the USD-5 test program, tow tests behind a C-130 aircraft with a 13.4-foot diameter ribbon

deceleration parachute reefed in various stages. The results of these tests are plotted in Figure 49, together with the U.S. Air Force Parachute Handbook data and the data published in Purdue in 1956. The data obtained in the C-130 tow tests agree extremely well with the summary data published by T. W. Knacke.

Figure 50 shows data evaluated from USD-5 and B-70 tests. These data are lower than ribbon parachute data and confirm the assumption that a considerable difference exists between drag area versus reefing line ratios of ribbon parachutes and extended skirt parachutes. Figure 49 contains a proposed curve for extended skirt parachutes which includes data obtained in this program as well as data obtained on solid flat parachutes in the late 1940's at Wright Air Development Center. Until better data become available, it is assumed that these data may be applicable for all flat or conical solid material parachutes.

6.0 COMPUTER ANALYSIS

6.1 Purpose

The calculation of the time-velocity-altitude-force history of an opening parachute is a complex procedure, especially if multiple step parachute systems and vehicle wake and dynamics on parachute opening has to be considered. Close solutions appear possible for parachutes that open unrestrained without reefing; however, it is uncertain if a close solution can be found for multiple step opening parachute assemblies. Manual calculations of the opening process generally result in time-consuming methods and frequent numerous attempts must be made in order to satisfy all of the recovery system requirements. It has long been felt that a problem of this nature would lend itself well to the utilization of modern high-speed computers. Several factors favor the computer approach:

(a) Greater accuracy

(b) The ability to consider many variables simultaneously

(c) Versatility

(d) Economy

In this study, an attempt was made to utilize parametric data obtained in the B-70 and the USD-5 analysis for the purpose of evolving a system suitable for use in the IBM-1620 computer available to Space Recovery Systems, at Vidya Corporation in Palo Alto, California. The obtained data were then compared with actual test data.

6.2 General Approach

The computer will generally determine from a set of given conditions, that means from the start of recovery, the velocity-altitude-force history with time serving as the independent variable. Starting conditions are generally altitude, horizontal and vertical velocity, and the initial weight. End conditions are normally landing altitude, landing weight, and desired rate of descent at landing. Limiting factors that are frequently introduced are: allowable parachute opening force, minimum altitude and minimum time. Any computer analysis of this type automatically introduces a discussion of drag area change versus time. In fact, the computer does not recognize the problem as one of parachute recovery, but only as an aerodynamic problem where drag area changes versus time in a certain predetermined pattern or a pattern to be determined by the computer. The various steps may be automatically selected by the computer based on maximum allowable parachute force as a

product of instantaneous drag area versus instantaneous dynamic pressure, or the computer may proceed with preselected times and preselected drag areas. In discussing drag area change versus time for opening parachutes, it is recognized that optimum conditions would be obtained by a drag area increase versus time, that results in a constant decelerating force. The mechanism of this system is generally referred to in parachute work as continuous disreefing. However, no such system has been developed at this time that is sufficiently reliable for operational use. Only parachute systems that open in steps, therefore, are considered in the computer study. The general system and definitions used are shown in Figures 36, 38 and 44.

6.3 Computer Procedure

6.3.1 General: Only the procedure for a single parachute, opening in two steps (single disreefing), will be discussed in this analysis. Multiple parachute systems are only an extension and repeat of the investigated procedure. It will be further assumed that the types of parachutes used, the number of parachutes in the system, and the types of reefing steps are generally preselected. In addition to this, the size of the final parachute is determined from the given requirements. A typical computer computation procedure will be discussed in the following paragraphs.

6.3.2 Reefed Opening: In order to utilize the computer fully, it is advantageous to feed in filling time and drag area in equation form given in Paragraphs 5.6 and 5.7. In the formula for filling time, (5.2),

$$t_f = \frac{n}{V_o \cdot 9} \qquad D_o \cdot \left(\frac{(C_D S)_R}{(C_D S)_o} \right) \qquad \frac{1}{2}$$

the bracketed expression times D_o is the referenced diameter of the reefed parachute and n is a value to be selected from Figure 41 or 42. Using the expression for drag area increase versus time, (5.4),

$$(C_D \cdot S)_{x_1} = (C_D \cdot S)_R \cdot (t_{x_1} / t_{f_1})^{m_1}$$

with m_1 equal to .5 to .52 introduces an interdependency between time and drag area that the computer cannot solve. When m is less than 1.0, the value of $(C_D S)_{x_1}$ approaches the preselected maximum value asymptotically. Thus, either the maximum value will be reached too soon, or it will never be reached. The drag area of the reefed parachute, therefore, has to be preselected with reasonable accuracy. The following two methods appear practical:

(a) Knowing maximum allowable parachute force, the parachute drag area in the reefed state can be obtained from the relation, $F_o = (C_D \cdot S)_R \cdot q \cdot x_o \cdot x_1$ where $(C_D S)_R$ is the allowable drag area of the

reefed parachute. The opening shock factor, x_o, has been found from previous evaluations in Paragraph 5.7, to be equal to 1.0 for reefed parachutes. x_1 can be determined with reasonable accuracy from the fact that the canopy loading $W/(C_D.S)_R$ for reefed main recovery parachutes generally varies from 20 lbs/sq ft to about 50 lbs/sq ft. Calculations show that this will result in an x_1 factor of approximately 0.7 to 0.9 (see paragraph 5.1). With this, a preliminary $(C_D.S)_R$ and t_{f_1} can be determined. The equations for t_{f_1} (5.2), as well as the drag area increase versus time equation (5.4), can now be fed into the computer. The computer will proceed along preselected time steps and will stop as soon as maximum parachute force is reached. If the drag area at this point varies from the drag area selected in the preliminary analysis, a correction has to be made, and the computer run has to be repeated so as to arrive at the proper value in the second or third run.

(b) Another simple approach uses the following method: It is assumed that the parachute will open reefed with a linear increase of $(C_D.S)_{x_1}$ versus time. Now the total filling time of the parachute, t_f, can be calculated from the known diameter D_o, and the known opening velocity. In this case, the computer will easily accommodate the formula, the only change being that the power factor, m, for the drag area increase versus time formula is equal to 1.0. Using this approach, it was found that the parachute force is about 25% too high, resulting in a drag area for the reefed parachute that is about 25% too low. Applying a corrected drag area value and using the equated approach will now give the right value. The result obtained from the linear solution for opening into the reefed stage could be used as a conservative approach, since it will always be on the safe side as far as parachute forces are concerned.

6.3.3 Reefed Drag Area: Once the reefed drag area has been obtained, based on the allowable maximum force, the computer will continue to advance at predetermined time increments either up to a previously selected time, or until terminal velocity is approached. It was found from experience that certain factors generally determine length of reefing time. Qualified reefing line cutters are available only in even seconds of 1, 2, 3, 4, 6, 8 and so on. In addition, waiting until the reefed parachute has reached terminal velocity generally results in unnecessary loss in time and altitude. It was found that starting disreefing at approximately 125% of terminal velocity in the reefed condition results in a practical solution.

6.3.4 Disreef to Full Open: At the point of disreef, the computer will program according to equation 5.3. A value for m must be selected from Figures 41 or 42. A preliminary value of 5 to 6 is recommended. Now the computer can continue to calculate the velocity decay until the maximum force and final rate of descent are reached. If the maximum force remains within the allowable limits, then no further problem exists. The point of maximum parachute force during final disreefing for recovery parachutes

generally occurs long before the parachute is fully opened. If, however, maximum force, F_o, is exceeded, it is necessary to return to the point of disreefing. If, at this time, the velocity is still above terminal, it might be advantageous to extend the reefed time. This will result in a further decrease in velocity before the start of final inflation. In the event that extending the reefed time does not sufficiently reduce the opening force, the only alternative would be to add a second stage of reefing or to increase the allowable maximum parachute force.

6.4 Result of Computer Calculations

Check runs were made in an attempt to match actual drop test data. Since force was for both the USD-5 as well as B-70, the ultimate design criteria, the obviously logical step was a comparison between computer and actual measured forces using the same starting and end conditions. Figures 51, 52 and 53 are profiles of computer data with experimental data superimposed. It can be seen that a rather good agreement exists between the experimental and computed force values. Quite a number of trajectories were calculated which all showed good agreement, generally considerably better than 10%.

6.5 Summary

The computer calculations show a good agreement with the actual test values, generally within or better than 10%. It has to be realized that the present evaluation is limited to extended skirt parachutes. The evaluated data may not cover a wide enough range to apply for solid material recovery parachutes in general, with the same accuracy as obtained in the presented sample calculations. What appears the most important conclusion is the fact that a computer analysis was possible using an equated approach for the step-wise parachute opening process that resulted in surprisingly good agreements between test data and computer data.

7.0 HANDBOOK COMPARISON

The following comparisons can be made with data contained in Reference 4: WADC TR-55-265, United States Air Force Parachute Handbook.

(a) Drag Coefficient of Extended Skirt Parachutes

Figures 17 and 37, as discussed in paragraph 5.3 of this report, show the drag coefficients obtained with single 34.5-foot diameter and 35.5-foot diameter, 10% extended skirt parachutes, and with single 71-foot diameter and a cluster of two 78-foot diameter conical fully extended skirt parachutes. The values obtained fall in the upper range of drag coefficient values given in Reference 4, page 2-1-20, and agree well with data published in References 7 and 8. For properly designed extended skirt parachutes, it is recommended to use a design drag coefficient (C_{D_o}) of .85 for small diameter parachutes at a rate of descent of approximately 20.0 fps, and a drag coefficient (C_{D_o}) of .75 to .8 for large parachutes descending at a rate of 25 fps.

(b) Filling Time

Reference 4, page 4-2-3, gives a generalized formula for parachute filling time. Equations 5.1, 5.2 and 5.3, and Figures 39 and 40 of this report show that the filling time of unreefed extended skirt parachutes, the reefed fill time, and the disreefed fill time will vary, based on velocity and parachute diameter. The n-factor, in Formula 5.1, given in Reference 4 as 8, will vary from 4 for large diameter parachutes opened at low speeds to 20 for reefed parachutes with small drag areas opened at high speeds (see Figures 41 and 42). It can be reasoned that a similar qualitative, and probably quantitative, trend can be assumed for solid flat and for solid conical parachutes.

(c) Drag Area Increase Versus Time

Reference 4 does not specifically deal with drag area increase versus time; however, it is known that drag area of ribbon parachutes increases approximately linearly with time. The drag area increase for extended skirt parachutes as evaluated from tests is shown in Figures 43 and 48, and analyzed in equations 5.4 and 5.5. The data show a convex type drag area increase from line stretch to reefed opening with a power factor of approximately .5, and a concave type drag area increase from disreef to fully open with a power factor of approximately 3 to 4.

(d) Drag Area Ratio Versus Reefing Line Ratio for Ribbon Parachutes

Data for the ribbon deceleration parachute of the USD-5 drone, as plotted in Figure 49, differ from those published in Reference 4, page 4-5-5, Figure 4-5-9. The data on the USD-5 ribbon deceleration parachute agree very well with the data obtained in numerous tests by the USAF 6511th Test Group at El Centro.

(e) Drag Area Ratio Versus Reefing Line Ratio for Extended Skirt Parachutes

The evaluated data show a distinct difference from the ribbon parachute data and the data contained in Reference 4. The ratios given in Figure 49 for extended skirt parachutes are accurate within the limited number of evaluated tests, but appear useful also for solid flat and solid conical parachutes until better data become available.

8.0 CONCLUSIONS

8.1 Final recovery parachutes presently used in missile and spacecraft systems are generally in the 200 to 250-knot deployment velocity range with drag area-to-weight ratios of 40 to 50 ft^2 per pound of parachute weight. This performance can be improved at the same velocity range to about 60 ft^2 of drag area per pound of parachute weight, or, at the same drag area-per-pound ratio to approximately 350 to 400 knots by using the following advanced design principles:

(a) Optimization of aerodynamic canopy design

(b) Optimization of construction

(c) Controlled deployment and parachute opening

8.2 Performance calculations of advanced recovery systems are quite complex if multiple stage parachute assemblies and vehicles with changing aerodynamic configurations have to be considered. The latter may include oscillating vehicles or vehicles changing from 0 to 90 degrees attitude with a resultant large change in drag area affecting trajectory velocity during a parachute opening. Performing these calculations by computers appears to be a logical solution considering the fact that closed solutions for parachute opening cannot account for staged parachute opening or changes in vehicle drag. It is, therefore, necessary to obtain parameters that are suitable for computer use. This includes clearly defined opening times obtained empirically and put into analytical form and drag area increases versus time during staged parachute opening.

8.3 The analysis of two test programs, conducted with the USD-5 Drone parachute recovery system and the B-70 encapsulated seat parachute system, shows that data useful for parametric analysis can be obtained from operational projects despite the fact that emphasis in these tests is generally on meeting performance requirements and tests schedules rather than on obtaining data. Data to be obtained should include trajectory velocities measured by phototheodolite or radar, forces obtained by strain gage telemetry, event coverage obtained by ground-to-air and air-to-air photography, and, quite important, accurate time coordination between velocity, force, and photo coverage.

8.4 Parachutes in a controlled deployment and opening system behave more regularly with regard to filling time and drag area increase versus time than is usually possible.

8.5 Filling times, as established in the Parachute Handbook, do not apply to extended skirt parachutes and n-values in Formula 5.1 for reefed opening, full opening and disreefing are not the same. Opening time n-factor in-

creases with velocity due to either higher velocity, or due to the influence of permanently attached pilot chute. Drag area increase versus time (m-factor) occurs with approximately 0.5 power for reefed opening and approximately 3.0 power for disreefing or opening without reefing.

8.6 Using the parametric data obtained in this report shows that within the limits of this investigation velocity-force-time data of closer than 10% compared with actually measured data can be obtained in computer analysis. This is a highly important fact and much better than previously expected.

8.7 There is good reason to assume that data obtained in this study with extended skirt parachutes may be useful for other types of solid material parachutes.

8.8 A relationship was established between drag area ratio and reefing line ratio for extended skirt parachutes which are different from data published for ribbon parachutes. It can be assumed that these data may be usable for other types of solid material parachutes until data on those parachutes become available.

8.9 No decrease in filling time could be observed in drops conducted at 15,000 feet altitude as compared with drops at 2,000 feet altitude.

APPENDIX I

DERIVATION OF PARACHUTE DISPLACEMENT ANGLE VERSUS TIME (STABILITY) ANALYSIS

This method was devised to analyze stability for the Recovery Parachute System of the B-70 Air Vehicle, Encapsulated Seat, from a single set of photographs. This was necessary because of the lack of Askania stability data. It will be found on investigating the method outlined in this report that a valid analysis can be made from a set of photographs viewing the parachute from one point, providing the distance from the camera to point of impact is known.

Two sets of measurements are taken from the photographs. First, the angle of oscillation is measured in the plane of the photograph with a protractor and denoted by θ. Second, the ratio of the minor and major axes is determined by measuring the observed ellipse to establish oscillation perpendicular to the plane of the photograph. This true angle of oscillation in the plane of the photograph is noted as B_1 on the sketch. When corrected to give an angle from a true vertical (or a projection of B_1 in a vertical plane through the line sight), it is denoted as $\emptyset$.

As rate of descent was always calculated from the weighted store, no correction was made for the distance from the store to the parachute skirt line. As this correction is proportional to the altitude analyzed, the error introduced only becomes apparent near impact.

It was determined by differential technique that a 5% error in all measurements resulted in a total error of 2.5% in the final form.

The remaining part of the process of analysis is presented following the diagram of the method of analysis.

The graphs are presented in the following manner. The center point of the graph represents the apex of the recovery parachute as a fixed point. The motions of the load beneath the parachute are plotted at approximately 0.45 second intervals. The points are then connected by a line which represents the path traveled by the weighted store attached to the suspension lines. As the photographs used were taken for rate of descent test, only the last 200 feet before impact can be analyzed.

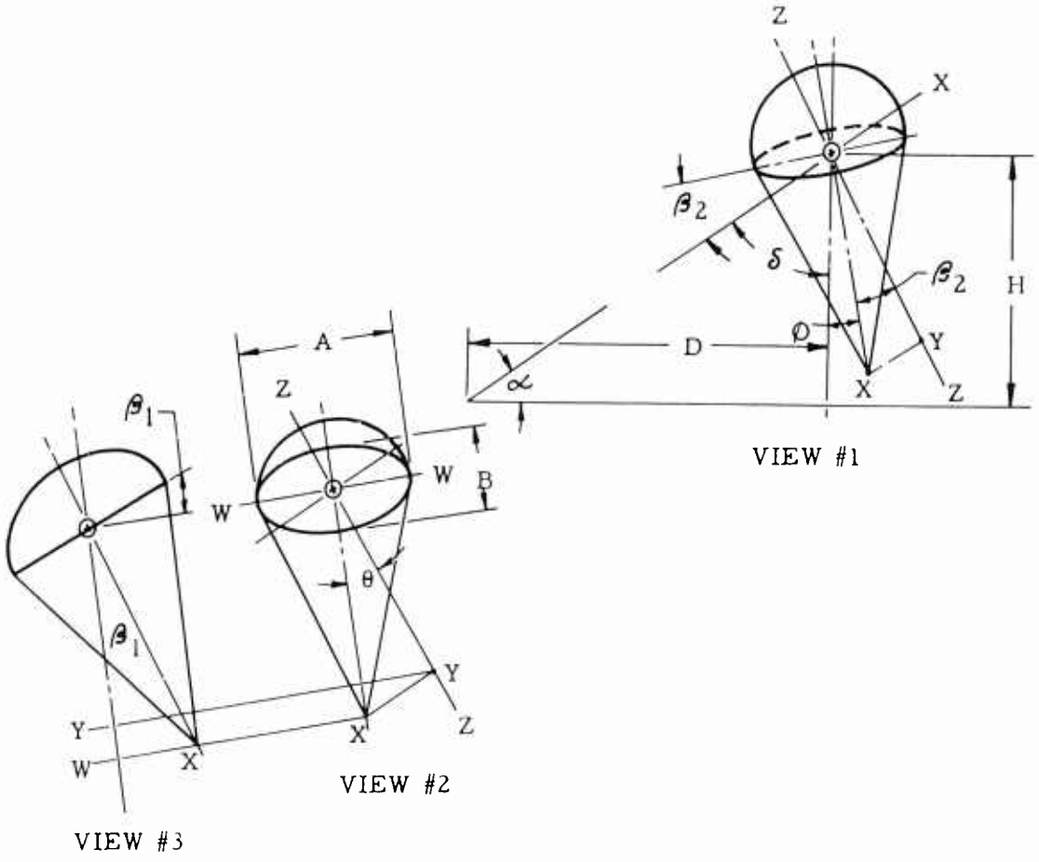

VIEW #1 Side view showing true view of α

VIEW #2 View represents photograph, and projection along line of sight X-X from View #1.

VIEW #3 Projection from View #2 along axis W-W to show true of $\beta_1 = \sin^{-1} \frac{B}{A}$.

Angle ϕ desired, angle of oscillation that is perpendicular to the plane of the photograph. If ϕ, α, and β_2 are positive as shown,

$$\phi = 90^\circ - \delta - \beta_2$$

$$= 180^\circ - 90^\circ - \alpha^\circ = 90^\circ - \alpha$$

$$\phi = 90^\circ - (90^\circ - \alpha) - \beta_2 = \alpha - \beta_2$$

Since Tan $\alpha = \frac{H}{D}$

$$\phi = \text{Tan}^{-1} \frac{H}{D} - \beta_2$$

Let the subscript indicate the view so that XY_1 is the length from X to Y in View #1, OX_3 is the length from X to Y in View #3, etc.

$$\text{Tan}\beta_2 = \frac{XY_1}{OY_1}$$

$$\text{Tan}\beta_1 = \frac{WX_3}{OW_3}$$

But $XY_1 = WX_3$ and $OW_3 = OX_2$ from projections

$$OX_2 \text{Tan}\beta_1 = OY_1 \text{ Tan}\beta_2 = WX_3 = XY_1$$

$$\text{Tan}\beta_2 = \frac{OX_2}{OY_1} \text{ Tan}\beta_1$$

But $OX_2 = \frac{OY_2}{\text{Cos }\Theta}$, from View #2, so that

$$\text{Tan}\beta_2 = \frac{OY_2}{\text{Cos }\Theta} \quad \frac{\text{Tan}\beta_1}{OY_1}$$

But $OY_1 = OY_2$ from projection so

$$\text{Tan}\beta_2 = \frac{\text{Tan}\beta_1}{\text{Cos }\Theta}, \text{ and}$$

$$\phi = \text{Tan}^{-1}\frac{H}{D} - \text{Tan}^{-1} \quad \frac{\text{Tan}\beta_1}{\text{Cos }\Theta}$$

$$= \text{Tan}^{-1}\frac{H}{D} - \text{Tan}^{-1} \quad \frac{\text{Tan Sin}^{-1}\frac{B}{A}}{\text{Cos }\Theta}$$

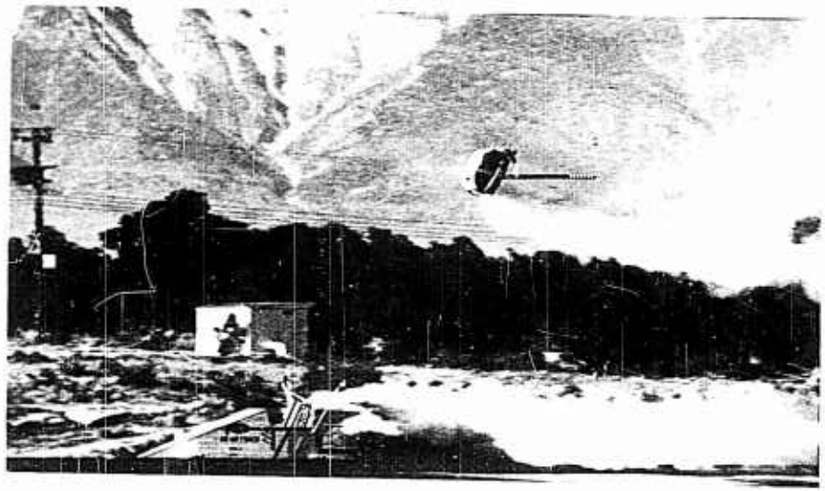

FIGURE 1

SLED TEST OF THE B 70
ENCAPSULATED SEAT PRCHT ASSY

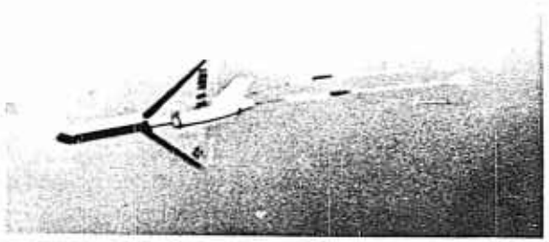

(1) PILOT CHUTES DEPLOY EXTRACTOR PARACHUTES

(2) EXTRACTOR PARACHUTES INFLATED

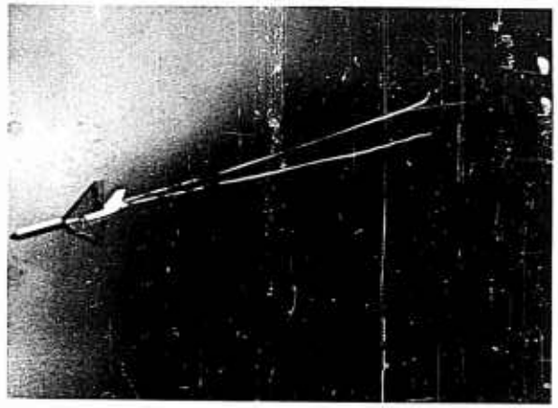

(3) EXTRACTOR PARACHUTES DEPLOY REEFED RECOVERY PARACHUTES

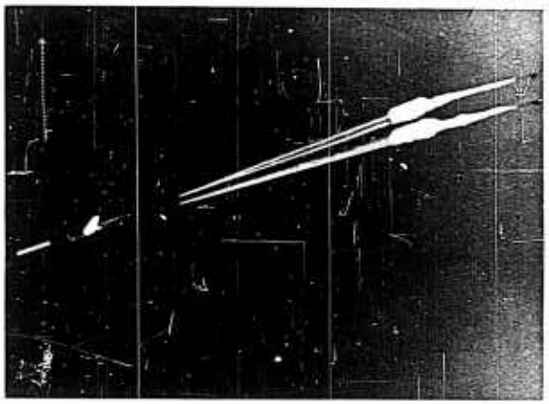

(4) REEFED INFLATION OF RECOVERY PARACHUTES BEGINS

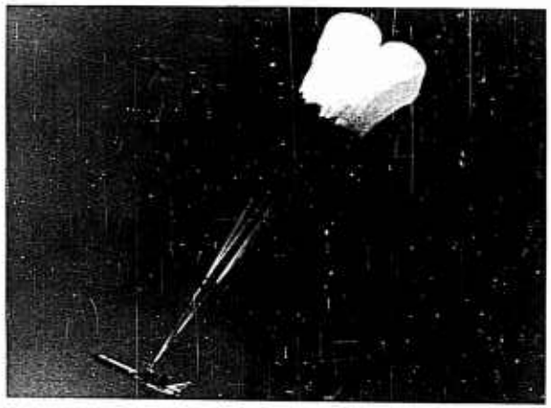

(5) RECOVERY PARACHUTES DISREEFING

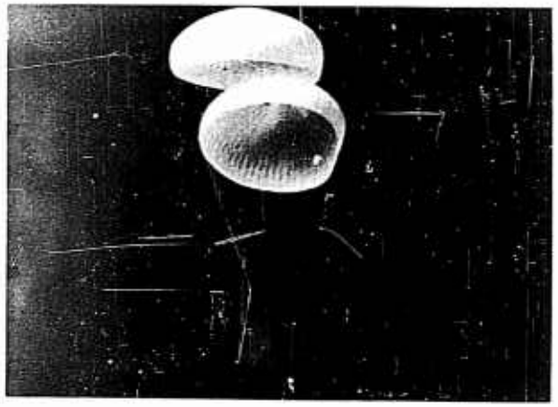

(6) RECOVERY PARACHUTES FULLY INFLATED

FIGURE 2

DEPLOYMENT OF THE USD-5 DRONE PARACHUTE ASSEMBLY

Parachute Type	Application	W Recovery Weight (lbs)	Parachutes		Parachute Performance		F Maximum Parachute Force (lbs)	W_p Parachute Weight (lbs)	C_{D_o} Drag Coefficient	$(C_D S)_o$ Parachute Drag Area (ft^2)	$(C_D S)_o / W_p$ Specific Drag Area (ft^2/lb)
			D_o (ft)	V_{eo} (fps)	IAS (knots)	Altitude (ft)					
Solid Flat (G11A)	Aerial Delivery	3,000	100	23	≥ 150	2,000	-	215	0.66	5,200	25.2
10% Ext. Skirt (T10)	Army Troop	200	34.9	16.0	≥ 150	2,000	-	13.75	0.69	620	47.9
Fully Ext. Skirt	Q2-B Drone	1,800	67.5	22.5	275	15,000	-	62	0.85	3,050	49.2
Solid Conical (Cluster of Three) *	Missile	10,000	100	22	260	2,500	23,000	168 (ea.)	0.74 (Cluster)	5,800 (ea.)	34.5
Ring Sail **	Mercury Capsule	2,300	63.1	26	150	10,000	10,000	55.4	0.75	2,350	42.5
Ext. Skirt	B-70 Encapsulated Seat	710	34.5	28	377	15,000	8,800	18.5	0.80	750	40.5
Ext. Skirt (Cluster of two)	USD-5 Drone	4,800	78	22.3	225	2,500	15,000	64.5 (ea.)	0.825 (Cluster)	3,940	61.0

* See Reference 2
** See Reference 3

Figure 3 Comparison of Final Recovery Parachutes

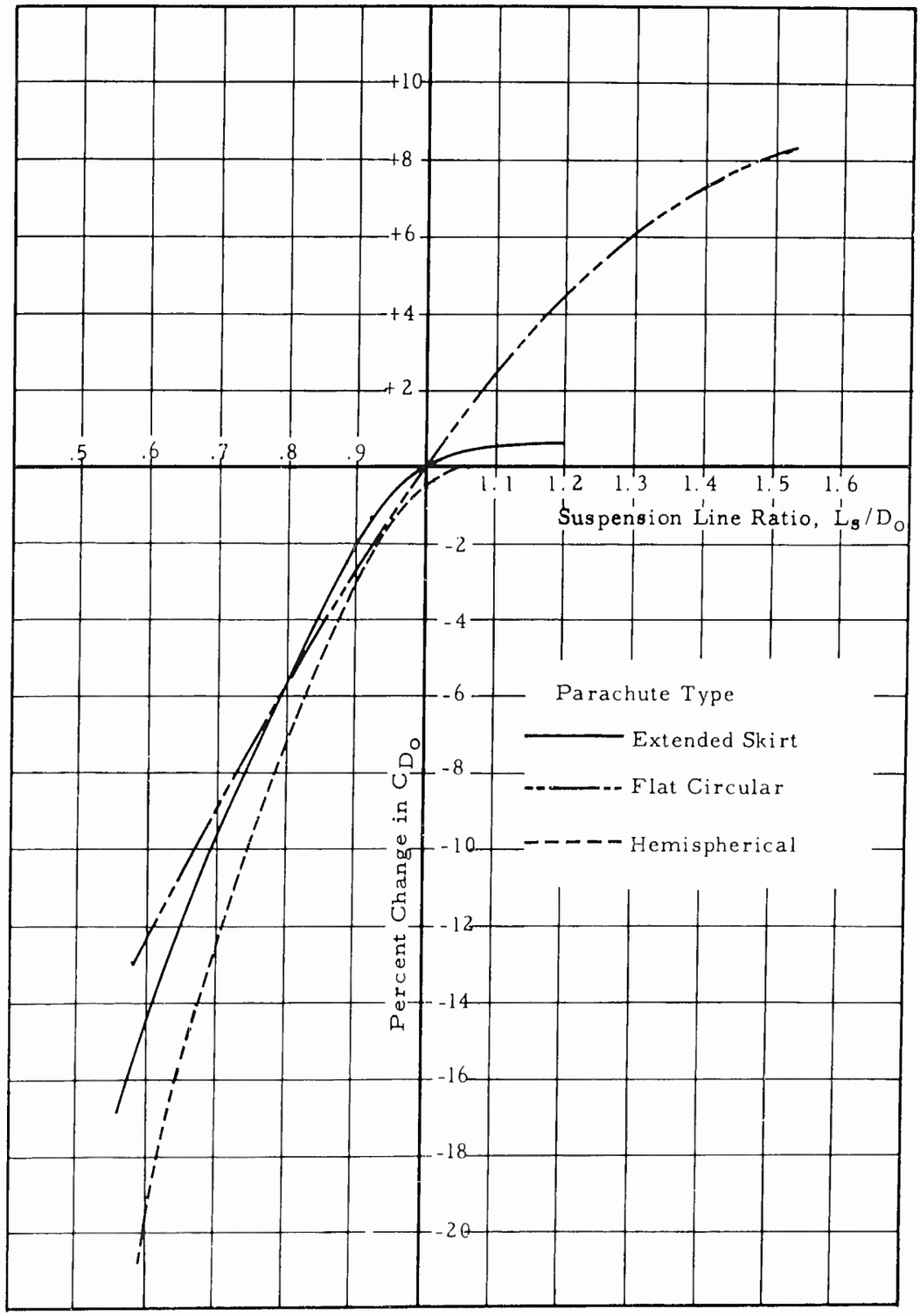

Figure 4 Change in Drag Coefficient C_{D_o} Vs. Ratio of Suspension Line Length to Nominal Diameter

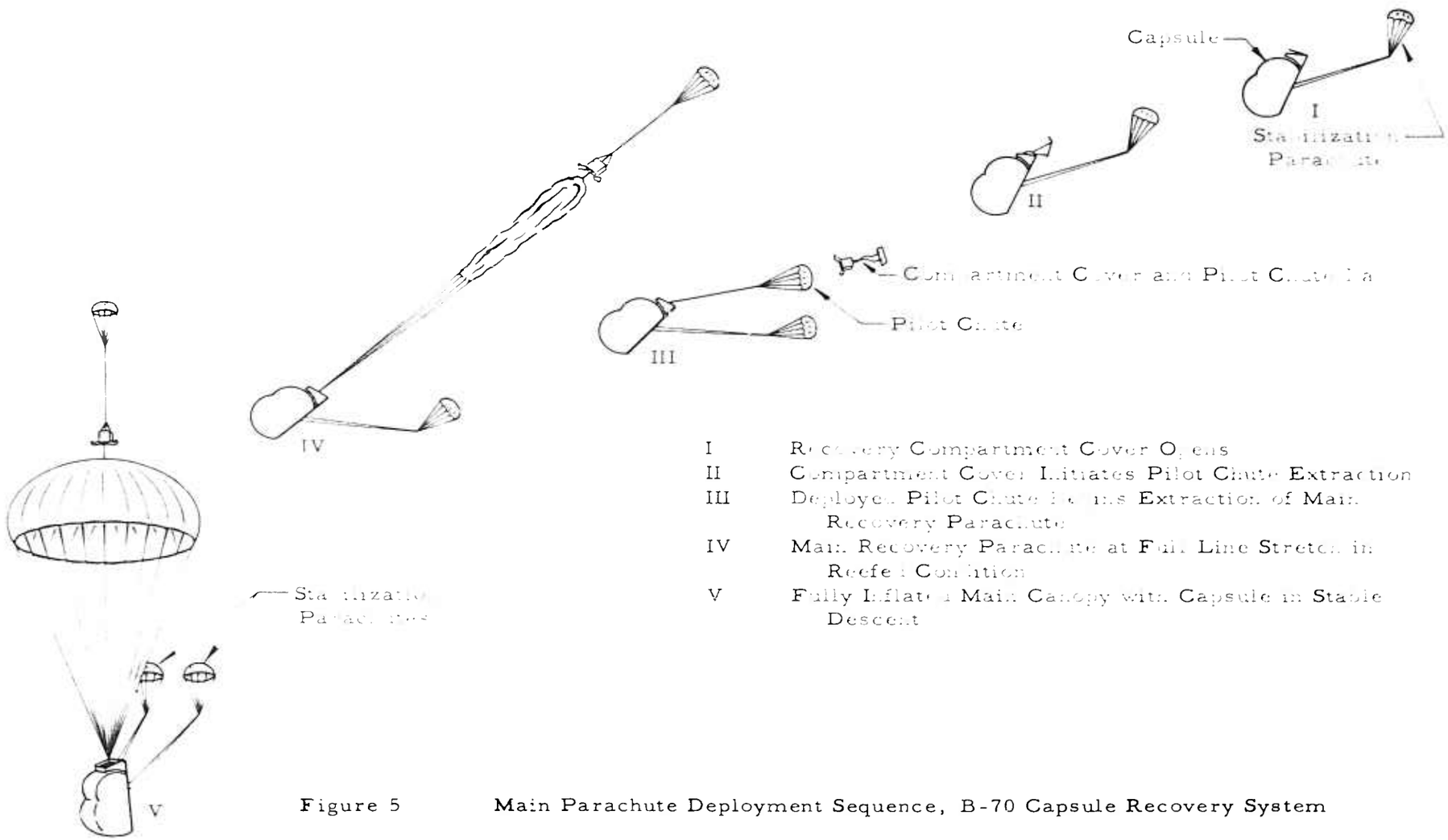

I Recovery Compartment Cover Opens
II Compartment Cover Initiates Pilot Chute Extraction
III Deployed Pilot Chute Initiates Extraction of Main Recovery Parachute
IV Main Recovery Parachute at Full Line Stretch in Reefed Condition
V Fully Inflated Main Canopy with Capsule in Stable Descent

Figure 5 Main Parachute Deployment Sequence, B-70 Capsule Recovery System

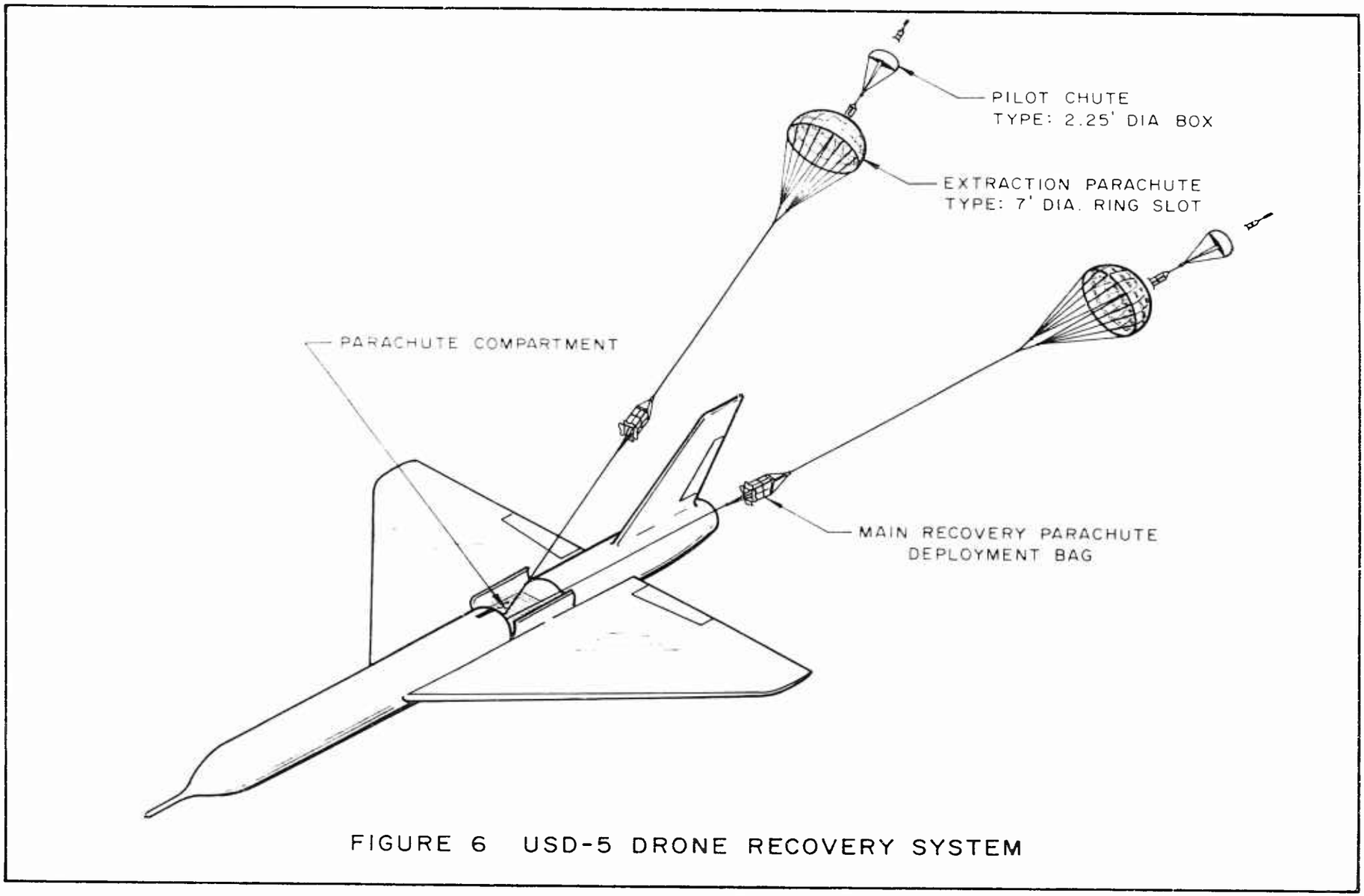

FIGURE 6 USD-5 DRONE RECOVERY SYSTEM

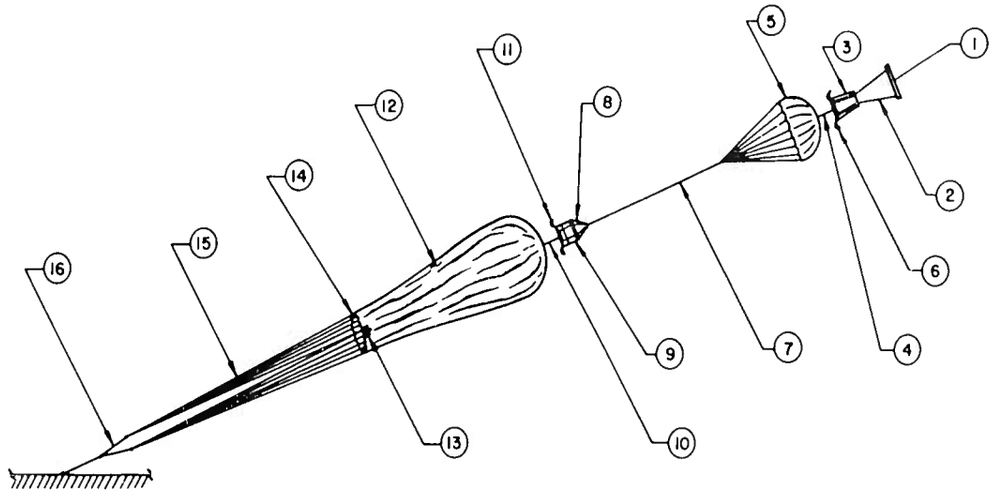

ITEM	DESCRIPTION	PART NO.	IDENT. NO.	WT. LBS.	QTY.	ITEM	DESCRIPTION	PART NO.	IDENT. NO.	WT. LBS.	QTY.
1	Container Cover	588-5000	-	-	1	10	Bridle, Apex	Part of 588-2310	MIL-W-4088 2 x 10,000 lb	-	1
2	Cover Bridle	-	4 Leg Steel Cable	-	1	11	Locking Loop, Closure Flap			-	1
3	Pilot Chute, Deployment Bag	588-2510	Handle 4 x 1000 lb	.25	1	12	Recovery Parachute, 34.5 Ft. Dia. Extended Skirt	588-2100 III-A	ESIO-40/90 -34.5-36-750	21.25	1
4	Apex Tie	-	2 Turns 5 Cord Cotton	-	1	13	Reefing Line	Nylon Cord	MIL-C-7515 Type III 750 lb	-	1
5	Pilot Chute, 5 Ft. Nominal Diameter	588-220	Conical Vane Type	2.50	1	14	Cutter, Reefing Line	Ord. Assoc. OA-D2		-	3
6	Mouth Tie		1 Turn 3 Cord Cotton	-	1	15	Suspension Lines	Part of 588-2100	MIL-C-7515 36 x 750 lb		36
7	Permanent Bridle	Part of 588-2310	MIL-W-4088 2 x 10,000 lb	2.00	1	16	Riser 2 Leg	588-2400	MIL-W-4088 2 x 10,000 lb	.75	2
8	Deployment Bag Extension and Bridle	Part of 588-2310		-	1		TOTAL WEIGHT			31.25	
9	Deployment Bag Recovery Parachute	588-2310		4.50	1		PACKED VOLUME = 1 cu. ft.				

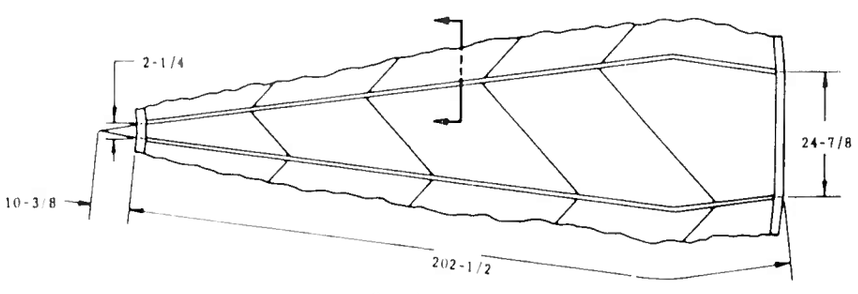

Gore Layout

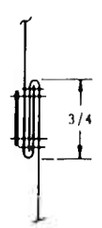

Main Seam Cross Section

Figure 7 B-70 Capsule Main Recovery Parachute Assembly

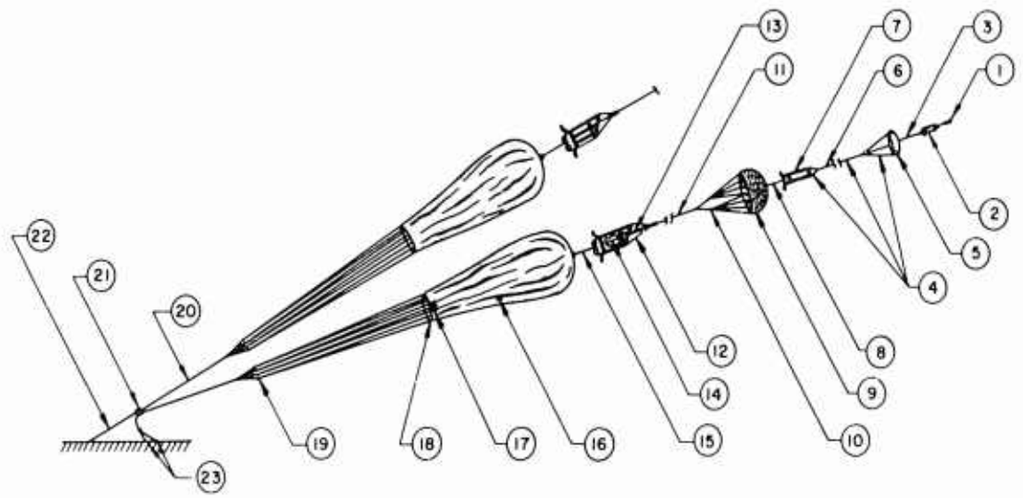

ITEM	DESCRIPTION	PART NO.	IDENT. NO.	WT. LBS.	QTY.	ITEM	DESCRIPTION	PART NO.	IDENT. NO.	WT. LBS.	QTY.
1	Slug, Drogue Gun	510-2818-1	-	1.0	2	13	Bridle, Deployment Bag	Part of 510-2212	MIL-W-4088 2 x 6000#	-	2
2	Deployment Bag, Pilot Chute	510-2232-1	Handle 4 x 1500 lb	0.2	2	14	Connector Link	52B6427	(Proof) 15,000	.53	2
3	Break Cord, Pilot Chute Apex	-	1 Turn 5 Cord Nylon	-	2	15	Bridle, Recovery Parachute Apex	Part of 510-2210-1	MIL-W-4088 2 x 6000#	-	2
4	Pilot Chute, Extractor Bag Ass'y.	510-2220-1	Consists of Items 5, 6, 7	0.93	2	16	Recovery Parachute 78 Ft Dia. Extended Skirt	510-2210-1	FESC 25-40-78-64-400	64.5	2
5	Pilot Chute, 2.25 Ft. Dia. Box Type	510-2231-1	SF-50-2.25 -4-550	0.22	2	17	Reefing Line Cutter	Ord. Assoc. OA-D2-6	-	0.3	6
6	Bridle, Pilot Chute	Part of 510-2220-1	MIL-W-5625 3/4 x 2250#	0.31	2	18	Reefing Line	Nylon Cord	MIL-C-7515 Type III 750 lb	.11	2
7	Deployment Bag, Extractor Parachute	510-2223-1	Handle 4 x 1000#	0.4	2	19	Connector Link	MS 22002-1 Opt. 55B660	(Proof) 3,000 lb	.17	8
8	Break Cord, Extractor Parachute, Apex	-	1 Turn MIL-T-7807 5 Cord Nylon	-	2	20	Riser, Recovery Parachute	510-2240-1	MIL-W-4088 2 x 10,000#	4.75	2
9	Extractor Parachute 7 Ft. Dia. Ring Slot	510-2221-1	RSC 25-90-7.0-12-1000	4.6	2	21	Disconnect, Parachute, 4 Pin	510-2840-1	-	4.72	1
10	Connector Link	MS 22002-1 Opt. 55B660	(Proof) 3,000 lb	.17	4	22	Riser, Vehicle, Forward Leg	510-2250-1	MIL-W-4088 4 x 10,000#	1.81	1
11	Bridle, Extractor Parachute	Part of 510-2212	MIL-W-4088 2 x 6000 lb	.56	2	23	Riser, Vehicle, Aft Leg	510-2250-2	MIL-W-4088 2 x 2 Ply 10,000#	1.97	1
12	Deployment Bag, Recovery Parachute	510-2212-1 & -2	Handle 2 x 10,000# 2 x 6,000#	6.0	2		TOTAL WEIGHT PACKED VOLUME = 6.6 cu. ft.			180.56	

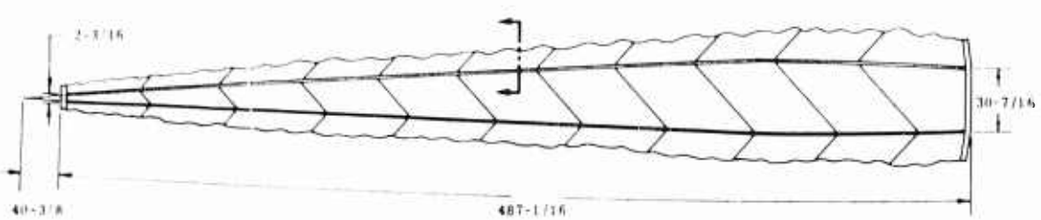

Gore Layout

Main Seam Cross Section

Figure 8 USD-5 Drone Main Recovery Parachute Assembly

GENERAL TEST DATA								PHOTO DATA			INSTRUMENTATION PHOTOGRAPHIC COVERAGE				TEST CONDITIONS						TEST RESULTS		
DROP NUMBER	DATE	FT. TROOP UNIT NO.	TEST PHASE	DROP AIRCRAFT TYPE	T-11 VEHICLE TYPE	PITCH CHUTE TYPE*	PARACHUTE CANOPY DIAMETER	RELEASE LINE LENGTH (INCHES)	LOAD MEASURED TO	AIR TO AIR	VEHICLE TO AIR	VEHICLE TO GROUND	ALTITUDE, FT.	DROP VELOCITY KNOTS I.A.S.	WIND VELOCITY KNOTS	TIME OF DAY	TEMPERATURE °F	GROSS WEIGHT LBS.	IMPACT WEIGHT, LBS.	TOTAL OPENING TIME, SEC.	TOTAL DROW TIME, SEC.	OSCILLATION, DEGREES	PERFORMANCE & DAMAGE N. D. (NORMAL DEPLOYMENT) N. O. (NORMAL OPENING) DAMAGE L (LIGHT) M (MEDIUM) H (HEAVY)	CALCULATED RATE OF DESCENT FT. SEC.
1	4-14	187	1	C-119	A-22	None	35ft	None	None	6mm	70mm	None	None	1500	13	4-5	100	93	Not known	Not known	2.7	48.0	25	N. D. N. O. No Damage	N. A
2	4-14	188								6mm	None					4-5	1000	93	Not known	Not known	2.5	48.0	15		N. A
3	4-15	4-5								6mm	7mm					2-4	1100	88	760	751	2.5	46.4	10		25.6
4	4-15	4-6								6mm	None					2-4	1100	88	762	753	2.5	54.0	10		24..
5	4-15	4-7								6mm	None	None				2-4	0800	88	762	753	3.4	54.2	20 30		25.
6	4-15	4-8								6mm	None	Dress A.C.				4-5	0800	92	760	751	2.4	56.1	25 45		25.4
7	4-21	4-9								7mm	None	None				4-5	0800	92	761	752	2.5	55.2	15 25		24.4
8	4-21	4-10					None		None	6mm	7mm					4-5	1000	92	762	753	2.6	51.4	15 25		25..
9	4-21	4-11						None		6mm	None					2-4	1000	88	774	767	2.1	53.0	5 15		26.7
10	4-22	4-12														2-4	1100	92	772	765	1.7	55.1	15 25		24.
11	4-22	4-13														12	1000	76	776	769	2.5	54.0	15 25		27.5
12	5-4	5-1	1	C-119	A-22	1	35ft	None	None	6mm	70mm	None	None	1500	13	12	08	77	778	771	Not Known	Not Known	15 25	N. D. N. O. No Damage	26.2

* See Table II for Pitch Chute Data.

Table III Test Summary Report, Bell Helicopter Company

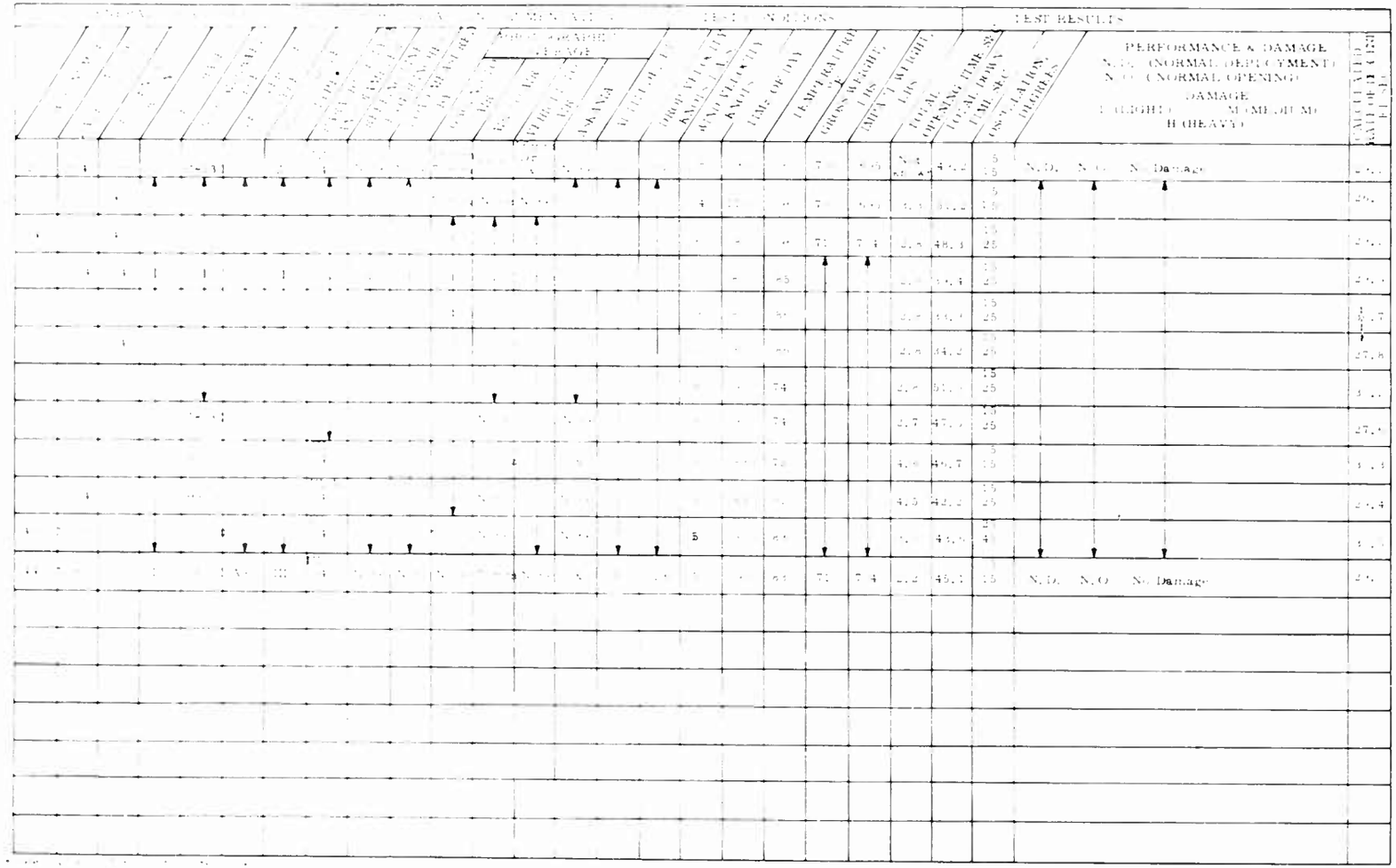
TEST RESULTS
PERFORMANCE & DAMAGE
N.D. (NORMAL DEPLOYMENT)
N.O. (NORMAL OPENING)
DAMAGE
L (LIGHT) M (MEDIUM)
H (HEAVY)
N.D. N.O. No Damage

GENERAL DROP DATA							PROJECTILE DATA		INSTRUMENTATION PHOTOGRAPHIC COVERAGE				TEST CONDITIONS							TEST RESULTS			
DROP NO.	TEST NO.	DATE	DROP POINT	DROP VEHICLE	TEST VEHICLE	PILOT CHUTE	PARACHUTE ASSEMBLY	REEFING LINE LENGTH	GROUND MET	AIR TO AIR	AIR TO VEHICLE	AIR TO GROUND	ALTITUDE, FT	DROP VELOCITY KNOTS TAS	WIND VELOCITY KNOTS	TIME OF DAY	TEMPERATURE °F	GROSS WEIGHT, LBS	IMPACT WEIGHT, LBS	TOTAL OPENING TIME SEC	TOTAL DRAG TIME SEC	OSCILLATION DEGREES	PERFORMANCE & DAMAGE N.D. (NORMAL DEPLOYMENT) N.O. (NORMAL OPENING) DAMAGE L (LIGHT) M (MEDIUM) H (HEAVY)	CALCULATED IMPACT VELOCITY FT/SEC
1	[illegible]	[illegible]	7-49	[illegible]	[illegible]	[illegible]	[illegible]	[illegible]	[illegible]	[illegible]	[illegible]	[illegible]	24	5	[illegible]	47	755	744	1.4	57.8	0 5		N.D. M On Opening	N/A
4	[illegible]	[illegible]	7-[illegible]	[illegible]	[illegible]	[illegible]	[illegible]	[illegible]	[illegible]	[illegible]	[illegible]	[illegible]	24	4	[illegible]	[illegible]	715	7.7	1.5	52.5	0 5		N.D. M On Opening	
5	[illegible]	[illegible]	[illegible]	[illegible]	[illegible]	[illegible]	[illegible]	[illegible]	[illegible]	[illegible]	[illegible]	[illegible]	24	2	[illegible]	42	7[illegible]	7[illegible]4	4.5	--	.5 25		N.D. N.O. No Damage	
[illegible]	[illegible]	[illegible]	[illegible]	[illegible]	[illegible]	[illegible]	[illegible]	[illegible]	[illegible]	[illegible]	[illegible]	[illegible]	24	4	[illegible]	45	[illegible]	7[illegible]	4.8	53.1	0 5		N.D. H At Reefed Open	N/A
[illegible]	[illegible]	[illegible]	[illegible]	[illegible]	[illegible]	[illegible]	[illegible]	[illegible]	[illegible]	[illegible]	[illegible]	[illegible]	24	[illegible]	[illegible]	44	[illegible]	7[illegible]4	4.5	7[illegible].2	5 15		N.D. N.O.	28.6
[illegible]	[illegible]	[illegible]	[illegible]	[illegible]	[illegible]	[illegible]	[illegible]	[illegible]	[illegible]	[illegible]	[illegible]	[illegible]	325	5	[illegible]	45	72	7[illegible]4	5.5	68.5	5 15		Pilot Chute Separated at Full Deployment, M at Reefed Open, Only 1 Cutter Fired.	30.8
[illegible]	[illegible]	[illegible]	[illegible]	[illegible]	[illegible]	[illegible]	[illegible]	[illegible]	[illegible]	[illegible]	[illegible]	[illegible]	325	[illegible]	[illegible]	43	7[illegible]	7[illegible]2	5.0	5[illegible].8	5 15		N.D. M After Full Inflation	N/A
[illegible]	[illegible]	[illegible]	[illegible]	[illegible]	[illegible]	[illegible]	[illegible]	[illegible]	[illegible]	[illegible]	[illegible]	[illegible]	320	[illegible]	[illegible]	[illegible]	72	7[illegible]4	4.2	7[illegible].4	5 15		N.D. N.O. L	
[illegible]	[illegible]	[illegible]	[illegible]	[illegible]	[illegible]	[illegible]	[illegible]	[illegible]	[illegible]	[illegible]	[illegible]	[illegible]	45	[illegible]	[illegible]	[illegible]	[illegible]	[illegible]	4.[illegible]	72.[illegible]	--		N.D. N.O. L	
[illegible]	[illegible]	[illegible]	[illegible]	[illegible]	[illegible]	[illegible]	[illegible]	[illegible]	[illegible]	[illegible]	[illegible]	[illegible]	32[illegible]	[illegible]	[illegible]	47	[illegible]	[illegible]	5.[illegible]	71.2	0 5		Pilot Chute Separated at Full Deployment, M at Reefed Open	
[illegible]	[illegible]	[illegible]	[illegible]	[illegible]	[illegible]	[illegible]	[illegible]	[illegible]	[illegible]	[illegible]	[illegible]	[illegible]	[illegible]	[illegible]	[illegible]	[illegible]	[illegible]	[illegible]	--	[illegible].2	0 5		Premature Canopy Deployment. H Damage, Two Reefing Cutters Torn Off, Third Cutter Fired. Chute Did Not Inflate.	N/A
[illegible]	[illegible]	[illegible]	A4[illegible]	[illegible]	[illegible]	[illegible]	[illegible]	[illegible]	[illegible]	[illegible]	[illegible]	[illegible]	[illegible]	[illegible]	[illegible]	[illegible]	[illegible]	[illegible]	4.[illegible]	6[illegible].8	5 15		N.D. N.O. Two Reefing Cutters Failed to Fire Due To Inverted Installation. Third Cutter Cut Reefing Line.	24.2
[illegible]	[illegible]	[illegible]	A4[illegible]	[illegible]	[illegible]	[illegible]	[illegible]	[illegible]	[illegible]	[illegible]	[illegible]	[illegible]	[illegible]	[illegible]	[illegible]	[illegible]	[illegible]	[illegible]	--	[illegible].[illegible]	0 5		N.D. Failed to Disreef. Reefing Cutters Failed to Fire Due to Inverted Installation.	N/A
[illegible]	[illegible]	[illegible]	A4[illegible]	[illegible]	[illegible]	[illegible]	[illegible]	[illegible]	[illegible]	[illegible]	[illegible]	[illegible]	[illegible]	[illegible]	[illegible]	[illegible]	[illegible]	[illegible]	5.4	56.7	5 15		N.D. N.O. No Damage	3[illegible].2
[illegible]	[illegible]	[illegible]	[illegible]	[illegible]	[illegible]	[illegible]	[illegible]	[illegible]	[illegible]	[illegible]	[illegible]	[illegible]	[illegible]	[illegible]	[illegible]	[illegible]	[illegible]	[illegible]	4.[illegible]	[illegible].7	5 15			24.7
[illegible]	[illegible]	[illegible]	A4[illegible]	[illegible]	[illegible]	[illegible]	[illegible]	[illegible]	[illegible]	[illegible]	[illegible]	[illegible]	24	[illegible]	[illegible]	[illegible]	[illegible]	[illegible]	4.[illegible]	[illegible].5	15 45			24.3
[illegible]	[illegible]	[illegible]	[illegible]	[illegible]	[illegible]	[illegible]	[illegible]	[illegible]	[illegible]	[illegible]	[illegible]	[illegible]	[illegible]	[illegible]	[illegible]	[illegible]	[illegible]	[illegible]	4.[illegible]	[illegible].2	5 15			47.6
[illegible]	[illegible]	[illegible]	[illegible]	[illegible]	[illegible]	[illegible]	[illegible]	[illegible]	[illegible]	[illegible]	[illegible]	[illegible]	[illegible]	[illegible]	[illegible]	[illegible]	[illegible]	[illegible]	4.5	[illegible]	5 15		N Damage	[illegible].7
[illegible]	[illegible]	[illegible]	[illegible]	[illegible]	[illegible]	[illegible]	[illegible]	[illegible]	[illegible]	[illegible]	[illegible]	[illegible]	[illegible]	[illegible]	[illegible]	[illegible]	[illegible]	[illegible]	4.[illegible]	[illegible].[illegible]	0 15		N.O. N.O. M	28.[illegible]

[illegible]

[illegible]

GENERAL TEST DATA / INSTRUMENTATION	ALTITUDE, FT	VELOCITY, KNOTS	WIND VELOCITY, KNOTS	TIME OF DAY	TEMPERATURE, F	GROSS WEIGHT, LBS	IMPACT WEIGHT, LBS	TOTAL OPENING TIME, SEC	TOTAL DOWN TIME, SEC	OSCILLATION, DEGREES	PERFORMANCE & DAMAGE N.D. (NORMAL DEPLOYMENT) N.O. (NORMAL OPENING) DAMAGE L (LIGHT) M (MEDIUM) H (HEAVY)	CALCULATED RATE OF DESCENT FT/SEC
[illegible]	[illegible]	[illegible]	[illegible]	[illegible]	72	7.4	4.5	48	[illegible]	5 15	N.D. N.O. L.	N/A
[illegible]	[illegible]	[illegible]	[illegible]	[illegible]			4.3	[illegible]	[illegible]	5 15	N.D. N.O. Pilot Chute Damaged During Deployment.	27.8
[illegible]	[illegible]	[illegible]	[illegible]	[illegible]			4.7	47	[illegible]	15 25	N.D. N.O. No Damage	N/A
[illegible]	[illegible]	[illegible]	[illegible]	[illegible]			4.5	44.4	[illegible]	[illegible]	N.D. N.O. No Damage	35.6
[illegible]	[illegible]	[illegible]	[illegible]	[illegible]	[illegible]	7.4	[illegible]	44.3	[illegible]	1 5	N.D. H At Full Inflation	N/A

GENERAL DROP DATA							PARACHUTE DATA		INSTRUMENTATION				TEST CONDITIONS							TEST RESULTS			
DROP NUMBER	DATE	A/C TYPE	A/C NO.	DROP POINT	DROP METHOD	TEST OBJECTIVE	PARACHUTE AND ASSEMBLY NO.	RIGGING LINE LENGTH (INCHES)	TOTAL WEIGHT DROPPED (LBS)	PHOTOGRAPHIC COVERAGE: GROUND TO AIR	PHOTOGRAPHIC COVERAGE: AIR TO AIR	PHOTOGRAPHIC COVERAGE: VEHICLE TO AIR	PHOTOGRAPHIC COVERAGE: ASHANIA	ALTITUDE, FT.	DROP VELOCITY KNOTS I.A.S.	WIND VELOCITY KNOTS	TIME OF DAY	TEMPERATURE °F	GROSS WEIGHT, LBS.	IMPACT WEIGHT, LBS.	TOTAL OPENING TIME, SEC.	TOTAL DOWN TIME, SEC.	OSCILLATION, DEGREES	PERFORMANCE & DAMAGE N.D. (NORMAL DEPLOYMENT) N.O. (NORMAL OPENING) DAMAGE L (LIGHT) M (MEDIUM) H (HEAVY)	CALCULATED RATE OF DESCENT FT/SEC
1*	[illegible]	[illegible]	5	27	A40	M-8	2	III A 44.5	[illegible]	Test Vehicle (Land)	None	None	None	None	2[illegible]	24	[illegible]	[illegible]	62	710	707	3.0	86.3	5 15	N.D. N.O. No Damage	30..
4	[illegible]	[illegible]	[illegible]	[illegible]	H-[illegible]	[illegible]	[illegible]	III A 44.5	[illegible]	Instrumented Vehicle (Land)	None	None	[illegible]	None	2[illegible]	55	15	[illegible]	77	[illegible]	[illegible]	4.8	59.5	15 25	N.D. N.O. No Damage	26..
5*	[illegible]	25[illegible]	[illegible]	[illegible]	B-[illegible]	[illegible]	[illegible]	III A 44.5	[illegible]	N.A.	None	None	None	None	200 230	425 445	12	1055	71	[illegible]	[illegible]	--	---	--	Dropped Off Range, No Data	N.A
6*	[illegible]	445	27	B-[illegible]	1	M-8	2	III A 44.5	[illegible]	Instrumented Vehicle (Land)	None	None	None	None	15000	323	2	1045	73	710	707	4.0	479.5	0 5	N.D. N.O. No Damage	28.3

* See Table II for Drop Data

Figure 3

Aerial Drop Test Summary, B-70 Recovery System

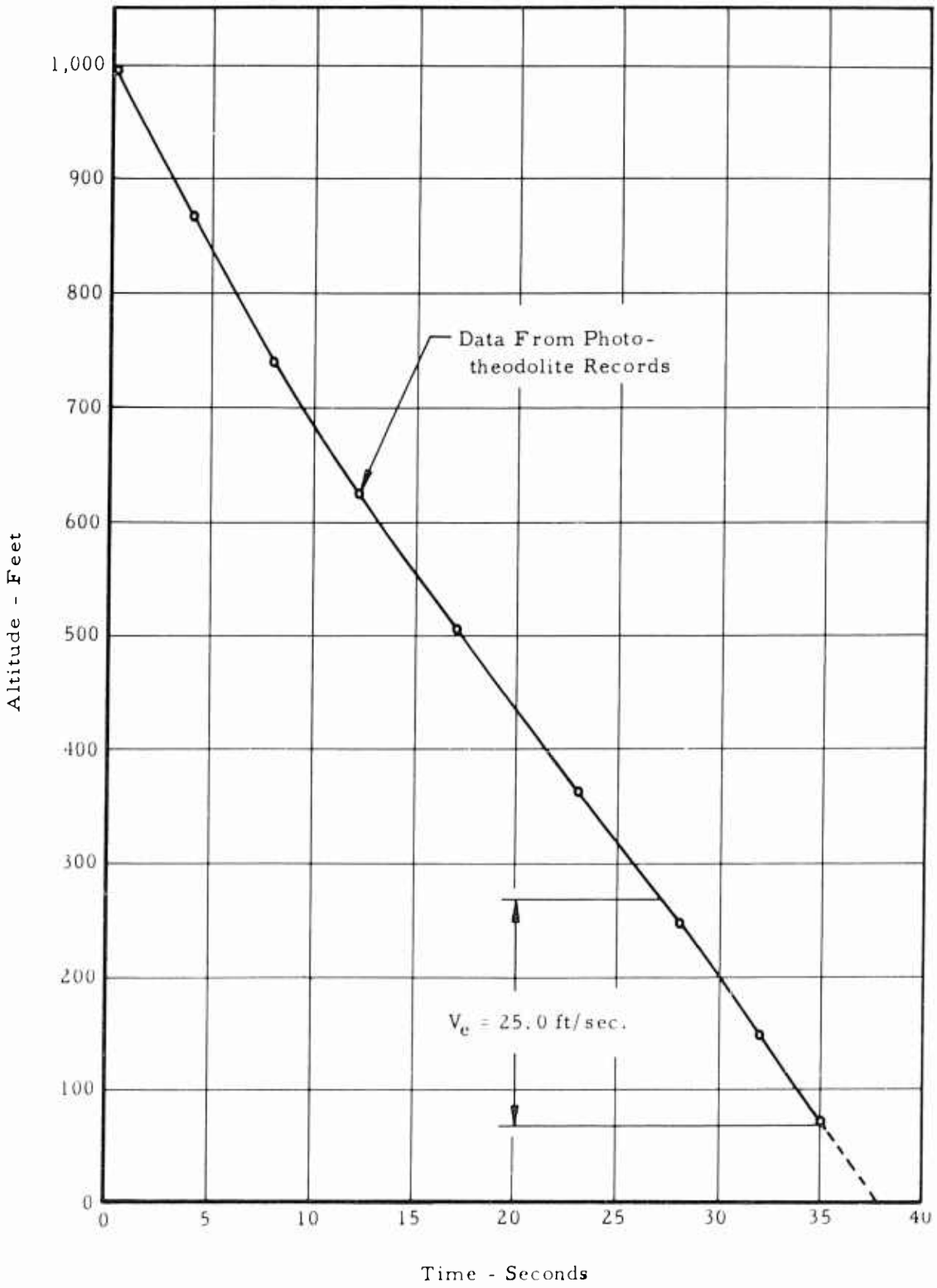

Figure 14 Altitude vs. Time (Rate of Descent), B-70 Test No. 35

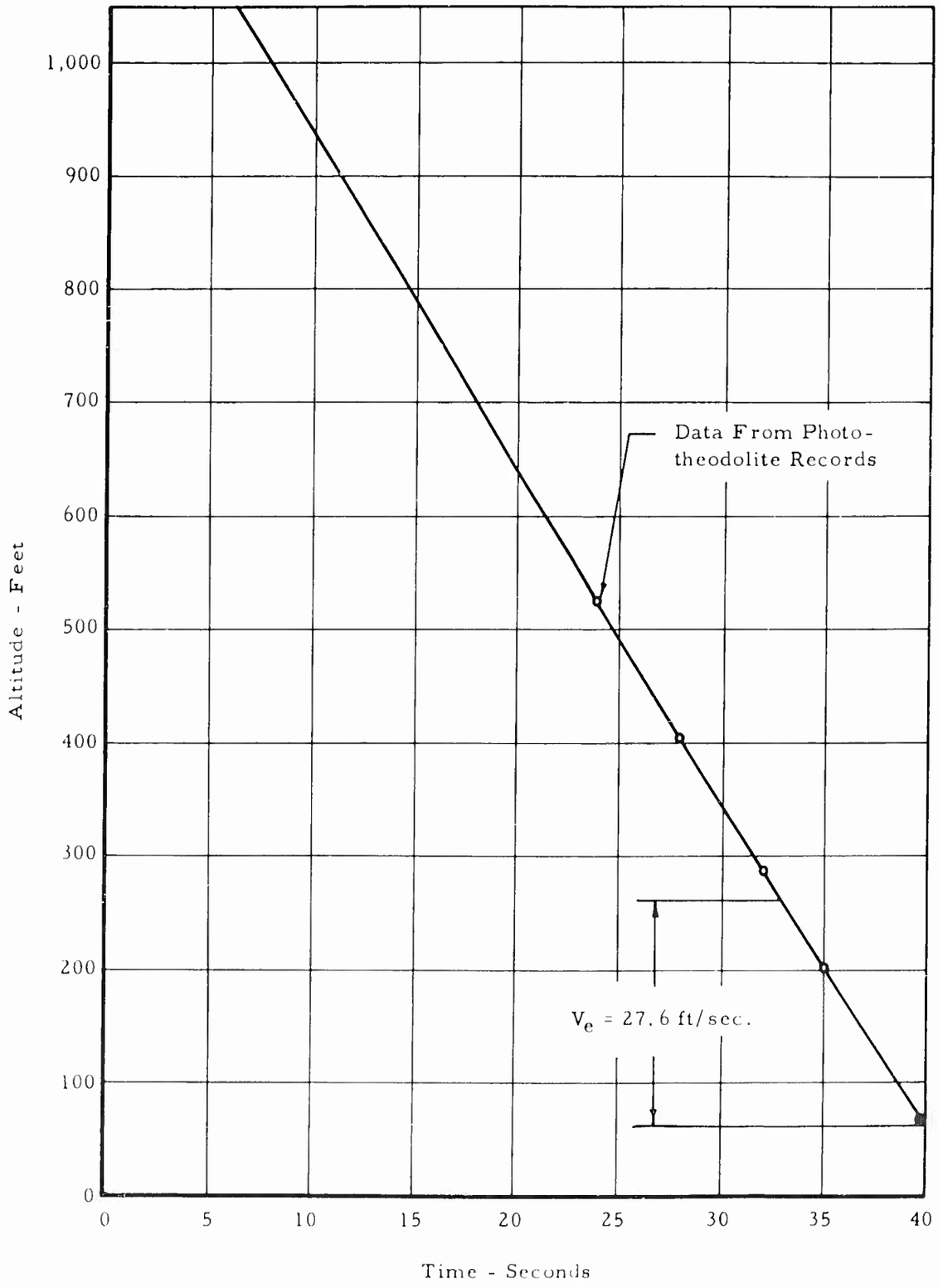

Figure 15 Altitude vs. Time (Rate of Descent), B-70 Test No. 47

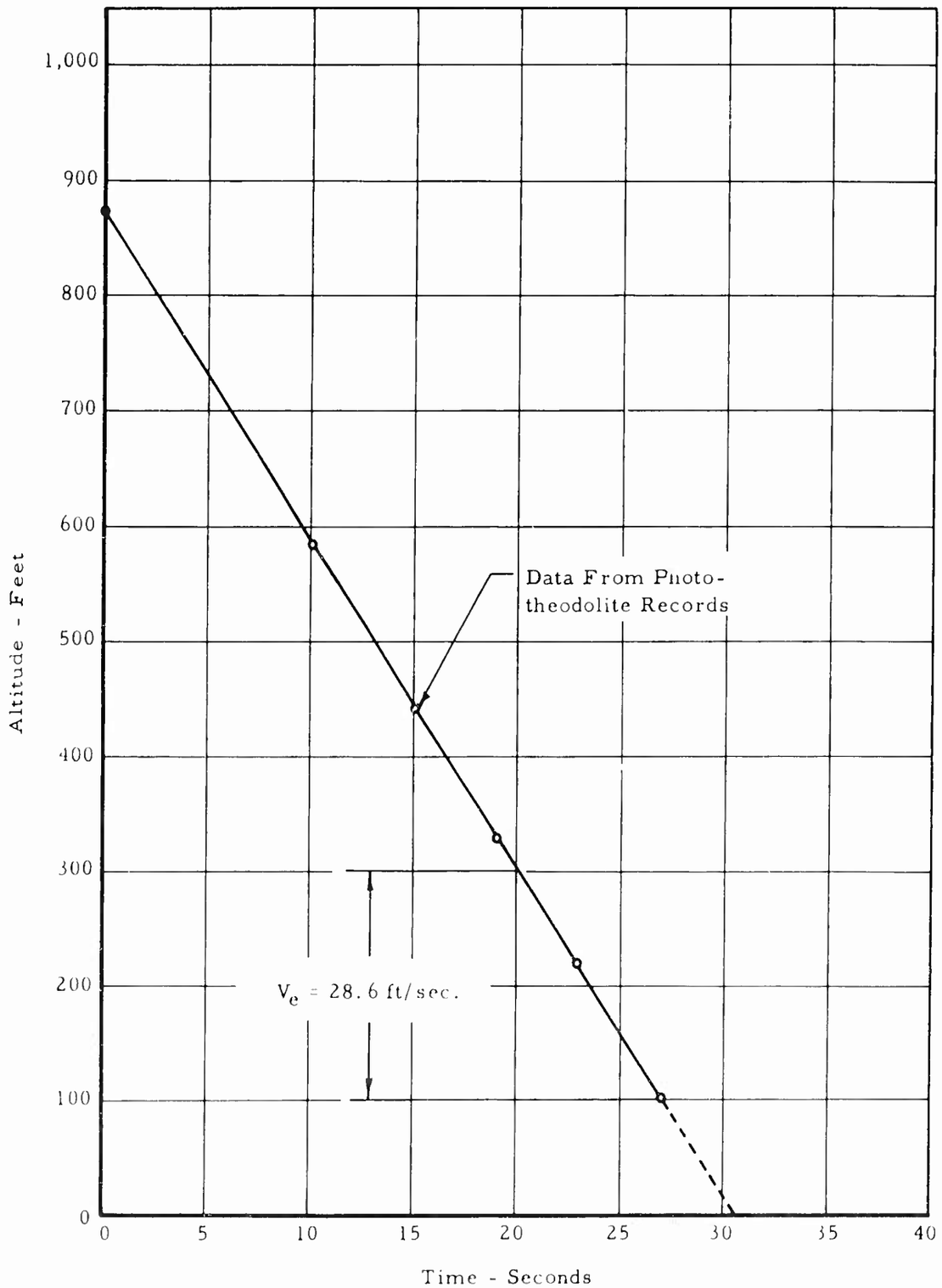

Figure 16 Altitude vs. Time (Rate of Descent), B-70 Test No. 55

Test Number	D_o Nominal Parachute Diameter (ft)	L_s/D_o Ratio of Suspension Line Length to D_o	W Impact Weight (lbs)	V_{eo} Rate of Descent (ft/sec)	V_{eo} Average Rate of Descent (ft/sec)	C_{D_o} Drag Coefficient	C_{D_o} Average Drag Coefficient	Data Acquisition Method
3	38	1.00	751	25.6	24.9	0.689	0.873	Drop Line
4			753	24.1		0.961		
5			753	25.0		0.891		
6			751	25.3		0.870		
7			752	24.4		0.940		
8			753	25.1		0.888		
9	38	0.87	767	28.7	27.3	0.691	0.771	Drop Line
10			765	24.9		0.918		
11			769	27.5		0.754		
12			771	28.2		0.720		
20	34.5	0.87	695	29.1	28.7	0.743	0.774	Drop Line
22			695	26.0		0.927		
24			704	29.1		0.751		
26			704	29.5		0.729		
27			704	30.7		0.674		
28			704	27.8		0.834		
30			704	30.1		0.700		
31			704	27.6		0.834		
35	34.5	0.95	704	24.2	28.3	1.081	0.805	Photo-theodolite
45				31.2		0.656		
47				26.7		0.889		
48				29.3		0.740		
51				27.6		0.834		
54				30.7		0.674		
55				28.3		0.795		
57				28.5		0.782		

Figure 17 Summary of Rate of Descent and Drag Coefficient Data, B-70 Test Program

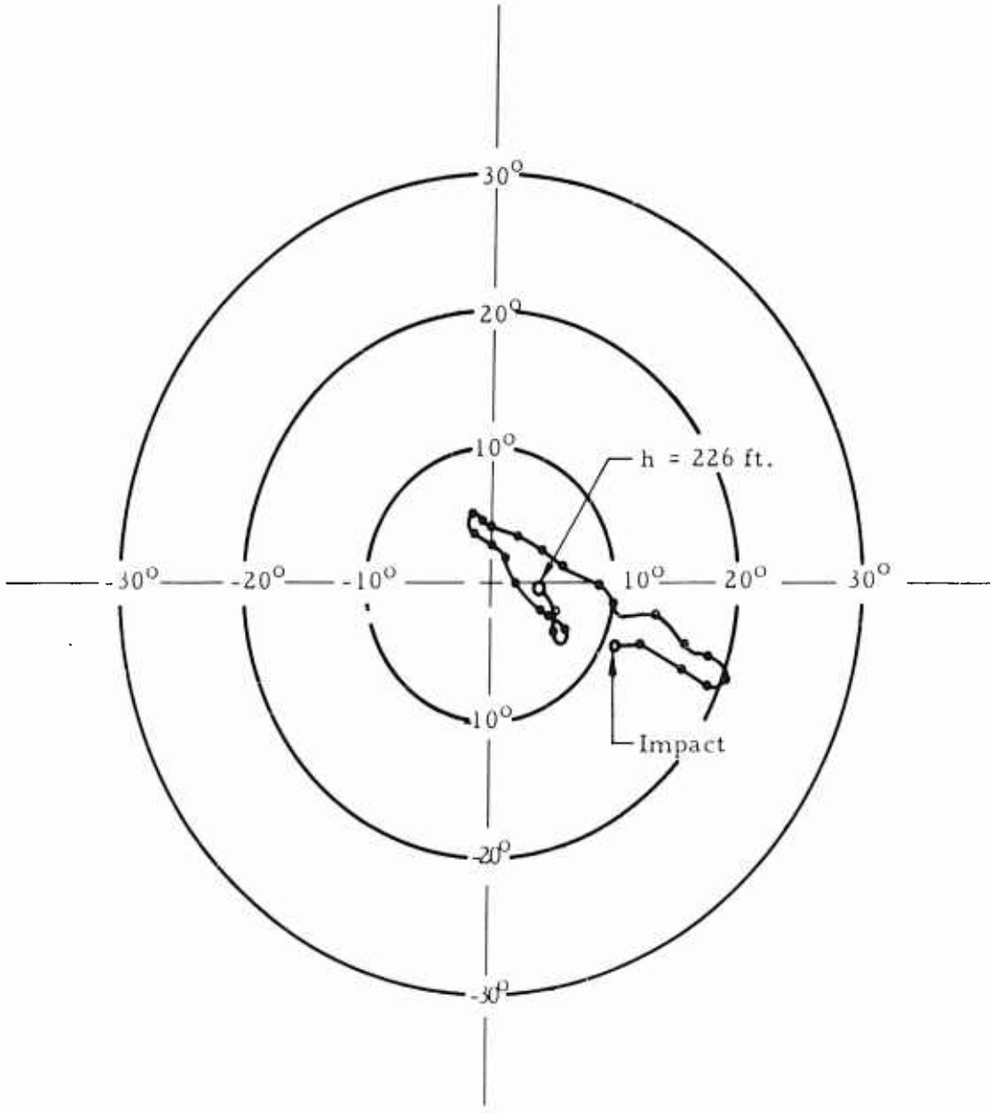

Data taken from Hulcher film
@ 0.28-second intervals

Figure 18 Stability Analysis, B-70 Test No. 24

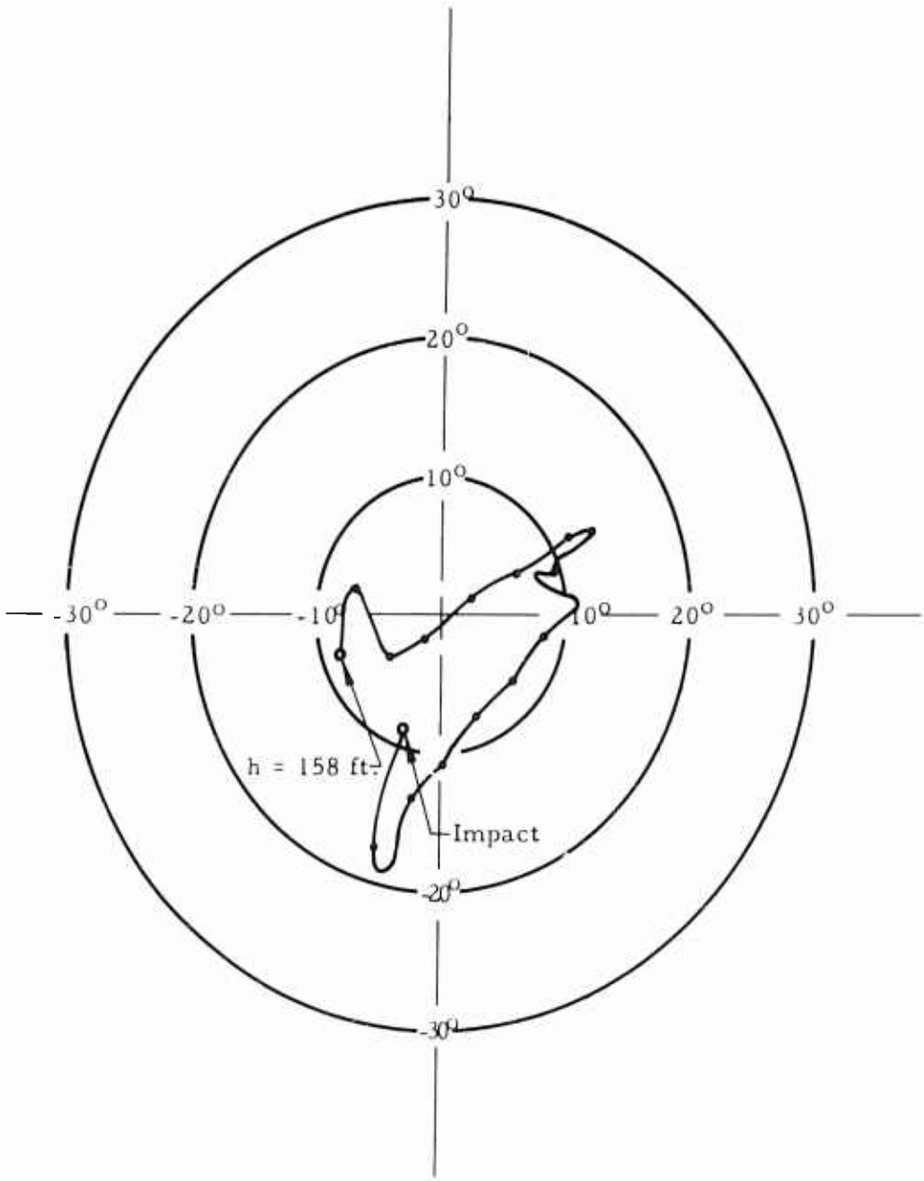

Data taken from Hulcher film
@ 0.27-second intervals

Figure 19 Stability Analysis, B-70 Test No. 26

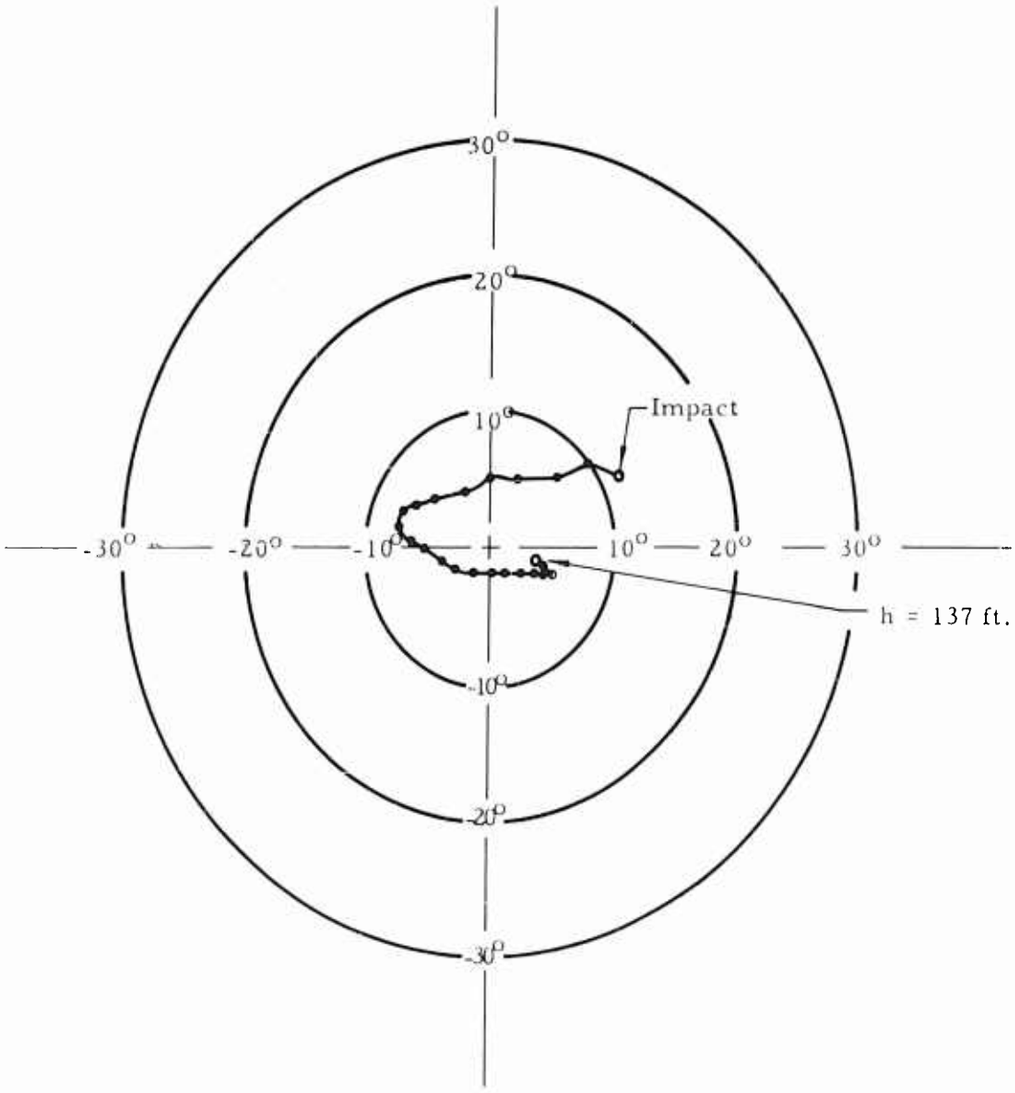

Data taken from Hulcher film
@ 0.21-second intervals

Figure 20 Stability Analysis, B-70 Test No. 51

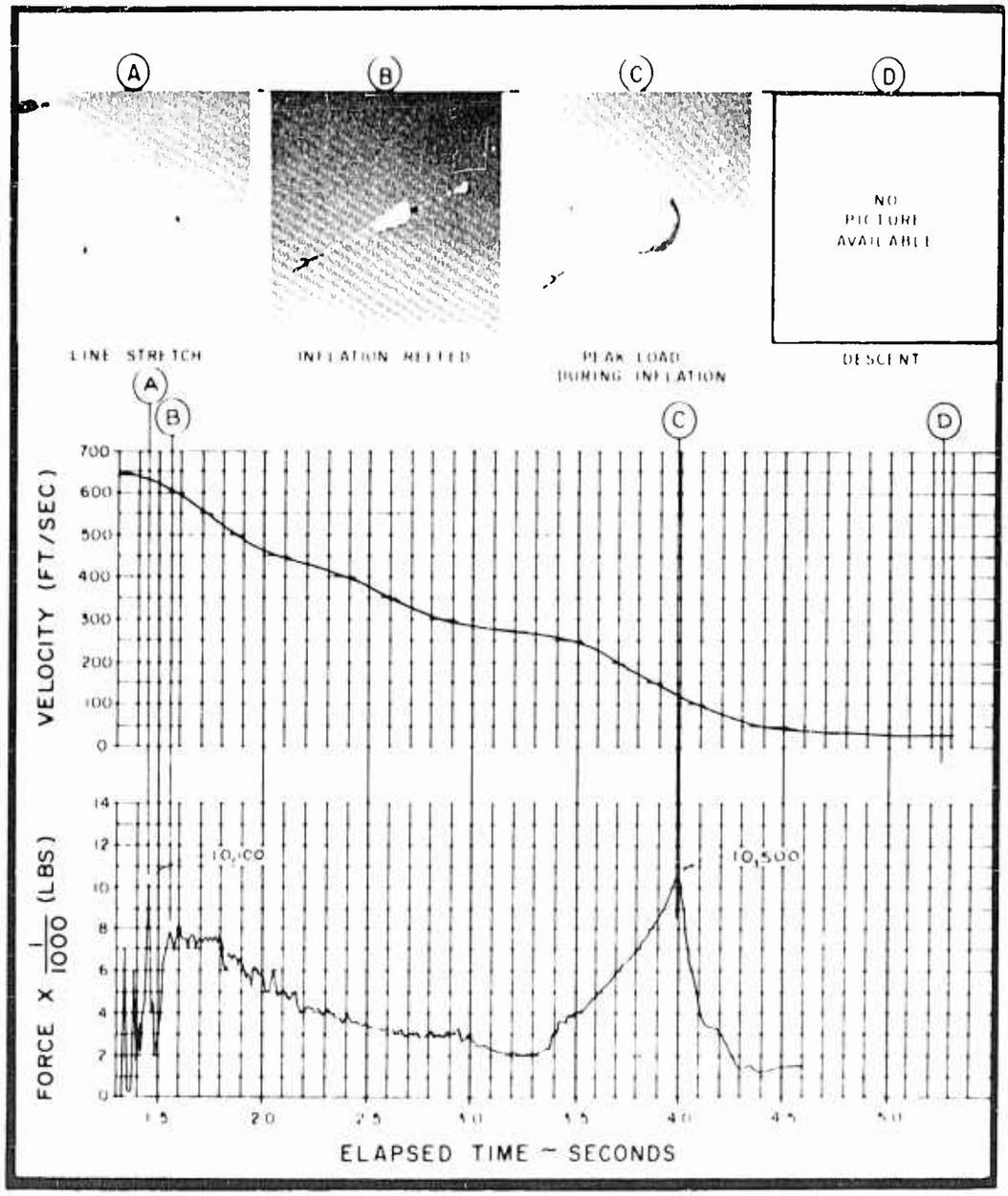

Figure 21: Force-Velocity-Time Profile, B-70 Test No. 29

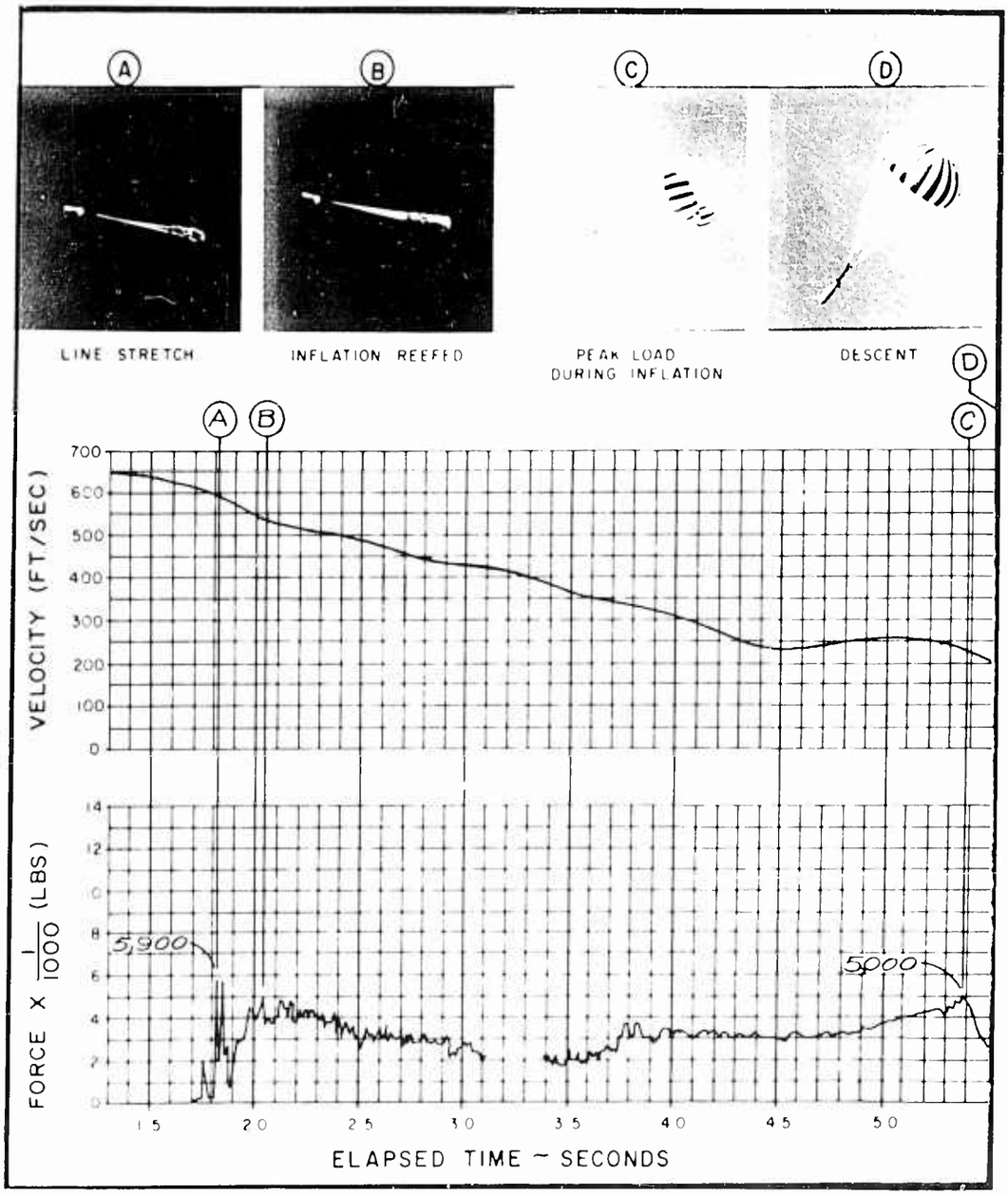

Figure 22: Force-Velocity-Time Profile, B-70 Test No. 33

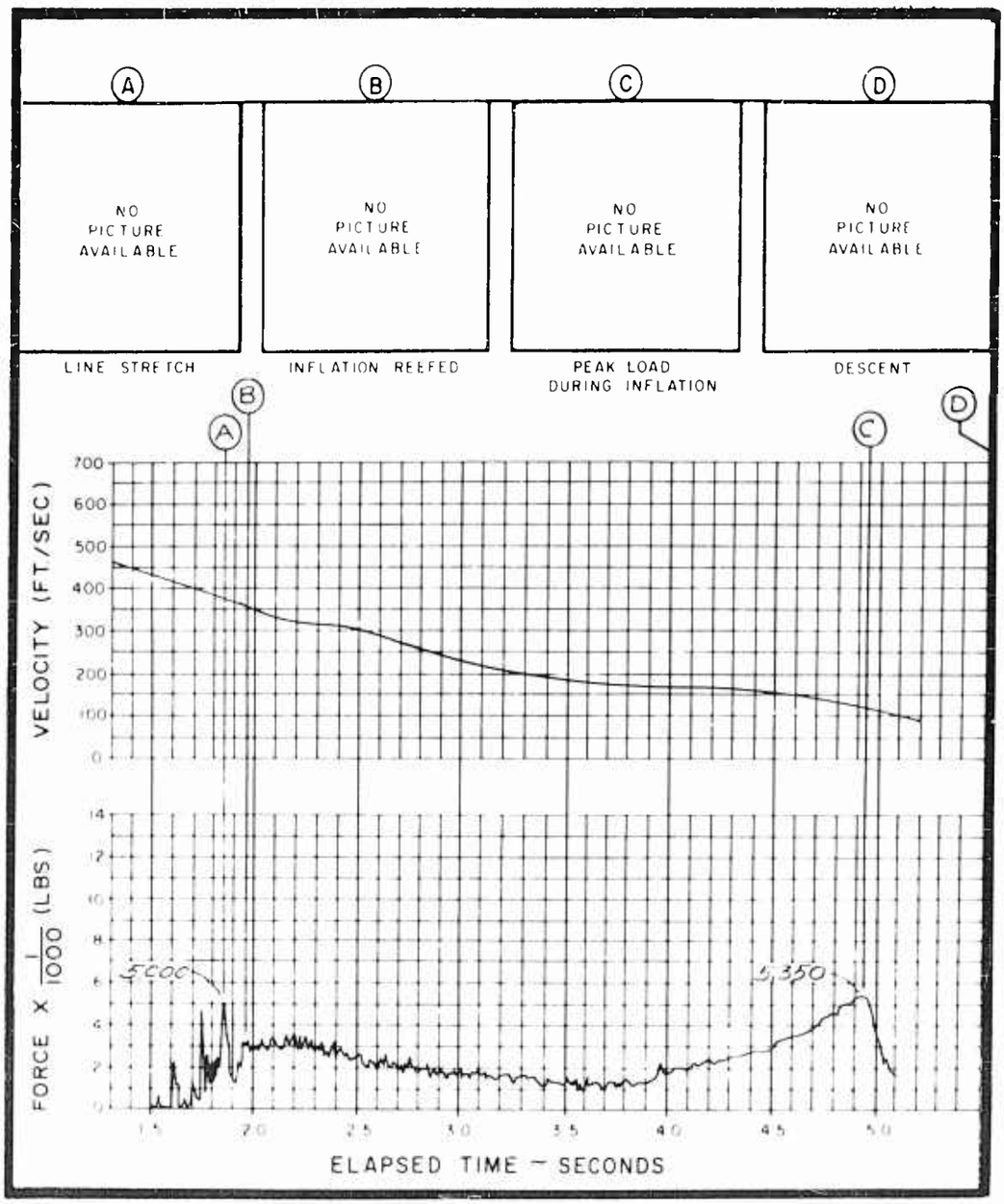

Figure 23: Force-Velocity-Time Profile, B-70 Test No. 48

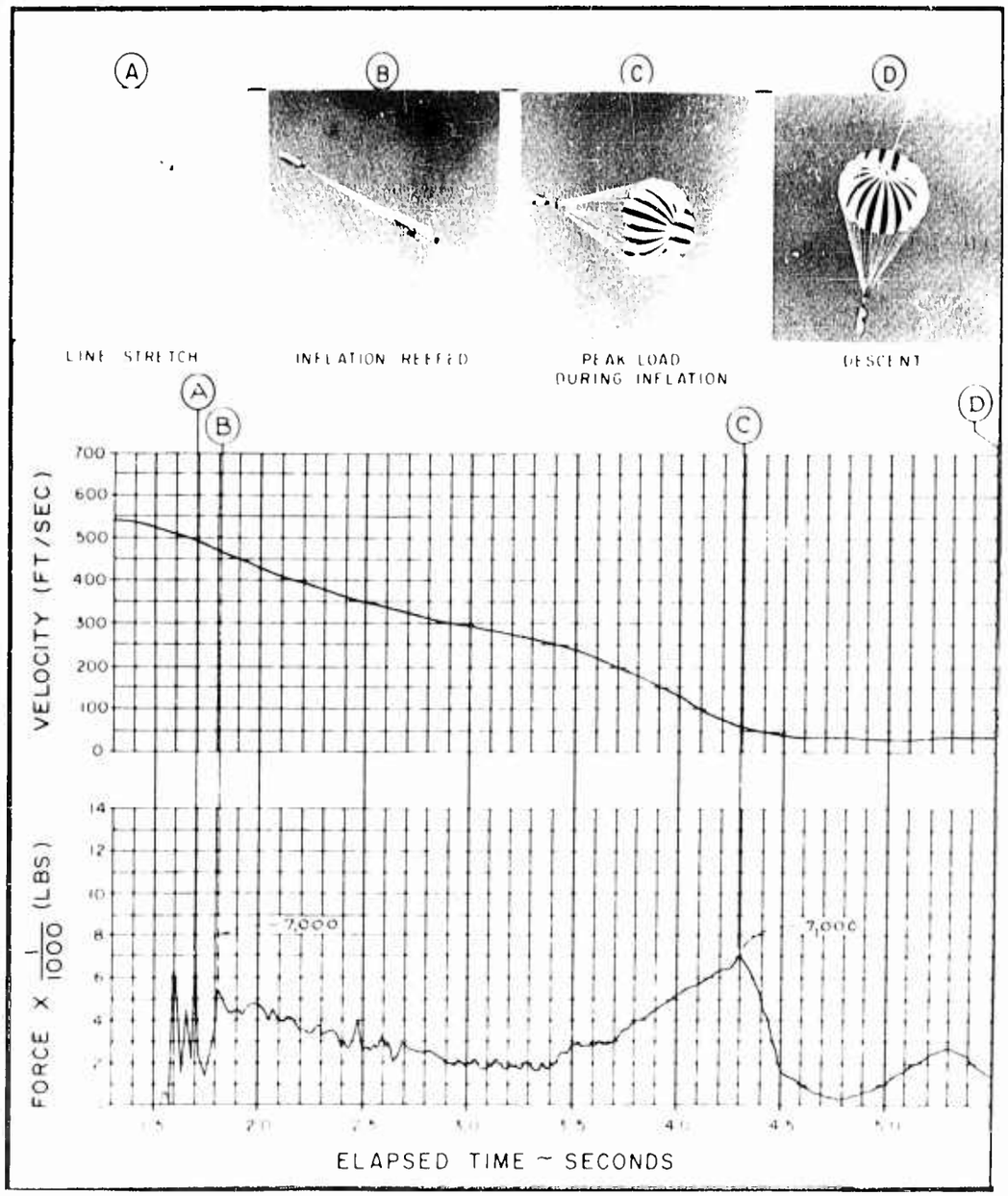

Figure 24: Force-Velocity-Time Profile, B-70 Test No. 51

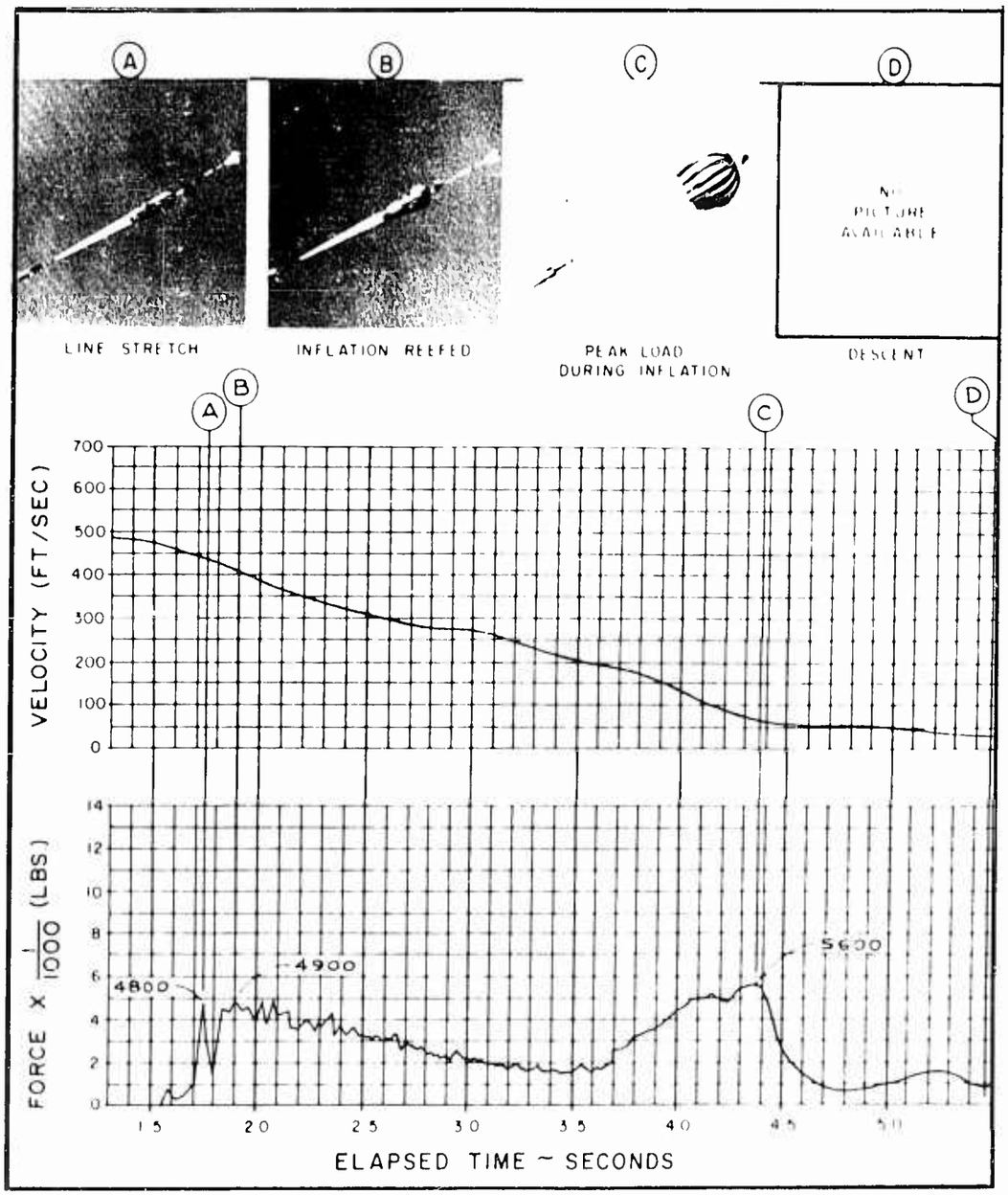

Figure 25: Force-Velocity-Time Profile, B-70 Test No. 54

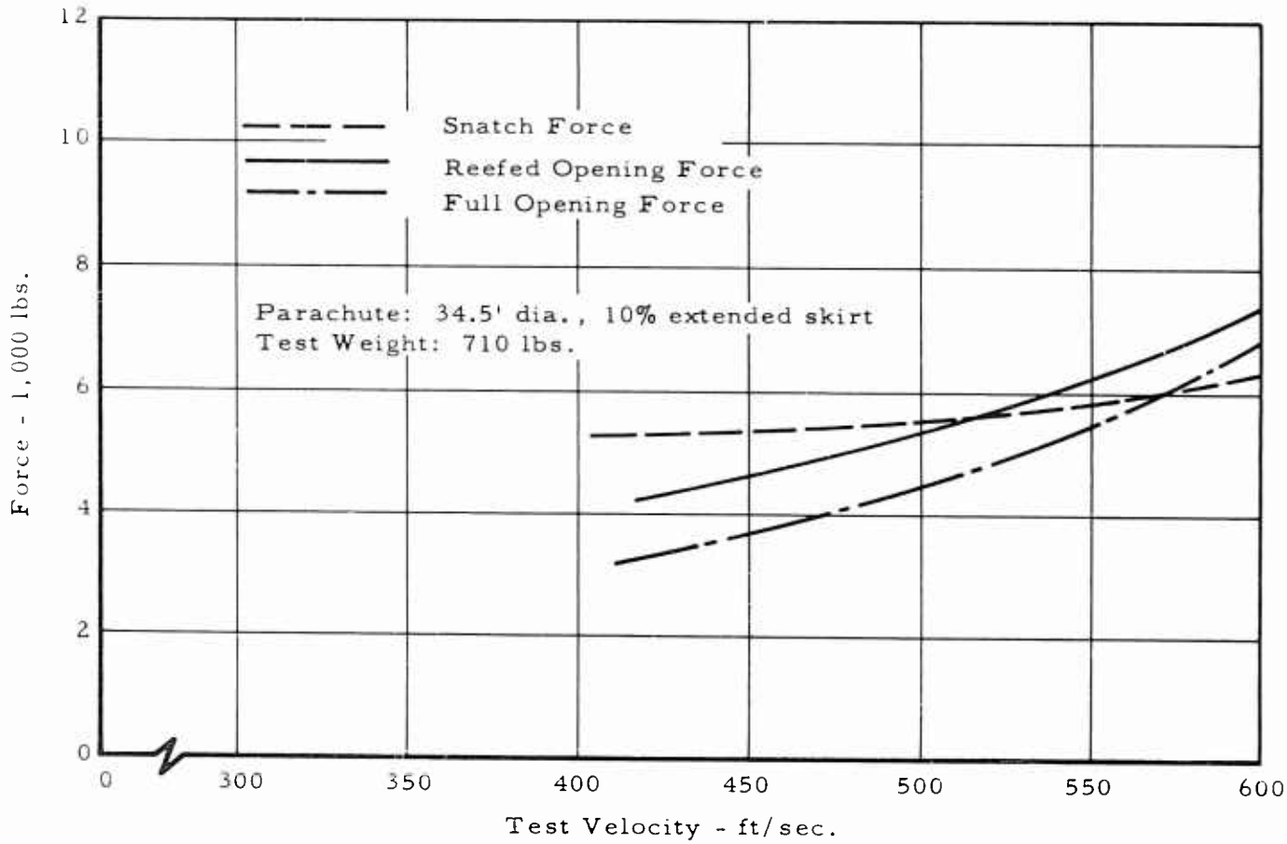

Figure 26 Force vs. Velocity, B-70 Tests

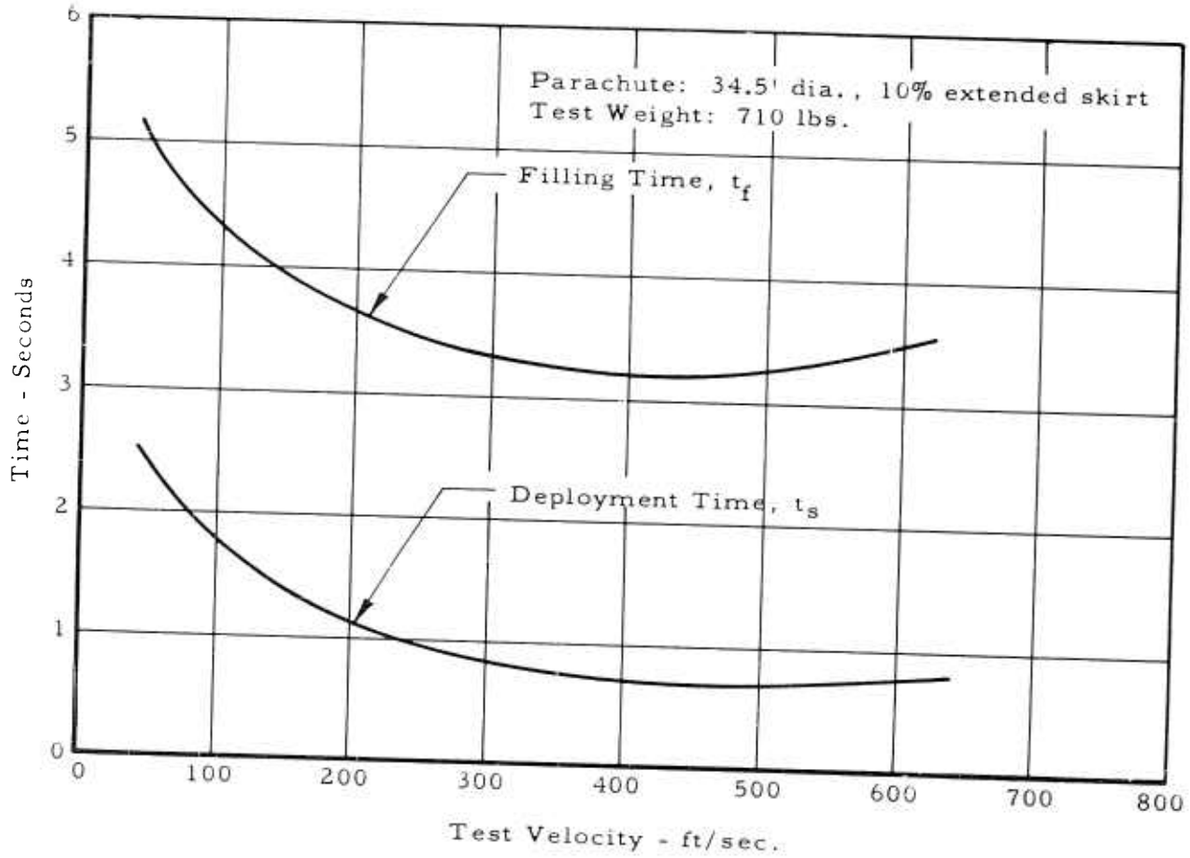

Figure 27 Parachute Times vs. Velocity, B-70 Tests

INSTRUMENTATION		PERFORMANCE	DAMAGE
FT-Force Tensiometer	AA-Air to Air Camera	ND-Normal Deployment	L-Light H-Heavy
TM-Telemetry	GA-Ground to Air Camera	NO-Normal Opening	M-Medium N-None
[illegible]	VA-Vehicle to Air Camera	NR-Normal Recovery	

[illegible columns]	Vehicle Type	Vehicle Weight	Total Drop Weight	Line Stretch	Reefed Open	Full Open	Snatch Force	Reefed Force	Open Force	Deployment	Opening	Aerial Damage	Recovery	COMMENTS
				sec	sec	sec	lbs	lbs	lbs					
[illegible]	AB	24[illegible]	257	---	---	---	155	2[illegible]5	---	ND	AO	H	None	Parachute failed in the vent area on opening
[illegible]	AB	---	24[illegible]	---	2.5 3.	[illegible]	---	---	---	ND	NO	L	NR	Tensiometer failed no load
[illegible]	AB	24[illegible]	2482	---	---	7.2	--- Peak [illegible]	---	---	ND	NO	L	NR	Tensiometer failed peak load only
[illegible]	AB	242[illegible]	251[illegible]	---	2.5	[illegible]2	---	---	---	ND	NO	L	NR	Tensiometer failed
[illegible]	AB	472[illegible]	4[illegible]	[illegible]7	7.5	17.5	37[illegible]	7[illegible]	[illegible],31	ND	NO	N	NR	Cluster Drop
[illegible]	AB	4720	4[illegible]	---	---	[illegible]2	365	[illegible]	[illegible], 2[illegible]	ND	NO	N	NR	Cluster Drop
[illegible]	AB	4[illegible]	[illegible]2[illegible]	---	---	[illegible]5	47[illegible]	[illegible]	[illegible]	ND	NO	N	NR	Cluster Drop
[illegible]	AB	4[illegible]	4[illegible]	---	---	[illegible]5	48[illegible]	[illegible]5	23,15[illegible]	ND	NO	N	NR	Cluster Drop
[illegible]	AB	4[illegible]	4[illegible]	---	---	---	51[illegible]	7025	24,15[illegible]	ND ND	AO NO	M H	NR	s/n #2 Open First s/n #3 slow opening, full at 20.4 sec
[illegible]	AB	24[illegible]5	24[illegible]	---	5.[illegible]	[illegible]2	2[illegible]	4[illegible]	[illegible]	ND	NO	M	NR	Parachute damage 2 gore sections & many small tears
[illegible]	[illegible]	474[illegible]	5[illegible]	4[illegible] 4[illegible]	5.47 5.3	[illegible]12 [illegible]	24[illegible] 2200	74[illegible] 4[illegible]	5[illegible] 42[illegible]	ND	OR OR	H H	NR	Parachute damaged at reefed opening, no full inflation times from load chart
[illegible]	[illegible]	474[illegible]	[illegible]	---	6.5	[illegible]3 [illegible]3	31[illegible] 2[illegible]	54[illegible] 54	53[illegible] [illegible]	ND	NO	N N	NR	Parachutes damaged after landing
[illegible]	[illegible]	474[illegible]	5	---	3.4	[illegible]8 14.4	25[illegible] 38[illegible]	[illegible] [illegible]000	[illegible],4 5[illegible]	ND	NO	N	NR	Telemetering did not function correctly - loads data questionable
[illegible]	[illegible]	474[illegible]	[illegible]	---	---	---	4160 [illegible]78	647 [illegible]	244[illegible] ---	---	---	H H	None	Test vehicle door malfunctioned normal parachute deployment not possible, both canopys badly damaged.
[illegible]	[illegible]	[illegible]	[illegible]	---	4.[illegible]	[illegible]	---	---	---	ND	[illegible]	N	NR	Rear legs of vehicle riser broken when parachute opened. Drone recovered on FWD vehicle riser
[illegible]	[illegible]	474[illegible]	5	2.7	4.[illegible]	[illegible]5	[illegible]	[illegible]	[illegible]	---	NO ---	N N	None	1 extractor parachute not connected to main parachutes. Only 1 parachute deployed - its riser failed

TYPE TEST VEHICLE
AB-Advanced Bomb CBU-Cluster Bomb Unit CD-Single Point Release Octagonal Pilot COP-Cluster with 6 in Octagonal Pilot
CV-Cargo Vehicle LAPES-Low Altitude Parachute Extraction System CPS-Cluster with Pilot & Extract Sys CPS-Cluster with Pilot & Extract Sys
VR-Vehicle Recy Prchts 35 & 78 FLTS CS -Complete System

TEST ASSEMBLYS

INSTRUMENTATION
ET-Exline Tensiometer AA-Air to Air Camera
TM-Telemetry GA-Ground to Air Camera
PT-Photothendolite VA-Vehicle to Air Camera

PERFORMANCE
ND-Normal Deployment L-Light H Heavy
NO-Normal Opening M-Medium N-None
NR-Normal Recovery

GENERAL DROP DATA											TEST ITEMS			INSTRU-MENTATION		TEST EQUIPMENT			TEST RESULTS											
																			TIMES-DROP TO			FORCES			PERFORMANCE				COMMENTS
SRS Drop No	Date	Rl Center Drop No	Test Phase	Drop A/C	Drop Velocity	Velocity at Line Stretch (Calculated)	Drop Altitude	Air Pressure	Air Temperature	Ground Wind	Test Parachute and Assemblies	Reefing Line Length and Line	Parachute System Weight	Force Measurement	Camera	Vehicle Type	Vehicle Weight	Total Drop Weight	Line Stretch	Reefed Open	Full Open	Snatch Force	Reefed Force	Open Force	Deployment	Opening	Aerial Damage	Recovery	
					KIAS	ft/sec	Feet	in Hg	F°	Knots	Type Feet	Inches Sec	Pound				Pound	Pound	Sec	sec	sec	lbs	lbs	lbs					
17	12 5 59	525 F	IH	B-66	150	274	2000	30.16	53	0	ES78 CPS	196 6	170	None	A-A G-A V-A	CV	4748	5000	---	2.5 3.5	12.2 14.3	---	---	---	ND	NO	N	NR	Parachute system recovery completely successful
18	12 14 59	527 F	III	B-47	150	274	2000	30.34	73	0	ES78 CS	196 6	170	None	A-A G-A V-A	DD	4748	4970	---	5.1 4.3	16.3 14.4	---	---	---	ND	NO	N	NR	Parachute system recovery complete successful
19	12 23 59	544 F	IH	B-66	175	320	2000	30.07	54	NW 2	ES78 CPS	196 6	170	TM	A-A G-A V-A	CV	4748	5000	2.22 2.22	3.5 3.6	13.5 15.6	3750 3660	5860 6950	5250 6590	ND	NO	N	NR	Parachute system recovery completely successful
20	1 5 60	13 F 60	IH	B-66	200	363	2000	30.35	37	0	ES78 CPS	196 6	170	None	A-A G-A V-A	CV	4748	4970	---	4.0	---	---	---	---	ND NO D	M ---	---	None	1 prcht not deployed the drogue gun projectile cut the tie to the pilot chute deployment bag the deployed prcht split skirt to apex
21	1 6 60	14 F 60	III	B-47	150	168	2000	30.33	66	0	ES78 CS	196 6	170	TM	A-A G-A V-A	DD	4748	4968	3.75	5.0	---	5700	9100	---	ND ND	NO ---	L N	NR	Reefing line cutters on one prcht not tied off prcht did not disreef other prcht split skirt to apex
22	1 6 60	15 F 60	IH	B-66	200	363	2000	30.21	64	0	ES78 CPS	196 6	170	None	A-A G-A V-A	CV	4748	4970	---	---	13.8 15.9	---	---	---	AND AND	NO NO	L L	NR	Static line did not remove cover drogue guns fired through cover
23	1 14 60	16 F 60	IH	B-66	225	397	2000	30.27	49	SE 2	ES78 CPS	196 6	170	None	A-A G-A V-A	CV	4748	4970	---	4.6 4.6	12.7 22.8	---	---	---	ND	NO	L H	NR	Heavy damage during reefed opening on 1 Main prcht torn gore vent to skirt
24	1 15 60	67 F 60	II	B-66	425	734	3000	28.975	58	NW 8	Ribbon 13.4 (1)	144 6	60	None	A-A G-A V-A	CV	4400	4610	---	---	---	---	---	---	NO ---	NO ---	--- ---	None	Deceleration prcht riser parted at deployment jump riser failed and did not deploy recy prchts (1) vehicle recy prchts-2 ea 16 ft ring slot prchts
25	2 1 60	182 F 60	III	B-47	175	320	2000	28.930	69	SE 7-10	ES78 CS	196 6	164	PT PM	A-A G-A V-A	DD	5018	5208	---	--- 10.4	13.3 15.2	2300	6750	---	ND	NO	L N	NR	Parachute system recovery completely successful
26	2 15 60	223 F 60	III	B-47	175	320	1500	30.18	49	0	ES78 CS	196 6	165	TM PT	A-A G-A V-A	DD	5159	5346	---	14.6 14.6	15.3 15.3	T/M	Failed		ND	NO	N L	NR	Telemetry failed Parachute system recovery completely successful
27	2 2 60	346 F 60	III	B-47	175	320	1300	30.18	51	E 2	ES78 CS	196 6	165	TM PT	A-A G-A V-A	DD	5196	5373	3.5	4.9 4.9	15.4 15.8	4000	6750	---	ND	NO	L L	NR	Parachute system recovery completely successful
28	2 15 60	418 F 60	IB	B-47	200	363	1500	30.25	52	SE 3	ES78 CPS	196 6	165	TM	G-A V-A	CV	4829	5021	3.2 3.2	3.8 3.9	--- 11.9	4600 4400	8800 8000	6500 6800	ND	NO	N	NR	Parachute system recovery completely successful
29	3 15 60	443 F 60	III	B-47	175	320	1500	30.20	85	SE 5	ES78 CS	196 6	165	TM	A-A G-A V-A	DD	5175	5360	3.65	4.5 4.6	14.5 15.9	4300	6600	---	ND	NO	N	NR	Parachute system recovery completely successful
30	3 24 60	523 F 60	IV	B-52	155	303	2300	28.936	73	NW 7	ES78 CS	196 6	165	PT TM	A-A G-A V-A	SD	4690	4875	3.75	4.75	---	5750	11500	---	ND	NO	N	NR	Parachute system recovery completely successful
31	4 4 60	586 F 60	III	B-47	200	363	1500	30.09	86	S 3	ES78 CS	196 6	165	---	---	DD	1575	5360	---	3.8 3.8	13.7 14.0	5000	8400	---	ND	NO	N	NR	Parachute system recovery completely successful
32	4 5 60	562 F 60	IB	B-66	180	346	1500	30.09	76	W 3	ES78 CPS	196 6	165	TM	---	CV	4844	5021	3.5 3.4	4.3 3.8	---	3800 4200	7800 8400	5800 5800	ND	NO	N	NR	Parachute system recovery completely successful

Figure 29

Aerial Drop Test Summary, USD-5

TYPE TEST VEHICLE

TEST ASSEMBLYS
COP-Cluster with 68ft Octagonal Pt
CPE-Cluster with Pilot & Extract Sys

INSTRUMENTATION
ET-Extra Tensiometer
TM-Telemetry
PT-Phototheodolite
AA-Air to Air Camera
GA-Ground to Air Camera
VA-Vehicle to Air Camera

PERFORMANCE
ND-Normal Deployment
NO-Normal Opening
NR-Normal Recovery

DAMAGE
L-Light
M-Medium
H-Heavy
N-None

GENERAL DROP DATA											TEST ITEMS			INSTRUMENTATION		TEST EQUIPMENT			TEST RESULTS										
																			TIMES-DROP TO			FORCES			PERFORMANCE				COMMENTS
SRS Drop No	Date	Ex Centro Drop No	Test Phase	Drop A/C	Drop Velocity	Velocity at Line Stretch (Calculated)	Drop Altitude	S.L. Pressure	S.L. Temperature	Ground Wind	Test Parachute and Assembly	Reefing Line Length and Time	Parachute System Weight	Force Measurement	Camera	Vehicle Type	Vehicle Weight	Total Drop Weight	Line Stretch	Reefed Open	Full Open	Stretch Force	Reefed Force	Open Force	Deployment	Opening	Aerial Damage	Recovery	
					KIAS	ft/sec	Feet	In Hg	F	Knots	Type Feet	Inches Sec.	Pounds				Pounds	Pounds	Sec.	Sec.	Sec.	lbs.	lbs.	lbs.					
11	[illegible]	562 F[illegible]	IV	B-52	[illegible]	34[illegible]	[illegible]2	2[illegible]	4	[illegible]	ES[illegible]	[illegible]	[illegible]65	TM PT	A-A G-A V-A	SD	46[illegible]	4875	3.5	4.4	---	72[illegible]	[illegible]4,800	---	ND	NO	N	NR	Parachute system recovery completely successful last SRS test.

Figure [illegible]

Aerial Drop Test Summary, USD-5

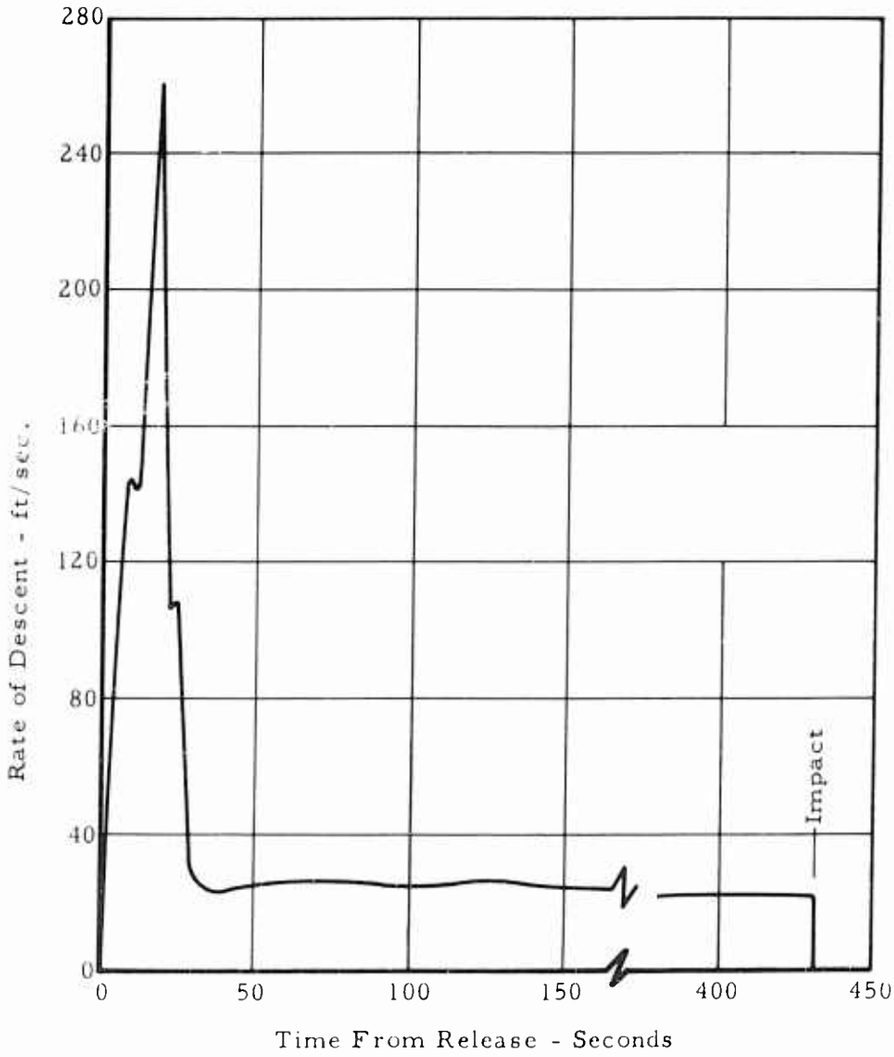

Figure 31 Rate of Descent vs. Time, USD-5 Test No. 45

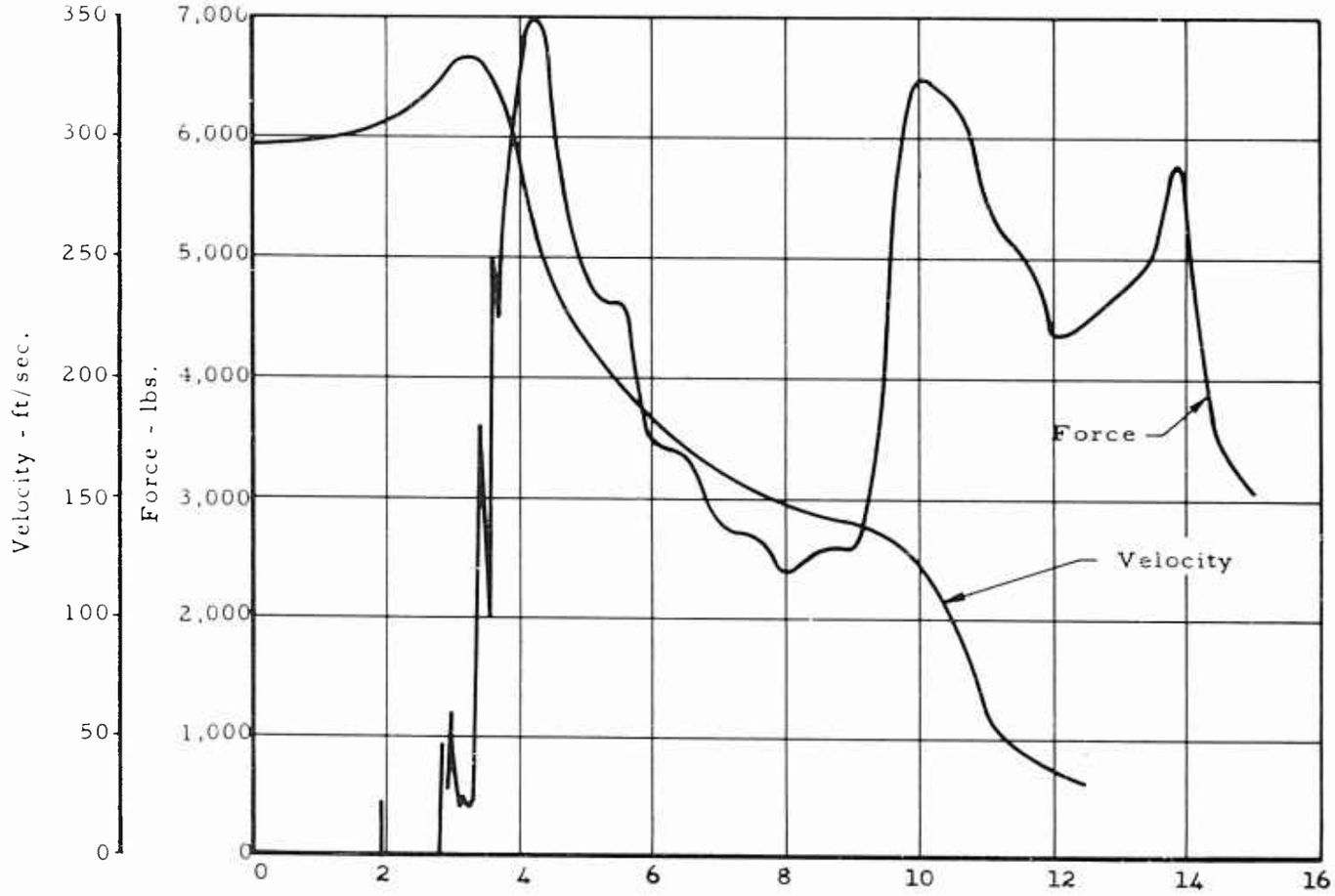

Figure 52 Force - Velocity - Time Profile, USD-5 Test No. 19-1

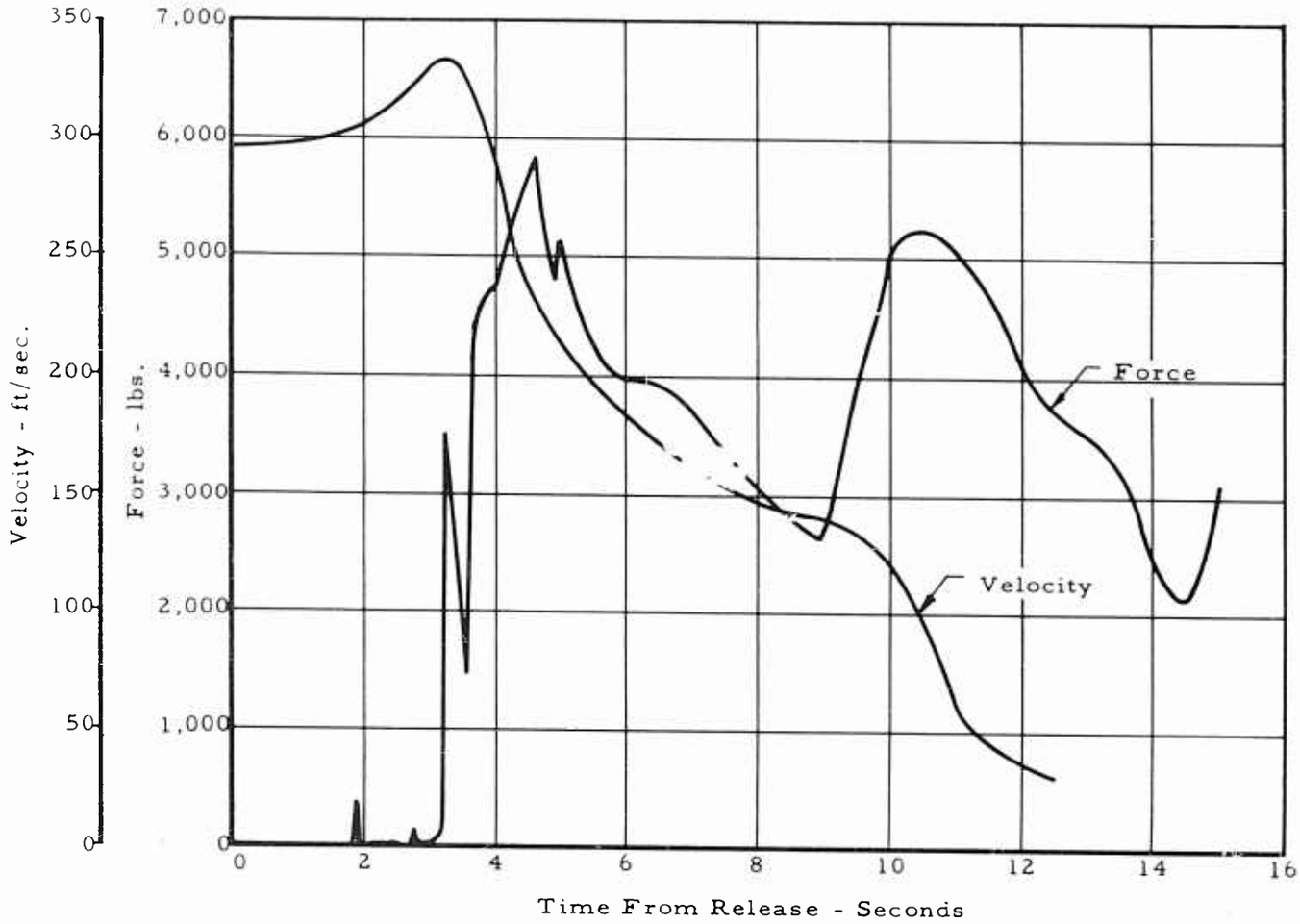

Figure 33 Force - Velocity - Time Profile, USD-5 Test No. 19-2

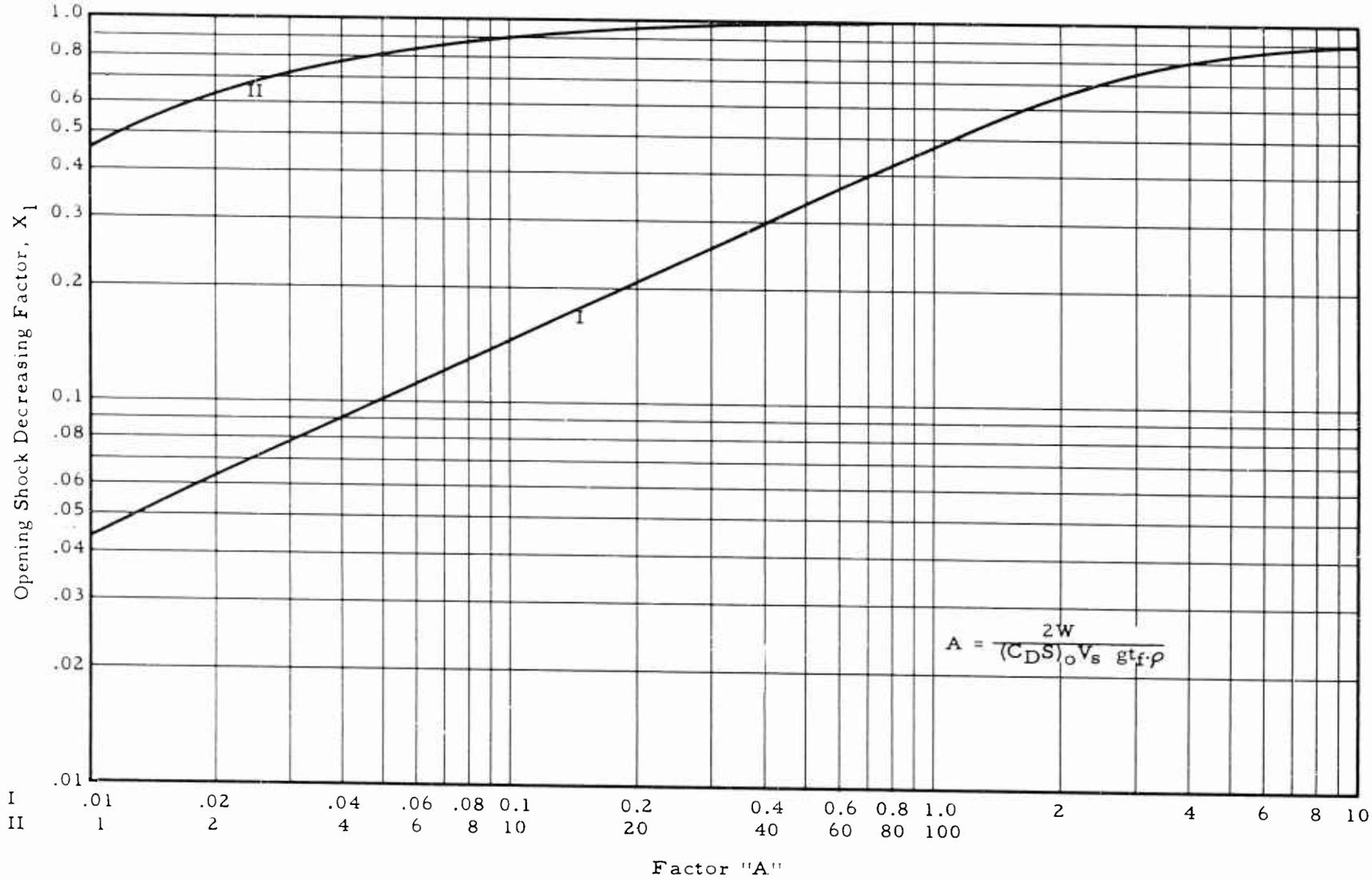

Figure 34 Opening Shock Decreasing Factor, X_1, Vs. Factor "A"

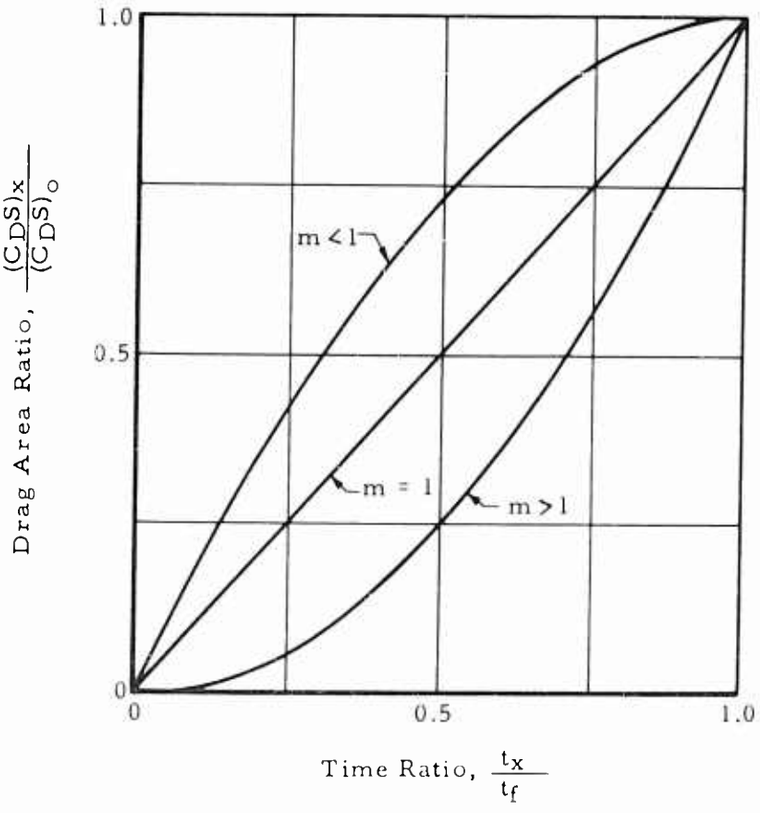

Figure 35 Typical Parachute Drag Area Growth Curves

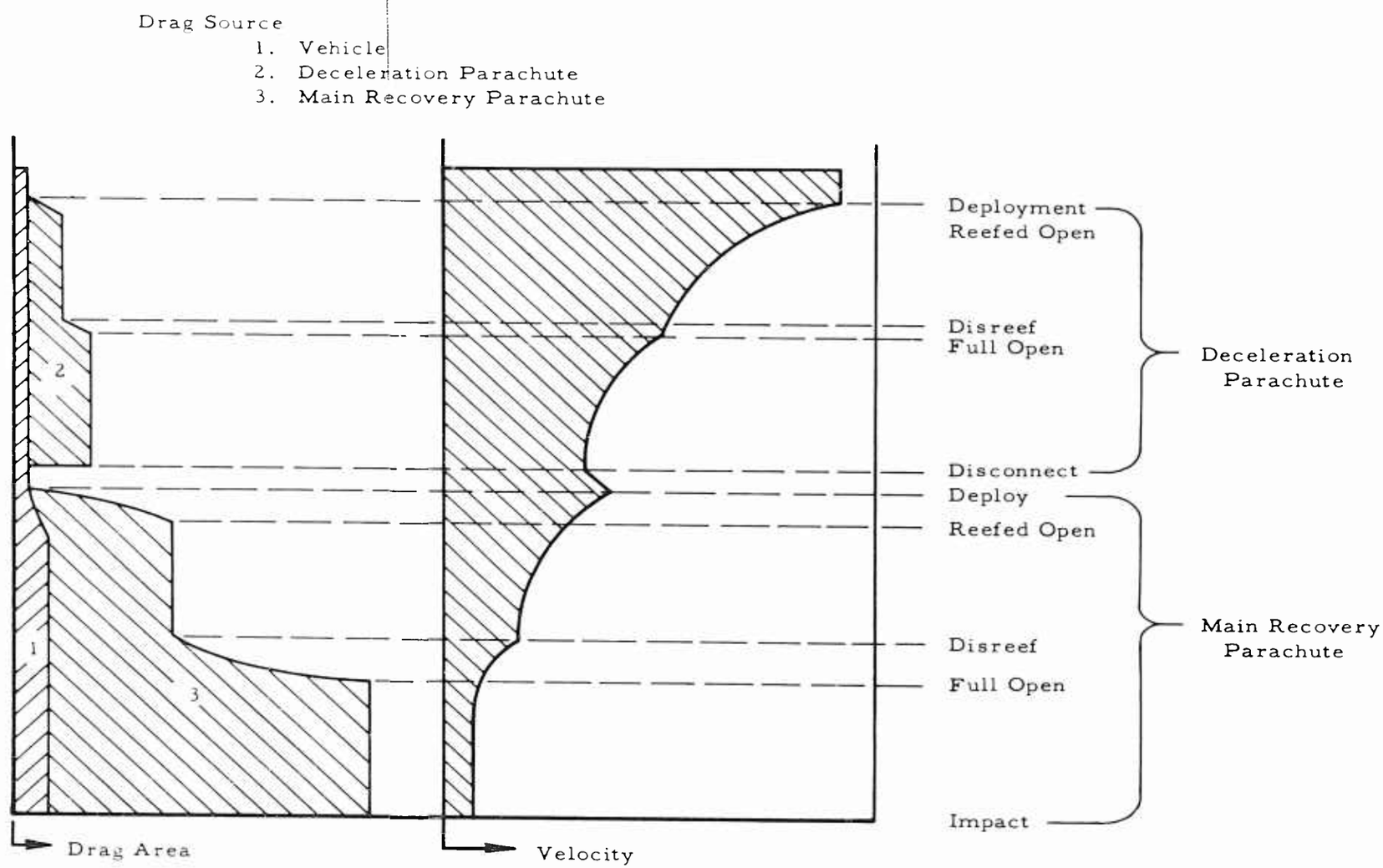

Figure 36 Typical Drag Area - Velocity - Time History of Multiple Stage Parachute Recovery System

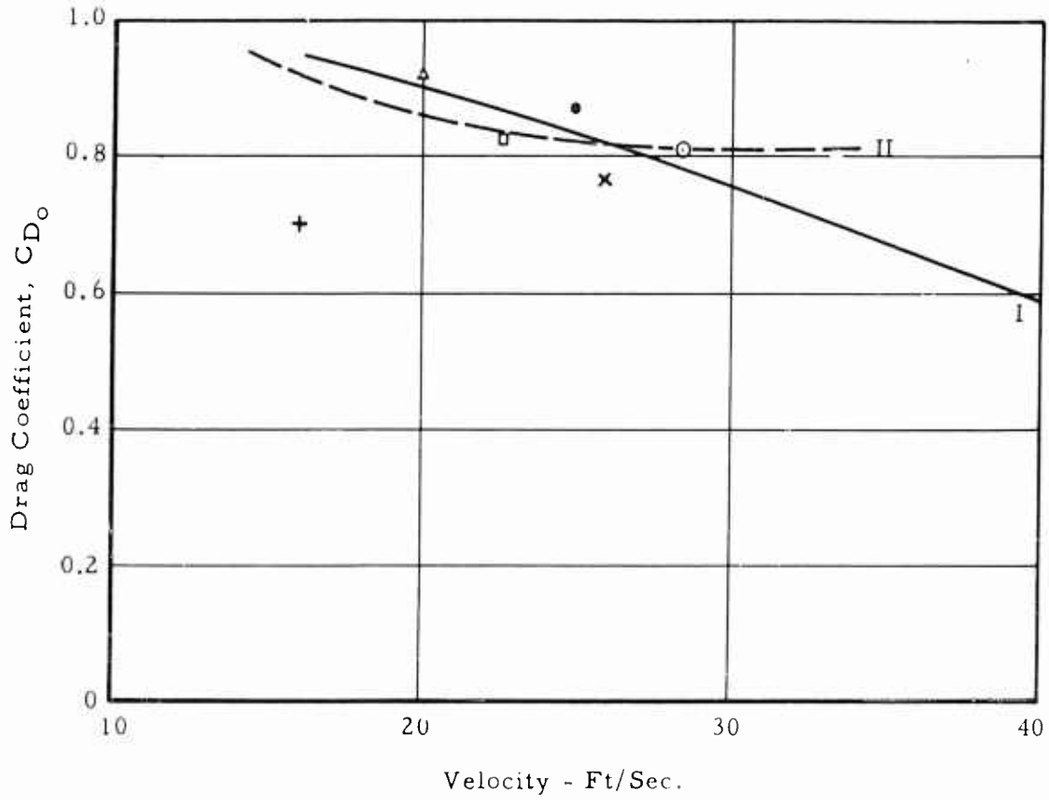

Symbol	Diameter, D_o, Ft.	Parachute Type	Use	Remarks
○	34.5	10% E.S.	B-70	Avg 6 tests
●	38	10% E.S.	B-70	Avg 8 tests
×	71	Full E.S.	USD-5	Cluster (2)
□	78	Full E.S.	USD-5	Cluster (2)
△	28	Mod. E.S.	Nike	---
+	35	10% E.S.	MC-1	---
I	67	Full E.S.	---	Refs 7 & 8
II	11.9	10% E.S.	---	Ref. 4

Figure 37 Drag Coefficient vs. Velocity for Extended Skirt Parachutes

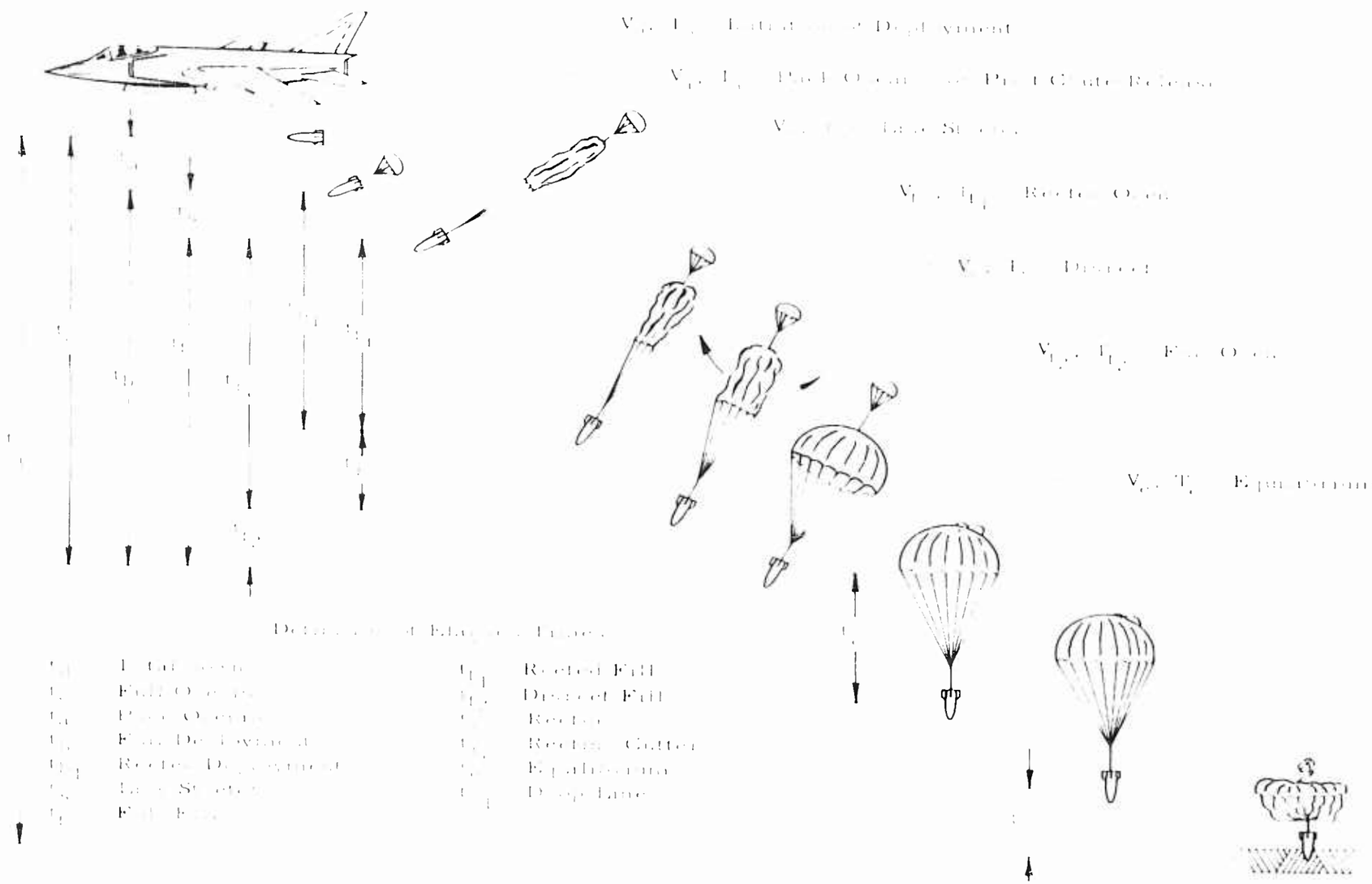

Figure 38 Nomenclature for Opening of Parachutes

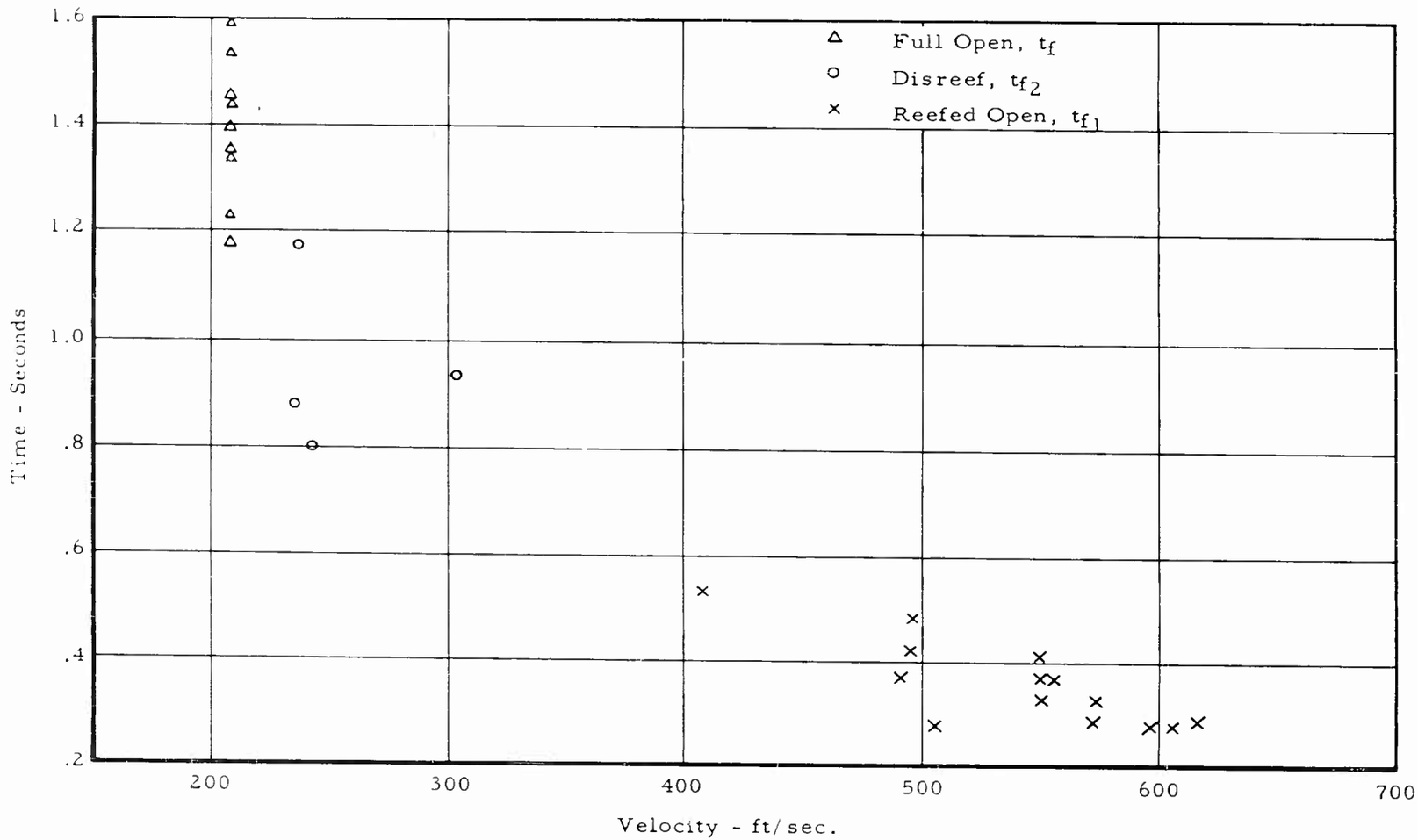

Figure 39 Filling Times vs. Velocity, B-70, 34.5 ft. Diameter, Extended Skirt Parachute

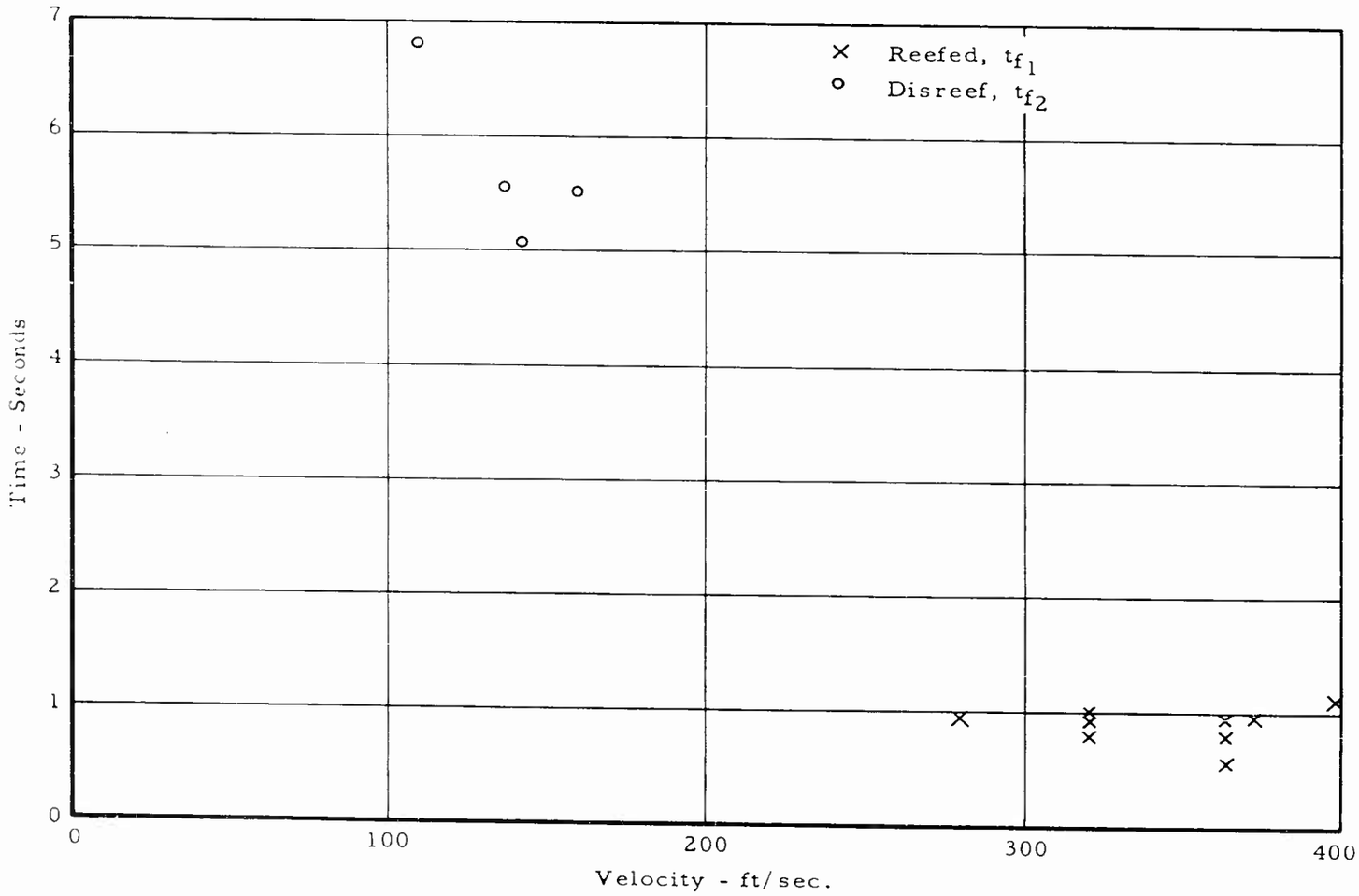

Figure 40 Filling Times vs. Velocity, USD-5, 78-foot Diameter, Extended Skirt Parachute

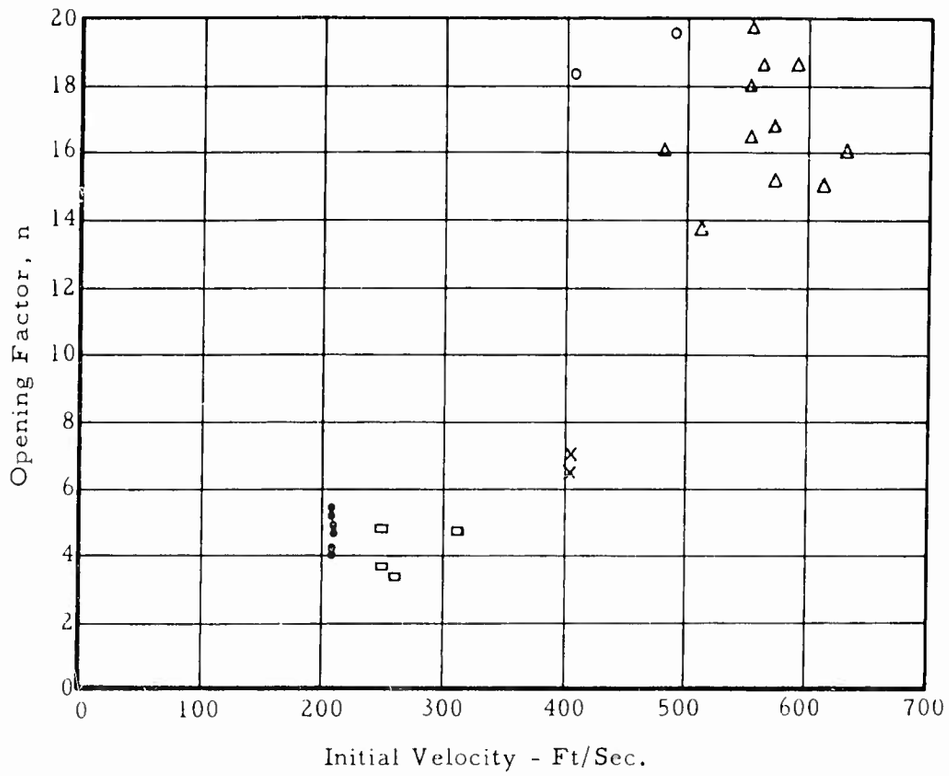

Symbol	Diameter, D_o	Type of Opening
△	34.5	Reefed
○	35.5	Reefed
▭	34.5	Disreef
×	35.5	Unreefed
•	38	Unreefed

Figure 41 Opening Factor vs. Velocity, B-70, Extended Skirt Parachute

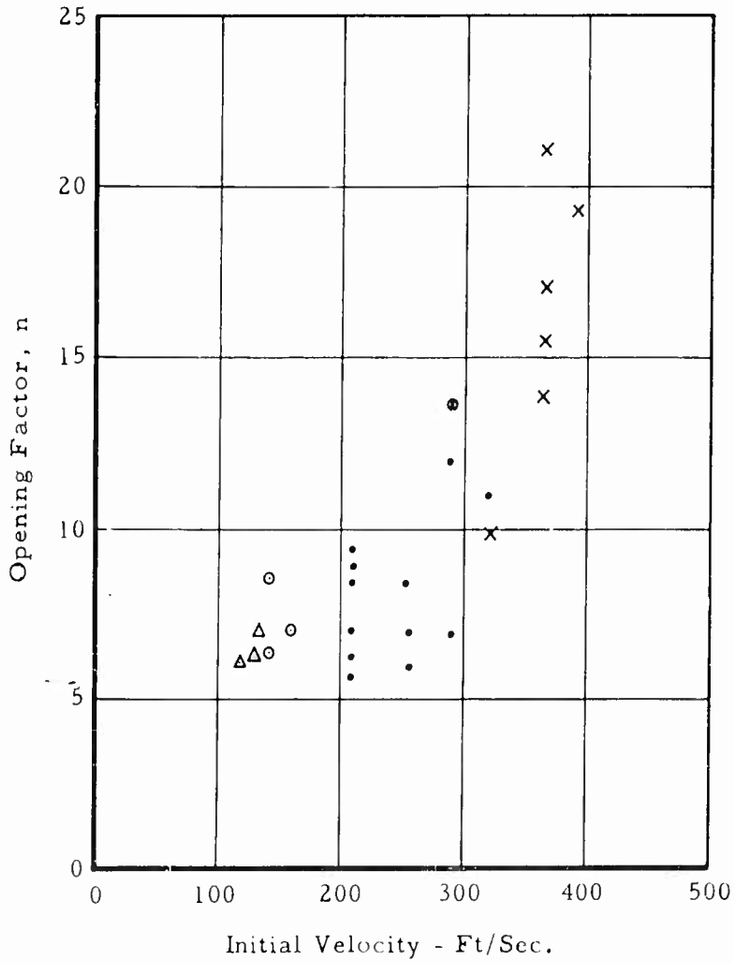

Symbol	Diameter, Do, Ft.	Type of Opening
•	71	Reefed
×	78	Reefed
o	71	Disreef
Δ	78	Disreef

Figure 42 Opening Factor vs. Velocity, USD-5, Extended Skirt Parachute

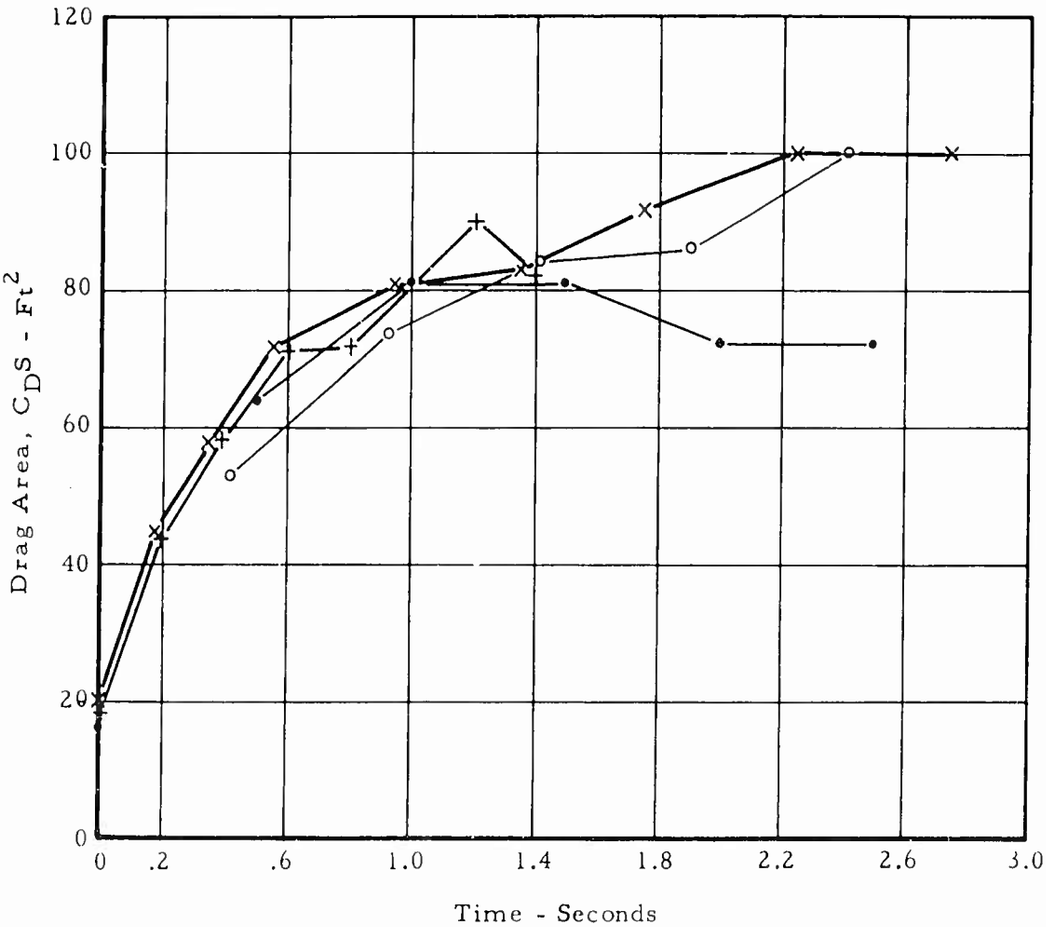

Symbol	Test No.	Diameter, D_o, Feet	Reefing Line Length - Ins
•	12	71	240
×	13	71	240
+	16	78	160
○	19	78	196

Figure 43 Drag Area Increase vs. Time for Reefed Opening, USD-5 Tests

Drag Area - Filling Time Relationships

$$t_{f_1} = \frac{n}{V_s \cdot g} \times D_o \left[\frac{(C_DS)_R}{(C_DS)_o}\right]^{1/2}$$

$$t_{f_2} = \frac{n}{V_s \cdot g} \times D_o \left[\frac{(C_DS)_o - (C_DS)_R}{(C_DS)_o}\right]^{1/2}$$

$$(C_DS)_{x_1} = (C_DS)_R \left[\frac{t_{x1}}{t_{f_1}}\right]^{m_1}$$

$$(C_DS)_{x_2} = (C_DS)_R + \left[(C_DS)_o - (C_DS)_R\right] \times \left[\frac{t_{x2}}{t_{f_2}}\right]^{m_2}$$

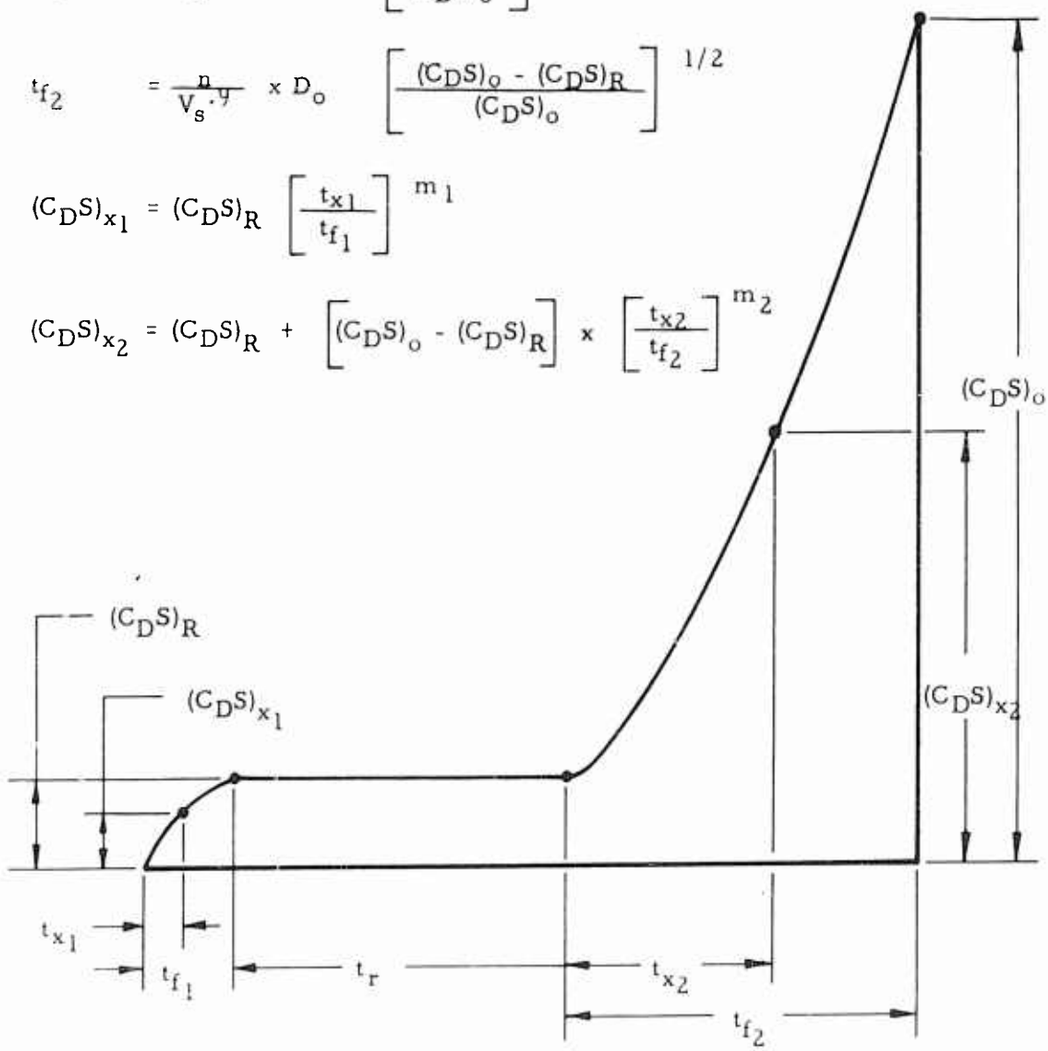

Figure 44 General Relationships for Parachute Opening with Single Stage Reefing

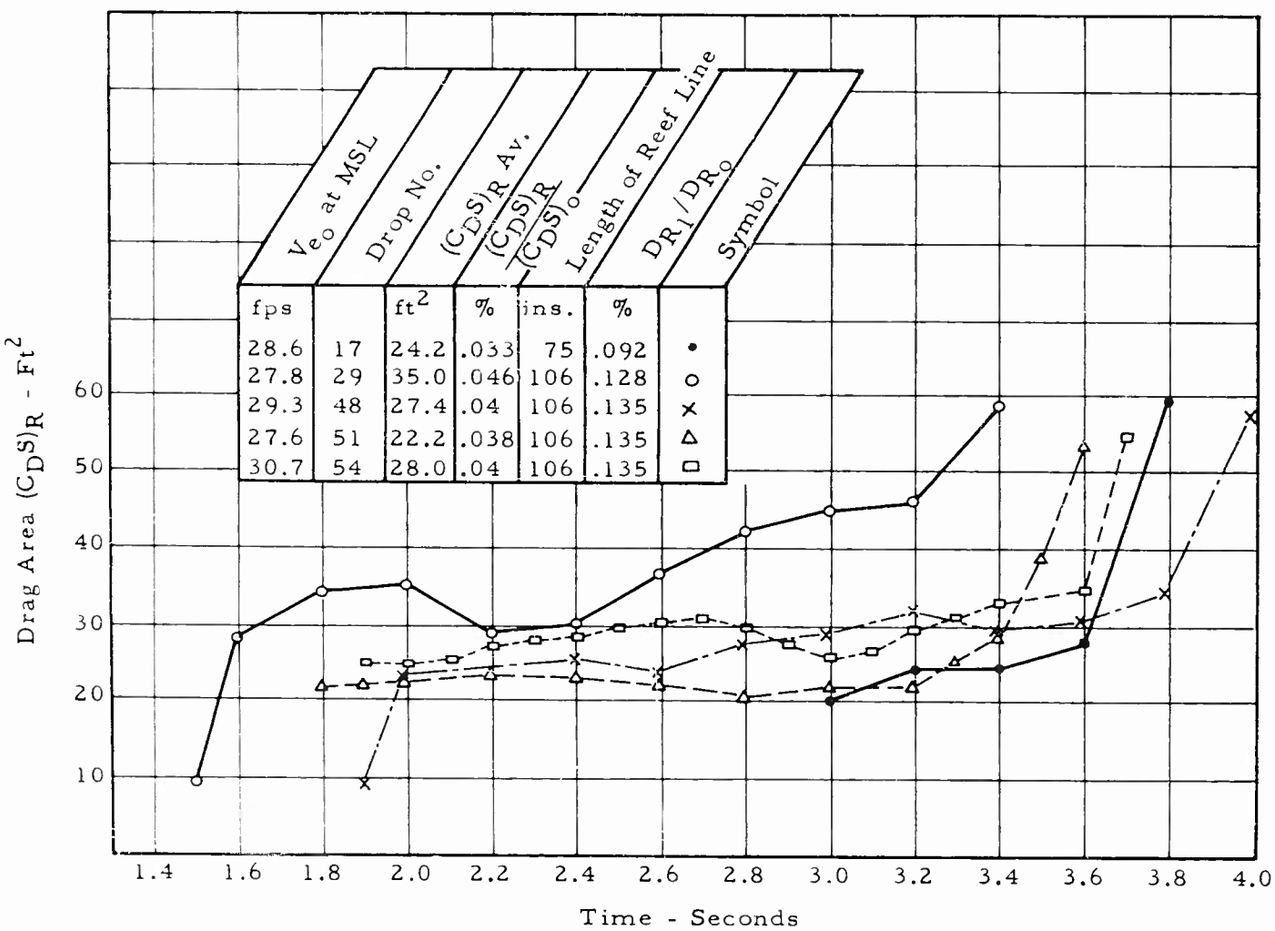

Figure 45 Drag Area Increase vs. Time to Disreef, B-70 Tests

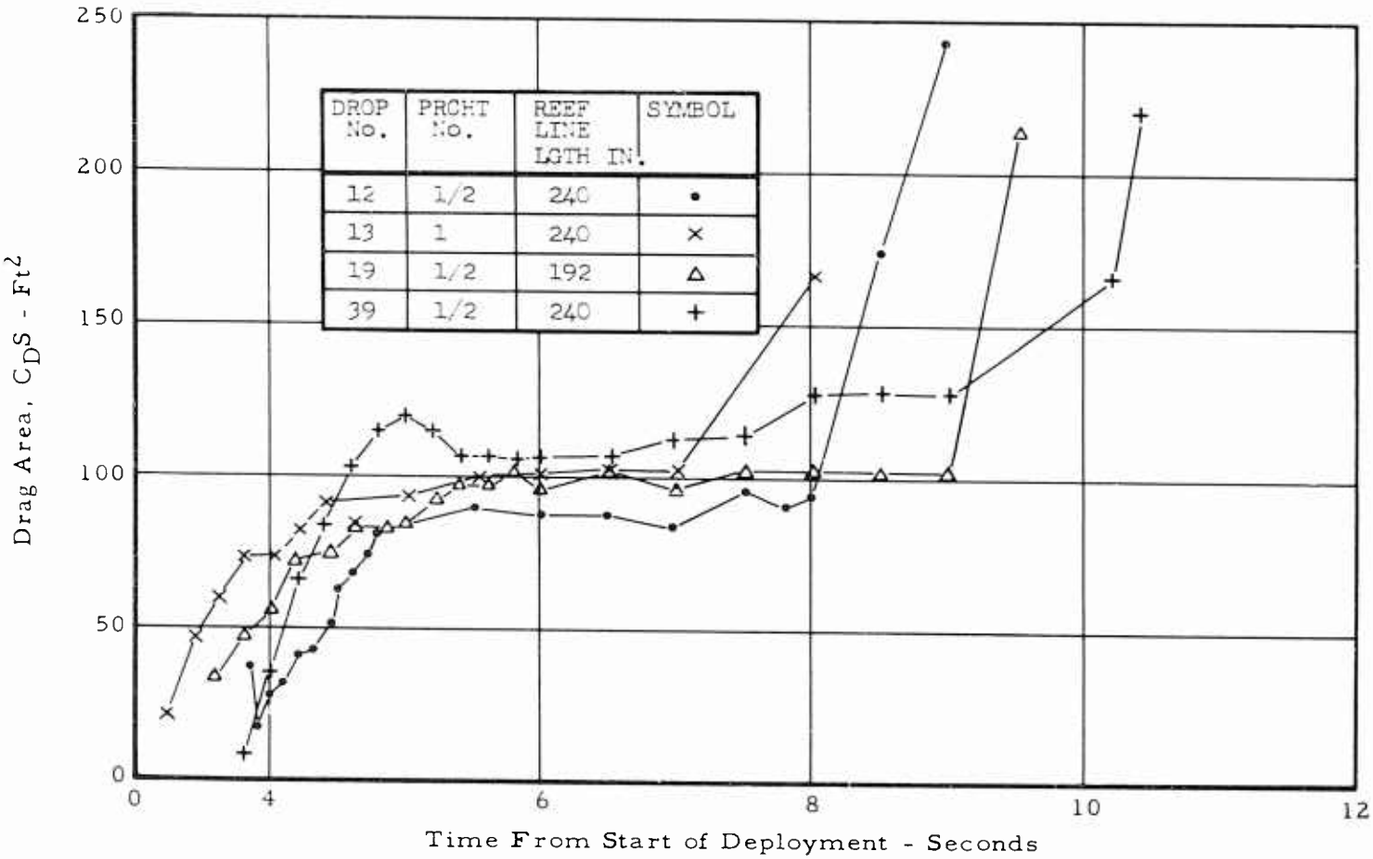

Figure 46 Drag Area vs. Time During Reefed Opening, USD-5 Tests

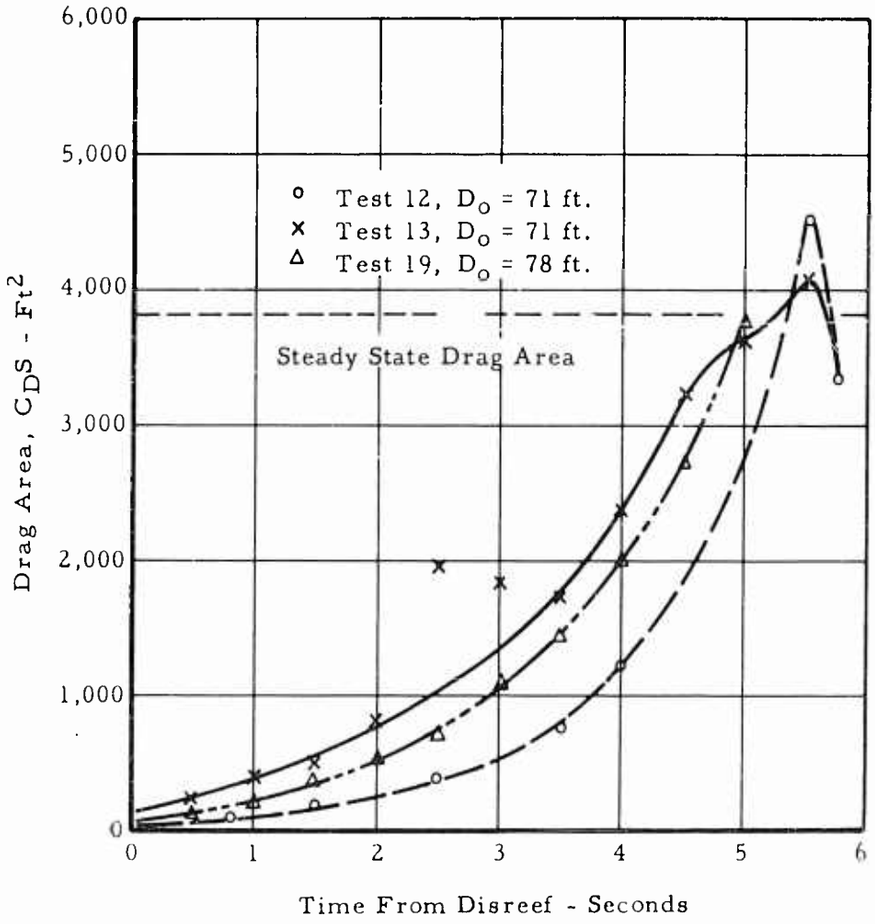

Figure 47 Drag Area vs. Time From Disreef to Full Open, USD-5 Tests

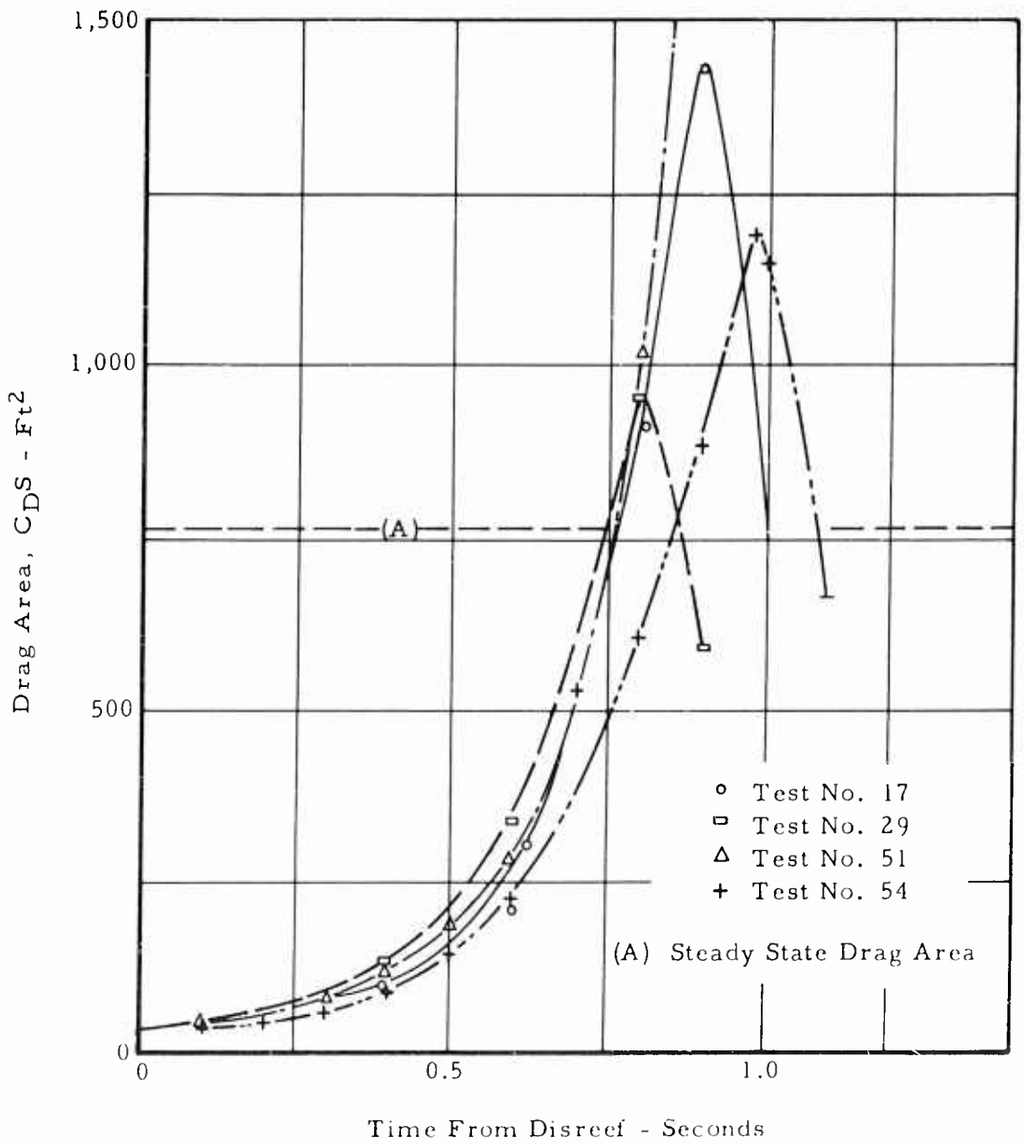

Figure 48 Drag Area vs. Time From Disreef to Full Open, B-70 Tests

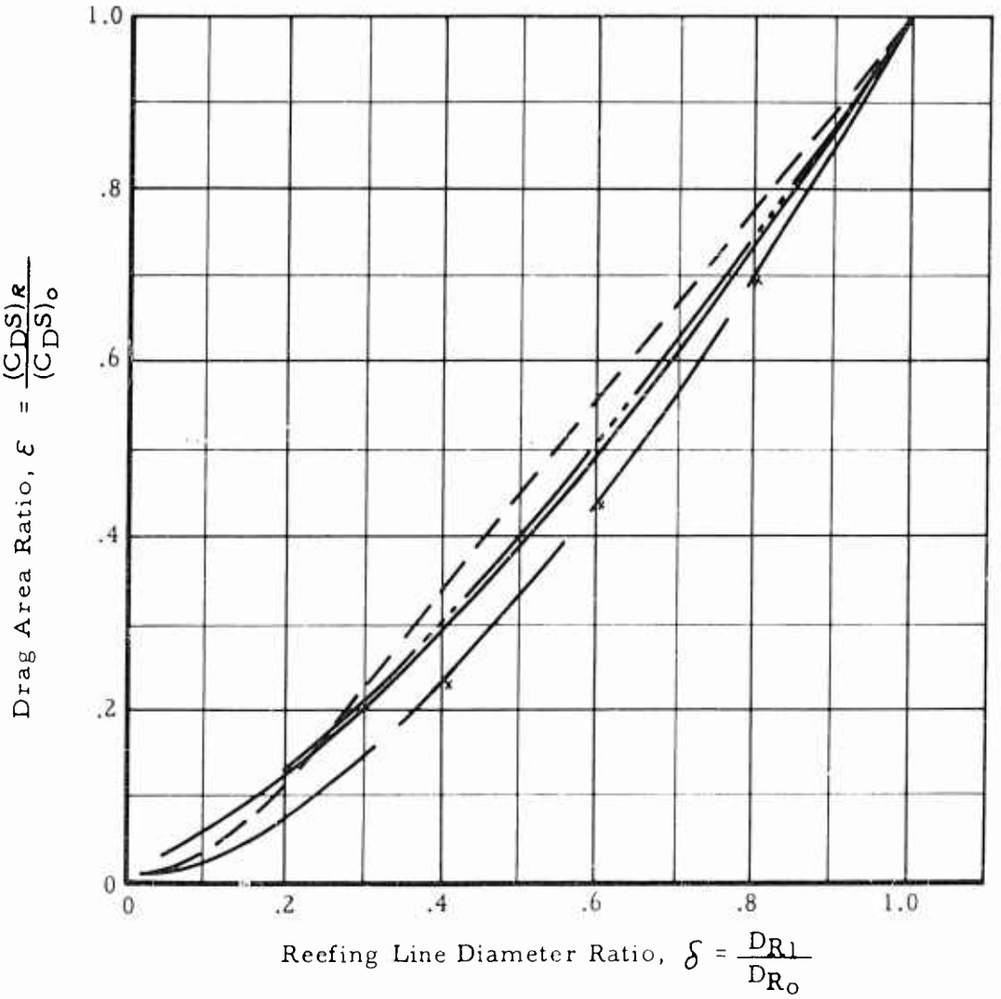

Figure 49 Drag Area Ratio vs. Reefing Line Diameter Ratio

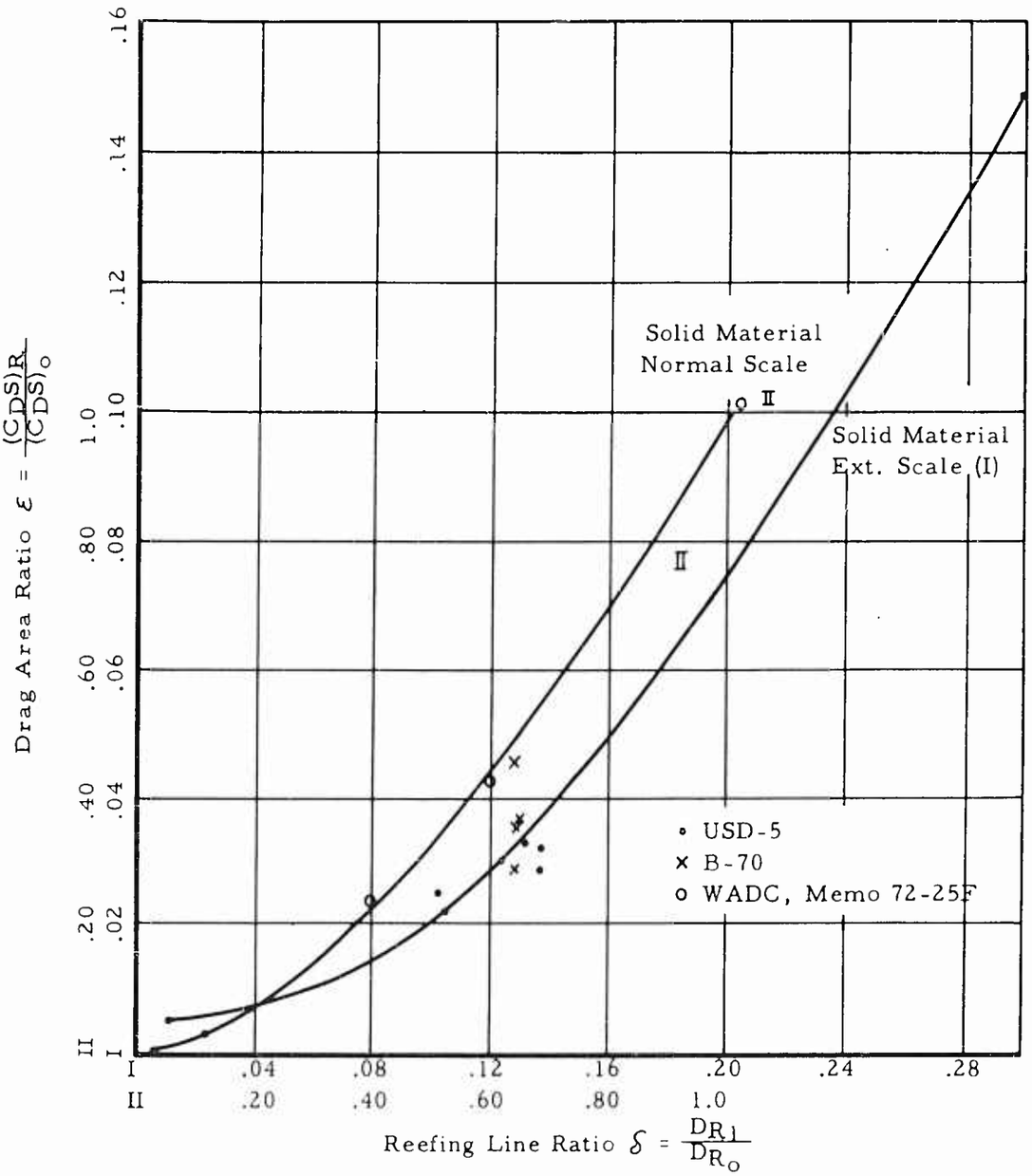

Figure 50 Drag Area Ratio vs. Reefing Line Diameter Ratio

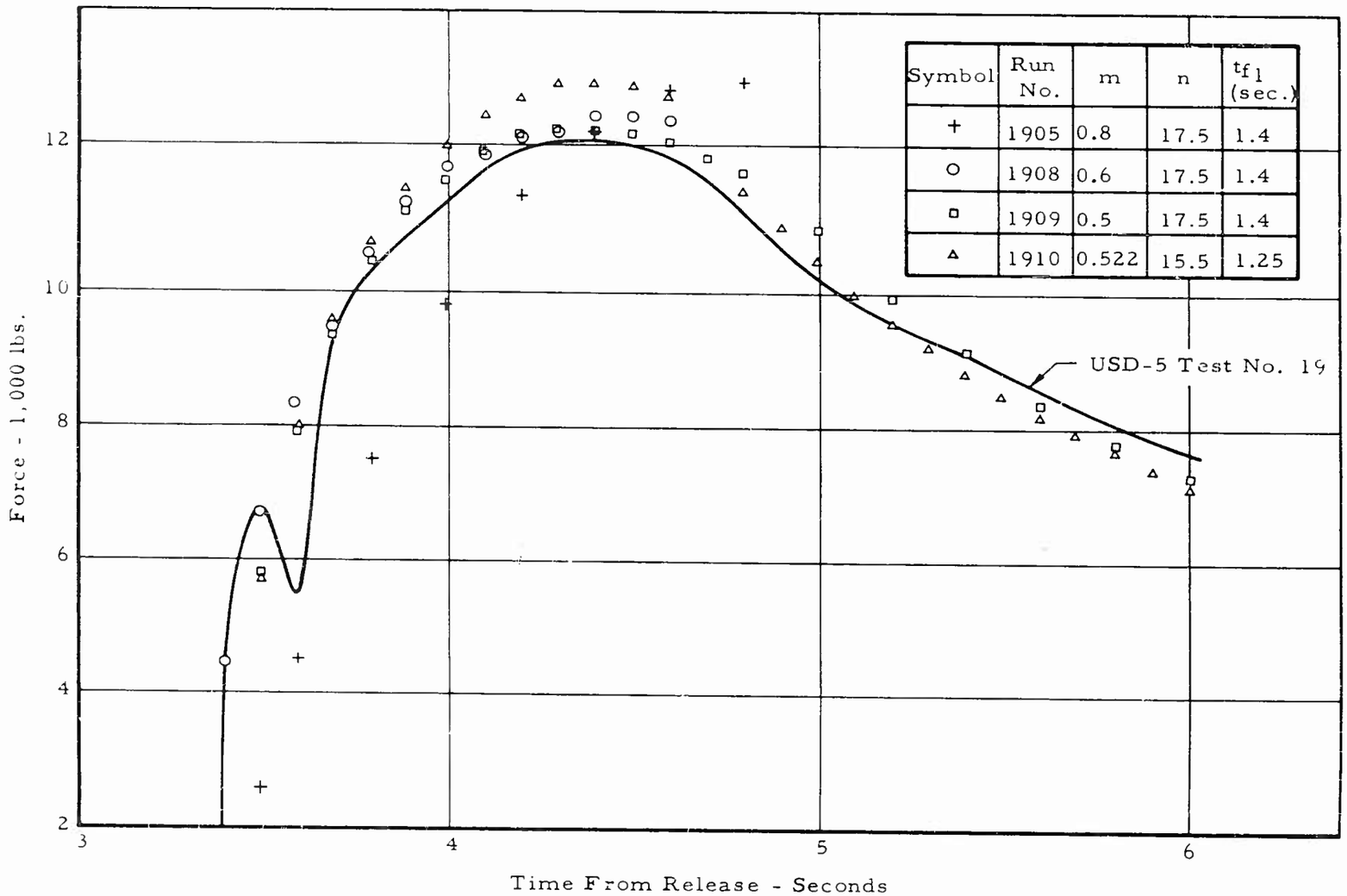

Figure 51 Comparison of Computed and Actual Force Data for Parachute Opening into the Reefed Condition

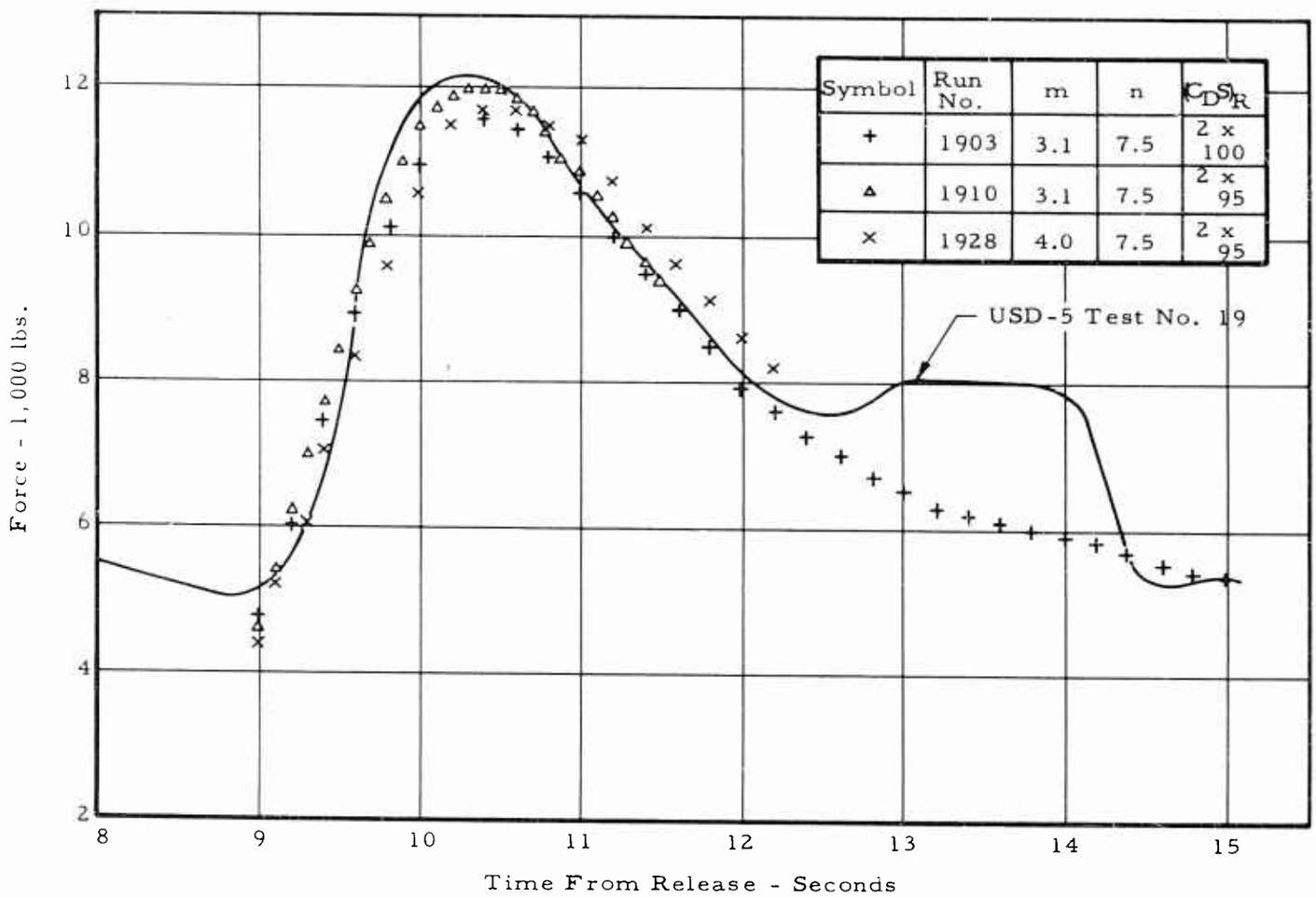

Figure 52 Comparison of Computed and Actual Force Data for Parachute Opening From Disreef to Full Open

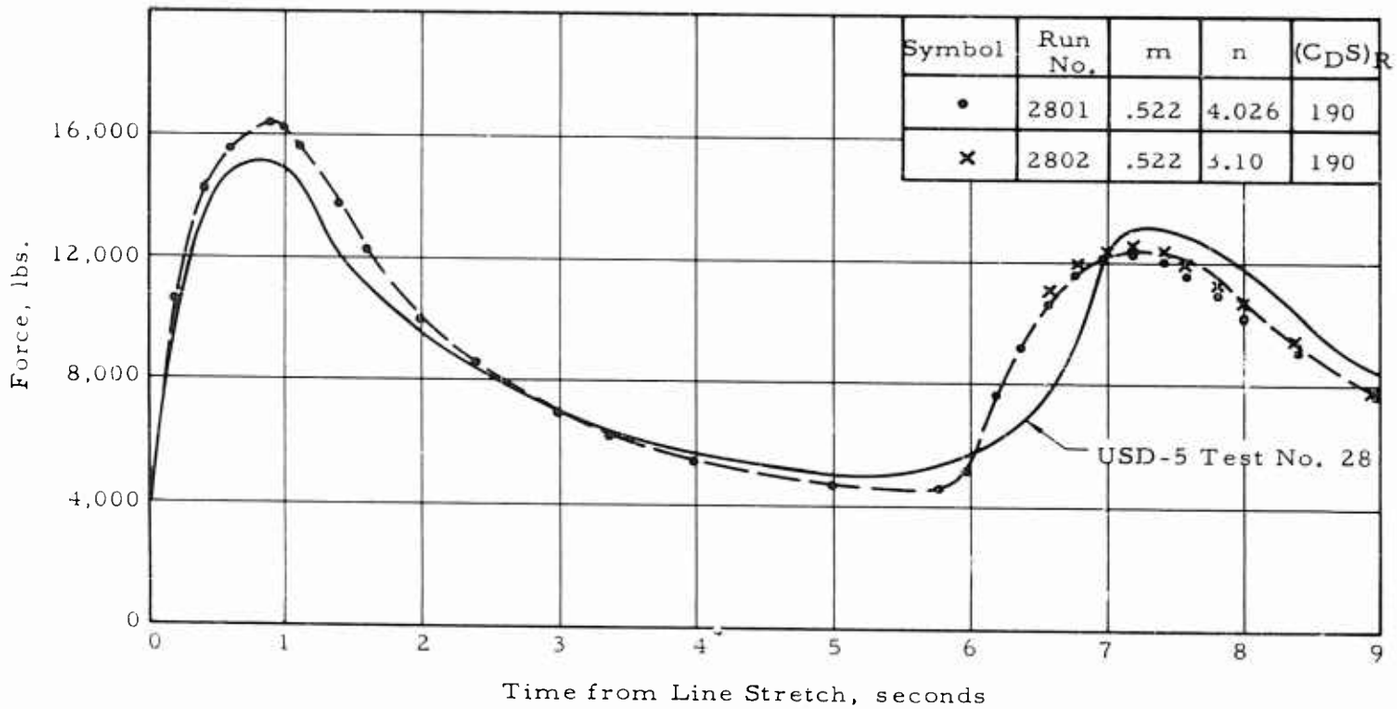

Figure 53 Comparison of Computed and Actual Force Data for Parachute Opening

REFERENCES

1. "Analysis of Parachute Qualification Tests for B-70 Encapsulated Seat", SRS Report 147-588

2. E. A. Gimalouski, "Development of a Final Stage Recovery System for a 10,000 Pound Weight", WADC Technical Report 59-109

3. E. G. Ewing, "Ring Sail Parachute Characteristics", Radioplane Report No. PTM-323-A

4. "USAF Parachute Handbook", WADC Technical Report 55-265

5. "Handbook of Astronautical Engineering", Chapter 22.5, McGraw-Hill Book Company

6. E. Pflanz, "Determination of the Retarding Forces in Unfolding Large Parachutes", (Translation), Part I, Report F-TS-811, ATI 26111, Part II, Report F-TS-3189, ATI 20126

7. "Parachute Recovery System Test for USAF Q-2B Drone", AFFTC Technical Note 59-11

8. "67.3-Foot Nominal Diameter Fully Extended Skirt Parachute", AFFTC Technical Note 55-9

Aeronautical Systems Division, Dir/Aeromechanics, Flight Accessories Lab, Wright-Patterson AFB, Ohio. Rpt Nr ASD TDR-62-75. DESIGN ANALYSIS OF FINAL RECOVERY PARACHUTES B-70 ENCAPSULATED SEAT AND THE USD-5 DRONE. Final report, Apr 62, 103p incl illus., 8 refs.

Unclassified Report

A performance analysis was conducted on two parachute recovery systems developed by Space Recovery Systems, Inc., for the North American Aviation B-70 encapsulated seat and the Fairchild Stratos Corp. USD-5 surveillance drone. Optimization of aerodynamic and textile design, controlled deployment and opening, and use of a cluster of two independently deployed parachutes for the USD-5 drone resulted in a highly predictable performance, in the highest known drag area per weight ratio for the

(over)

USD-5 system, and a high velocity capability for the B-70 system.

Equations were developed through data analysis for the opening process and the drag area increase versus time during parachute opening for extended skirt parachutes. These equations permitted a computer analysis of the total parachute deceleration process with computer results showing less than 10% deviation from actual test data. The developed computer method may well be suitable for performance analysis of recovery processes using ribbon, ring slot, and other solid material type parachutes.

1. Aerial delivery
2. Recovery parachute performance analysis
3. Computer approach to parachute performance analysis
I. AFSC Project 6065, Task 606503
II. Contract AF33(616)-8371
III. Space Recovery Systems, Inc, El Segundo, Calif.
IV. T.W. Knacke and L.I. Dimmick
V. In ASTIA collection
VI. Not Aval fr OTS

Aeronautical Systems Division, Dir/Aeromechanics, Flight Accessories Lab, Wright-Patterson AFB, Ohio. Rpt Nr ASD-TDR-62-75. DESIGN ANALYSIS OF FINAL RECOVERY PARACHUTES B-70 ENCAPSULATED SEAT AND THE USD-5 DRONE. Final report, Apr 62, 103p incl illus., 8 refs.

Unclassified Report

A performance analysis was conducted on two parachute recovery systems developed by Space Recovery Systems, Inc., for the North American Aviation B-70 encapsulated seat and the Fairchild Stratos Corp. USD-5 surveillance drone. Optimization of aerodynamic and textile design, controlled deployment and opening, and use of a cluster of two independently deployed parachutes for the USD-5 drone resulted in a highly predictable performance, in the highest known drag area per weight ratio for the

(over)

USD-5 system, and a high velocity capability for the B-70 system.

Equations were developed through data analysis for the opening process and the drag area increase versus time during parachute opening for extended skirt parachutes. These equations permitted a computer analysis of the total parachute deceleration process with computer results showing less than 10% deviation from actual test data. The developed computer method may well be suitable for performance analysis of recovery processes using ribbon, ring slot, and other solid material type parachutes.

1. Aerial delivery
2. Recovery parachute performance analysis
3. Computer approach to parachute performance analysis
I. AFSC Project 6065, Task 606503
II. Contract AF33(616)-8371
III. Space Recovery Systems, Inc, El Segundo, Calif.
IV. T.W. Knacke and L.I. Dimmick
V. In ASTIA collection
VI. Not Aval fr OTS

Aeronautical Systems Division, Dir/ Aeromechanics, Flight Accessories Lab, Wright-Patterson AFB, Ohio. Rpt Nr ASD TDR 62-75. DESIGN ANALYSIS OF FINAL RECOVERY PARACHUTES B-70 ENCAPSULATED SEAT AND THE USD-5 DRONE. Final report, Apr 62, 103 p incl illus., 8 refs.

Unclassified Report

A performance analysis was conducted on two parachute recovery systems developed by Space Recovery Systems, Inc., for the North American Aviation B-70 encapsulated seat and the Fairchild Stratos Corp. USD-5 surveillance drone. Optimization of aerodynamic and textile design, controlled deployment and opening, and use of a cluster of two independently deployed parachutes for the USD-5 drone resulted in a highly predictable performance, in the highest known drag area per weight ratio for the

(over)

USD-5 system, and a high velocity capability for the B-70 system.

Equations were developed through data analysis for the opening process and the drag area increase versus time during parachute opening for extended skirt parachutes. These equations permitted a computer analysis of the total parachute deceleration process with computer results showing less than 10% deviation from actual test data. The developed computer method may well be suitable for performance analysis of recovery processes using ribbon, ring slot, and other solid material type parachutes.

1. Aerial delivery
2. Recovery parachute performance analysis
3. Computer approach to parachute performance analysis
I. AFSC Project 6065, Task 606503
II. Contract AF33(616)-8371
III. Space Recovery Systems, Inc, El Segundo, Calif.
IV. T.W. Knacke and L.I. Dimmick
V. In ASTIA collection
VI. Not Aval fr OTS

Aeronautical Systems Division, Dir/ Aeromechanics, Flight Accessories Lab, Wright-Patterson AFB, Ohio. Rpt Nr ASD-TDR-62-75. DESIGN ANALYSIS OF FINAL RECOVERY PARACHUTES B-70 ENCAPSULATED SEAT AND THE USD-5 DRONE. Final report, Apr 62, 103 p incl illus., 8 refs.

Unclassified Report

A performance analysis was conducted on two parachute recovery systems developed by Space Recovery Systems, Inc., for the North American Aviation B-70 encapsulated seat and the Fairchild Stratos Corp. USD-5 surveillance drone. Optimization of aerodynamic and textile design, controlled deployment and opening, and use of a cluster of two independently deployed parachutes for the USD-5 drone resulted in a highly predictable performance, in the highest known drag area per weight ratio for the

(over)

USD-5 system, and a high velocity capability for the B-70 system.

Equations were developed through data analysis for the opening process and the drag area increase versus time during parachute opening for extended skirt parachutes. These equations permitted a computer analysis of the total parachute deceleration process with computer results showing less than 10% deviation from actual test data. The developed computer method may well be suitable for performance analysis of recovery processes using ribbon, ring slot, and other solid material type parachutes.

1. Aerial delivery
2. Recovery parachute performance analysis
3. Computer approach to parachute performance analysis
I. AFSC Project 6065, Task 606503
II. Contract AF33(616)-8371
III. Space Recovery Systems, Inc, El Segundo, Calif.
IV. T.W. Knacke and L.I. Dimmick
V. In ASTIA collection
VI. Not Aval fr OTS

Aeronautical Systems Division, Dir/ Aeromechanics, Flight Accessories Lab, Wright Patterson AFB, Ohio. Rpt Nr ASD-TDR-62-75. DESIGN ANALYSIS OF FINAL RECOVERY PARACHUTES B-70 ENCAPSULATED SEAT AND THE USD-5 DRONE. Final report, Apr 62, 103p incl illus., 8 refs.

Unclassified Report

A performance analysis was conducted on two parachute recovery systems developed by Space Recovery Systems, Inc., for the North American Aviation B-70 encapsulated seat and the Fairchild Stratos Corp. USD-5 surveillance drone. Optimization of aerodynamic and textile design, controlled deployment and opening, and use of a cluster of two independently deployed parachutes for the USD-5 drone resulted in a highly predictable performance, in the highest known drag area per weight ratio for the

(over)

USD-5 system, and a high velocity capability for the B-70 system.

Equations were developed through data analysis for the opening process and the drag area increase versus time during parachute opening for extended skirt parachutes. These equations permitted a computer analysis of the total parachute deceleration process with computer results showing less than 10% deviation from actual test data. The developed computer method may well be suitable for performance analysis of recovery processes using ribbon, ring slot, and other solid material type parachutes.

1. Aerial delivery
2. Recovery parachute performance analysis
3. Computer approach to parachute performance analysis
I. AFSC Project 6065, Task 606503
II. Contract AF33(616)-8371
III. Space Recovery Systems, Inc, El Segundo, Calif.
IV. T.W. Knacke and L.I. Dimmick
V. In ASTIA collection
VI. Not Aval fr OTS

Aeronautical Systems Division, Dir/ Aeromechanics, Flight Accessories Lab, Wright-Patterson AFB, Ohio. Rpt Nr ASD-TDR-62-75. DESIGN ANALYSIS OF FINAL RECOVERY PARACHUTES B-70 ENCAPSULATED SEAT AND THE USD-5 DRONE. Final report, Apr 62, 103 p. incl illus., 8 refs.

Unclassified Report

A performance analysis was conducted on two parachute recovery systems developed by Space Recovery Systems, Inc., for the North American Aviation B-70 encapsulated seat and the Fairchild Stratos Corp. USD-5 surveillance drone. Optimization of aerodynamic and textile design, controlled deployment and opening, and use of a cluster of two independently deployed parachutes for the USD-5 drone resulted in a highly predictable performance, in the highest known drag area per weight ratio for the

(over)

USD-5 system, and a high velocity capability for the B-70 system.

Equations were developed through data analysis for the opening process and the drag area increase versus time during parachute opening for extended skirt parachutes. These equations permitted a computer analysis of the total parachute deceleration process with computer results showing less than 10% deviation from actual test data. The developed computer method may well be suitable for performance analysis of recovery processes using ribbon, ring slot, and other solid material type parachutes.

1. Aerial delivery
2. Recovery parachute performance analysis
3. Computer approach to parachute performance analysis
I. AFSC Project 6065, Task 606503
II. Contract AF33(616)-8371
III. Space Recovery Systems, Inc, El Segundo, Calif.
IV. T.W. Knacke and L.I. Dimmick
V. In ASTIA collection
VI. Not Aval fr OTS

Aeronautical Systems Division, Dir/ Aeromechanics, Flight Accessories Lab, Wright-Patterson AFB, Ohio. Rpt Nr ASD-TDR-62-75. DESIGN ANALYSIS OF FINAL RECOVERY PARACHUTES B-70 ENCAPSULATED SEAT AND THE USD-5 DRONE. Final report, Apr 62, 103 p. incl illus., 8 refs.

Unclassified Report

A performance analysis was conducted on two parachute recovery systems developed by Space Recovery Systems, Inc., for the North American Aviation B-70 encapsulated seat and the Fairchild Stratos Corp. USD-5 surveillance drone. Optimization of aerodynamic and textile design, controlled deployment and opening, and use of a cluster of two independently deployed parachutes for the USD-5 drone resulted in a highly predictable performance, in the highest known drag area per weight ratio for the

(over)

USD-5 system, and a high velocity capability for the B-70 system.

Equations were developed through data analysis for the opening process and the drag area increase versus time during parachute opening for extended skirt parachutes. These equations permitted a computer analysis of the total parachute deceleration process with computer results showing less than 10% deviation from actual test data. The developed computer method may well be suitable for performance analysis of recovery processes using ribbon, ring slot, and other solid material type parachutes.

1. Aerial delivery
2. Recovery parachute performance analysis
3. Computer approach to parachute performance analysis
I. AFSC Project 6065, Task 606503
II. Contract AF33(616)-8371
III. Space Recovery Systems, Inc, El Segundo, Calif.
IV. T.W. Knacke and L.I. Dimmick
V. In ASTIA collection
VI. Not Aval fr OTS

FOREWORD

This report was prepared by Space Recovery Systems, Inc., a division of Itek Corporation, in compliance with Contract No. AF 33(616)-8371, Project No. 6065 and Task No. 606503. The Retardation and Recovery Branch, Flight Accessories Laboratory, Aeronautical Systems Division, was the initiating agency with Mr. L. L. Watson serving as Project Officer.

The work at Space Recovery Systems was conducted by Mr. W. W. Knacke, Vice President Research and Engineering and Mr. L. I. Dimmick, Chief Aeromechanics Section. Staff members that contributed to the report include, Mr. B. A. Engstrom, Chief Paramechanics Department, and Mr. C. L. Byrd, Senior Engineer. Work was initiated on 1 May 1961 and completed on 31 December 1961.

This is the final report under contract AF33(616)-8371. The contractor's report number is SRS project No. 716.